TECHNISCHE UNIVERSITÄT WIEN

DISSERTATION

Biophysical Characterisation of Adeno-Associated Virus Vectors Using Advanced Analytical Technologies

Thema

ausgeführt zum Zwecke der Erlangung des akademischen Grades einer Doktorin der Naturwissenschaften unter der Leitung von

(Betreuung) Univ. Prof. Ruth Birner-Grünberger

Name

E164

Institutsnummer

Institut für Chemische Technologien und Analytik

Institutsbezeichnung

eingereicht an der Technischen Universität Wien

Technische Chemie

Fakultät

von

(VerfasserIn) Christina Wagner

Name

01301700

Matrikelnummer

Wien, am 09.02.2024

[redacted]

Acknowledgements

I would like to express my deepest appreciation to my sponsor, Dr. Birgit Seyfried, for offering me the position and financial support to conduct my PhD at Takeda. Furthermore, I am extremely grateful to Dr. Martin Lemmerer for his motivating words, patience, and guidance throughout the whole time. In addition, this endeavour would not have been possible without the generous support of Dr. Barbara Kraus and Robert Pletzenauer, who allowed me to carry out my experiments at the gene therapy site in Orth/Donau. I would also like to thank Univ.-Prof. Dr. Ruth Birner-Gruenberger from the Technical University of Vienna for her support during this time.

Special thanks to Bernd Innthaler and Dr. Felix Fuchsberger for editing and proofreading my published articles, their advice, and suggestions throughout the process of writing and submitting and their knowledge and expertise that they shared with me. Furthermore, I would like to acknowledge all my other colleagues for their moral and practical support during this time, especially Lucas Bock and Laura M. Nagel.

I am also grateful to my colleagues from the upstream and downstream processing teams for introducing me to the topic and showing me all the process steps within the gene therapy development platform relevant for my practical work.

Lastly, I would like to recognize my family and friends for their emotional support and for keeping up my spirits and motivation during this process.

Table of Contents

Abstract II
Zusammenfassung III
Abbreviations IV
Publications in connection with this thesis V
Brief Summary 1
Introduction 2
Aims 3
Methods 4
IEC-MALS 4
Mass Photometry 7
Results and Discussion 8
Concluding Remarks 10
References 11
Scientific Articles 16

Abstract

Adeno-associated viruses (AAV) are one of the most commonly used vehicles in gene therapies for the treatment of rare diseases. During the AAV manufacturing process, particles with little or no genetic material are co-produced alongside the desired AAV capsids containing the payload of interest. Due to potential adverse effects of these byproducts, they are considered impurities and require to be monitored thoroughly together with several other critical quality attributes (CQAs), such as capsid titer and viral genome integrity for example to ensure the safe and efficacious application of the gene therapeutic. Today, several analytical techniques, including size-exclusion chromatography (SEC), analytical ultracentrifugation (AUC), transmission electron microscopy (TEM), charge-detection mass spectrometry (CDMS), qPCR or ELISA, are used jointly for the characterisation of a gene therapy product. However, no universal technique for the simultaneous determination of multiple CQAs is currently available. Furthermore, most of these methods are associated with long-turnaround times, lack of high sample throughput and complex data analysis. In this study, a novel and robust ion-exchange chromatography method coupled to light scattering detectors was developed for the comprehensive characterisation of empty and filled AAVs concerning product titer, full-to-total ratio, capsid size, polydispersity, and absolute molar masses of the protein and nucleic acid omitting baseline-separation of both subpopulations prior to data analysis. Furthermore, it was demonstrated that mass photometry (MP) can be used as a fast and simple orthogonal technique to AUC to accurately quantify the proportions of empty, partially filled, full and overfull particles in an AAV samples with minimal sample preparation, low sample volumes (5-10 uL) and short analysis times (1-2 min.). To expand this further, a purification procedure was developed based on single-domain monospecific antibody fragments immobilised on either a poly(styrene-divinylbenzene) resin or on magnetic beads prior to MP analysis which enables the assessment of AAV subpopulations at early stages of the development platform within the upstream process. This should aid in selecting promising harvest conditions (transfection reagent, cell line, transgene, etc.) yielding high quantities of filled AAV capsids omitting cumbersome cleanup procedures such as diafiltration, ultracentrifugation or chromatography-based separation techniques.

Zusammenfassung

Adeno-assoziierte Viren (AAV) sind eines der am häufigsten verwendeten Transportsysteme bei Gentherapien zur Behandlung seltener Erkrankungen. Während der AAV-Produktion werden neben den gewünschten AAV-Kapsiden, die das Transgen von Interesse enthalten, auch Partikel mit Bruchstücken oder ohne genetisches Material produziert. Da diese Nebenprodukte potenziell gesundheitsgefährdend sind, gelten sie als Verunreinigungen und müssen zusammen mit verschiedenen anderen kritischen Qualitätsmerkmalen (CQAs), wie z. B. dem Kapsidtiter und der Integrität des viralen Genoms, sorgfältig überwacht werden, um die sichere und wirksame Anwendung des Gentherapeutikums zu gewährleisten. Heutzutage werden verschiedene Analysetechniken wie Größenausschlusschromatographie (SEC), analytische Ultrazentrifugation (AUC), Transmissionselektronenmikroskopie (TEM), Ladungsdetektions-Massenspektrometrie (CDMS), qPCR oder ELISA gemeinsam zur Charakterisierung eines Gentherapieprodukts eingesetzt. Derzeit gibt es jedoch keine universelle Technik für die gleichzeitige Bestimmung mehrerer CQAs. Darüber hinaus sind die meisten dieser Methoden mit langen Durchlaufzeiten, geringem Probendurchsatz und komplexer Datenanalyse verbunden. In dieser Arbeit wurde ein neuartiges und robustes Ionenaustausch-Chromatographieverfahren gekoppelt an Lichtstreudetektoren für die umfassende Charakterisierung von leeren und gefüllten AAVs in Bezug auf Kapsidtiter, das Verhältnis von vollen zu Gesamtkapsid-Zahl, Größe der Partikel, Polydispersität und absolute Molmassen des Proteins und der Nukleinsäure entwickelt, wobei eine Basislinientrennung beider Subpopulationen vor der Datenanalyse entfällt. Darüber hinaus wurde gezeigt, dass die Massenphotometrie (MP) als schnelle und einfache orthogonale Technik zur AUC eingesetzt werden kann, um die Anteile leerer, teilweise gefüllter, voller und überfüllter Partikel in einer AAV-Probe mit minimaler Probenvorbereitung, geringen Probenvolumina (5-10 uL) und kurzen Analysezeiten (1-2 Min.) genau zu quantifizieren. Um dies weiter auszubauen, wurde ein Aufreinigungsverfahren entwickelt, das auf monospezifischen Einzeldomänenantikörper basiert, die entweder auf einem Poly(styrol-divinylbenzol)-Harz oder auf magnetischen Beads immobilisiert sind. Dies ermöglicht die Bestimmung von AAV-Subpopulationen in Zellmaterial während der Entwicklung neuer Transfektionsbedingungen. Dies sollte bei der Auswahl vielversprechender Erntekonditionen (Transfektionsreagenz, Zelllinie, Transgen usw.) helfen, welche die größten Ausbeuten an gefüllten AAV-Kapsiden liefern, ohne dass aufwändige Reinigungsverfahren wie Diafiltration, Ultrazentrifugation oder chromatografische Trennverfahren erforderlich sind.

Abbreviations

A260/280	Absorbance ratio at 260 and 280 nm
Ad	Adenovirus
AUC	Analytical ultracentrifugation
c	concentration
CDMS	Charge-detection mass spectrometry
Cp	Capsids
CQA	Critical quality attributes
(Cryo-) TEM	(Cryo-)Transmission electron microscopy
DLS	Dynamic light scattering
dn/dc	Differential refractive index increment
ELISA	Enzyme-linked immunosorbent assay
EMA	European Medicines Agency
FDA	Food and Drug Administration
F/E ratio	Full/empty ratio
HSV	Herpes Simplex Virus
IEC	Ion-exchange chromatography
I_s	Intensity of scattered light
LS	Light scattering
MALS	Multi-angle light scattering
MP	Mass photometry
Mw	Molecular weight
pI	Isoelectric point
(q)PCR	(quantitative) Polymerase chain reaction
R	Rayleigh ratio
R%	Recovery
rAAV	Recombinant adeno-associated virus
Rg	Radius of gyration
Rh	Hydrodynamic radius
Rms	Root-mean-square radius (synonym for Rg)
SEC	Size-exclusion chromatography
VP	Viral protein
θ	theta

Publications in connection with this thesis

I. Biophysical Characterization of Adeno-Associated Virus Vectors Using Ion-Exchange Chromatography Coupled to Light Scattering Detectors

Wagner C, Innthaler B, Lemmerer M, Pletzenauer R, Birner-Gruenberger R.

Int. J. Mol. Sci. **2022**, 23, 12715.

This research article presents a novel and innovative ion-exchange chromatography method coupled to multi-angle light scattering detectors for the in-depth characterisation of empty and filled AAVs of multiple serotypes with respect to AAV particle titer, full-to-total ratio, absolute molar masses of protein and packaged genomic material and the capsid size.

Contributions of the first author: experiment planning and conduction, data analysis and visualisation, writing of the original draft.

II. Quantification of Empty, Partially Filled and Full Adeno-Associated Virus Vectors Using Mass Photometry

Wagner C, Fuchsberger F F, Innthaler B, Lemmerer M, Birner-Gruenberger R.

Int. J. Mol. Sci. **2023**, 24, 11033.

This research article demonstrates the high potential of mass photometry as orthogonal method to analytical ultracentrifugation for the quantification of the proportions of empty, partially filled, full and overfull species in AAV samples. In addition, it was shown, that mass photometry can be used to confirm the molecular weight of the encapsidated nucleic acid in filled AAV particles.

Contributions of the first author: experiment planning and conduction, data analysis and visualisation, writing of the original draft.

III. Automated Mass Photometry of Adeno-Associated Virus Vectors from Crude Cell Extracts

Wagner C, Fuchsberger F F, Innthaler B, Pachlinger R, Schrenk I, Lemmerer M, Birner-Gruenberger R.

Int. J. Mol. Sci. **2024**, 25, 838.

This research article highlights the differences in the various operating modes of the mass photometer and their advantages and drawbacks in AAV analysis. Furthermore, potentially promising harvest conditions that yield large numbers of the desired AAV capsids containing the genomic material of interest can be identified during the early stages of the viral vector development platform using single-domain monospecific antibody fragments immobilised on either a poly(styrene-divinylbenzene) resin or on magnetic beads followed by mass photometry analysis.

Contributions of the first author: experiment planning and conduction, data analysis and visualisation, writing of the original draft.

Brief Summary

Introduction

Recombinant adeno-associated virus (rAAV) vectors are one of the leading platforms for the delivery of gene therapeutics in vivo for the treatment of severe and rare diseases in patients. Compared to other viral vector-based vehicles such as retroviruses or lentiviruses, rAAVs stand out by their low immunogenicity, non-pathogenicity, long-term gene expression and different tissue tropisms due to a broad variety of serotypes [1-4]. To date, there are 13 different AAV serotypes differing in their receptor binding domains on the capsid surface arising from virion assembly which allow the specific targeting of tissues and cells [5,6]. In addition, the genetic engineering of rAAV vectors that feature an improved transduction efficiency and cope with immunological barriers have become more attractive and expand the gene therapy portfolio [6,7]. The great potential of rAAVs in human gene therapy is reflected in the many clinical trials which are currently ongoing worldwide in the field of ocular diseases, cardiovascular diseases, and cancer [8]. Furthermore, seven gene therapy products approved by the US Food and Drug Administration (FDA) or the European Medicines Agency (EMA) are currently on the market aiming at the treatment of lipoprotein lipase deficiency (Glybera), retinal dystrophy (Luxturna), spinal muscular atrophy (Zolgensma), Duchenne muscular dystrophy (Elevidys) and Hemophilia B (Hemgenix), aromatic L-amino acid decarboxylase (AADC) deficiency (Upstaza) and haemophilia A (Roctavian) respectively [9-16]. Additionally, the lentivirus-based gene therapy product Zynteglo has been approved by the EMA and FDA for patients suffering from beta thalassemia intermedia and major [17,18].

The non-enveloped AAV capsids belong to the genus *Dependoparvovirus* within the family *Parvoviridae* and are about 25 nm in diameter [19,20]. For efficient replication they depend on a helper virus, such as Herpes Simplex Virus (HSV) or Adenovirus (Ad) [21,22]. The AAV capsid is made up from three viral proteins: VP1, VP2 and VP3, which occur in a ratio of 1:1:10, with an overall sum of 60 interlocking proteins shaping the characteristic icosahedral capsid structure [23-25]. The protein monomers share a common region which is defined as VP3 and represents the shortest sequence variant with a molecular weight of 62 kDa. VP1 is the longest protein sequence variant and consists of VP2 with an additional N-terminal extension. VP1 and VP2 have molecular weights of 87 kDa and 73 kDa, respectively [26-28]. The packaging capacity of the virus particle is limited to a single-stranded DNA of ~4.7 kb, which is rather low in comparison with other viral vectors e.g., Ad or HSV, which are capable of transporting double-stranded DNA up to ~8 kb and ~40 kb, respectively [4,11,29].

This low packaging capacity is compensated due to the aforementioned structural simplicity and safety profile of AAVs. To guarantee the safe and efficacious application

of a gene therapeutic for patients, it is crucial to monitor certain critical quality attributes (CQAs), such as capsid titer, packaging efficiency (empty, partially filled, full and overfull), viral genome integrity, aggregation content and other impurities generated during the AAV production process as they pose potential adverse health effects to the recipient [30-33]. This demands robust and reliable analytical tools with a high throughput and little effort. To date, these parameters are captured with different techniques, varying in their accuracy and precision. While ELISA, PCR and light scattering are applied to determine the product titer, vector genome titer and aggregation content, respectively [34], analytical ultracentrifugation (AUC), transmission electron microscopy (TEM) and charge-detection mass spectrometry (CDMS) are frequently used in the biopharmaceutical industry and provide information on the AAV subpopulations (empty, partially filled, full and overfull). However, these methods share the lack in high sample throughput, long turnaround times, and often require adaption of the method for a specific serotype. This makes AUC, TEM, and CDMS less desirable for application in routine analysis and process development [30,31,35-39].

Aims

The aim of this study was to develop and apply new and advanced analytical techniques for the assessment of multiple CQAs focusing on the reduction of sample preparation and analysis duration, the increment of sample throughput and the broad applicability to various serotypes. The first analytical technique was based on ion-exchange chromatography coupled to dynamic (DLS) and static multi-angle light scattering (MALS) detectors for the determination of the capsid titer, full-to-total ratio, capsid size, polydispersity and molar masses of protein and genomic cargo of different serotypes without adaption of method parameters. Therefore, suitable mobile phases and IEC columns should be carefully selected as the separation of AAVs depends on the isoelectric point, the composition of the buffer system and the stability of the capsids at that specific pH. The chromatographic separation should be optimised, and the robustness of the method should be guaranteed to ensure the generation of reliable results. The second approach should consist of the establishment of an orthogonal analytical technique to AUC for the quantification of empty, partially filled, full and overfull AAV capsids. This method should be faster, simpler and should offer a higher sample throughput as opposed to AUC as the latter is less suitable for application in routine analysis due to its limited number of seven samples that can be analysed simultaneously in a 5 – 6-hour run. The developed methods should function as

orthogonal methods to the already established analytical techniques and aid in optimising the in-process analytical platform.

Methods

IEC-MALS

To circumvent the issues of long turnaround times and lack in high sample throughput that are often associated with multiple analytical techniques, orthogonal methods based on chromatographic separation prior to sample analysis, such as size-exclusion chromatography (SEC) for the quantification of aggregates, provide a faster response and allow the screening of large sample numbers. In AAV analytics, SEC is often coupled to light scattering detectors as this setup enables the determination of the capsid titer, polydispersity, capsid size, full-to-total ratio and absolute molar mass of protein and nucleic acid in one single measurement [40,41]. However, the unsatisfactory resolution of the SEC column as a consequence of the separation mechanism being based on the hydrodynamic radius is mirrored in the lack of baseline separation of oligomeric species from the monomers. . Due to the unproportionally high light scattering (LS) signal of the neighbouring oligomeric forms, the measured molar mass of the monomer is often compromised [40,42].

Ion-exchange chromatography (IEC) represents an alternative separation technique. IEC is frequently applied for the separation and relative quantification of empty and filled AAV capsids and allows the adjustment of multiple parameters for the optimisation of the chromatographic resolution of both AAV subspecies as opposed to SEC. This includes variation of the buffer systems, pH, temperature, flow rate, salt concentration and composition, gradient slope and column properties. The principle of separation is premised on the interaction of a charged stationary phase with complementarily charged AAV particles [40]. While an anion-exchange column comprises positively charged quaternary amine groups, a cation-exchanger contains negatively charged sulfonyl groups. The pH of the buffer media and the stability of AAV vectors at that specific pH define the type of ligand required for separation. For anion-exchange columns, the isoelectric point (pI) must be inferior to the pH of the buffer to guarantee an overall negative charge of the AAV capsids and vice versa when using cation-exchange columns [43-45].

Like SEC, IEC can be used in combination with light scattering detectors. This setup allows a more in-depth characterisation of the AAV capsids due to a separation of both subspecies prior to data analysis. This innovative application enables the determination of multiple CQAs in one single measurement, such as the product titer, the full-to-total capsid ratio, the polydispersity, the shape factor, the absolute molar

mass of nucleic acid and protein, as well as the hydrodynamic radius and radius of gyration. The physical principle of MALS is premised on the polarisability of matter, where the intensity of scattered light (I_s) at a certain angle (theta, θ) is directly proportional to the molecular weight (M_w), the concentration (c) of the analyte and the excess Rayleigh ratio (R) at angle theta provided that the differential refractive index increment (dn/dc) is a constant value of 0.185 mL/ g at ~660 nm (applicable to unmodified proteins in aqueous solution) (Equation (1)) [41,46-49]:

$$I_s(\theta)\ \alpha\ c * M_w * \left(\frac{dn}{dc}\right)^2 * R(\theta) \qquad (1)$$

The excess Rayleigh ratio, R(θ), is defined as the scattered light intensity at a certain angle (θ) of a suspension comprising particles with a defined molar mass (M_w) at a certain concentration (c) in excess of the light scattered by the pure solvent in which the particles are present (Equation (2)) [50]:

$$R(\theta) = \frac{f[I(\theta) - I_s(\theta)]}{I_0} \qquad (2)$$

I(θ) and I_s(θ) represent the measured scattered light intensity of the sample and the pure solvent at angle θ, respectively. I_0 is defined as the light intensity of the incident light beam and f as the absolute calibration constant (depending on the geometry of the light scattering device) [50]. Extrapolation to angle zero (R(0°) = 1) and concentration zero (c = 0) yields the weight-averaged molar mass by the intercept on the y-axis in the Zimm plot, while the slope of the extrapolation of the concentration determines the z-averaged root-mean-square radius (rms) [51]. For the assessment of the molar masses of protein and genomic cargo, two detectors are required. This can be UV/RI or a UV detector measuring at two different wavelengths e.g., 280 nm for the protein content and 260 nm for the amount of nucleic acid. However, when using IEC in combination with a salt gradient, the use of an RI detector becomes redundant as the change in the refractive index arising from the increasing salt concentration during elution hampers the data analysis. Hence, the use of dual wavelength UV-absorption detection is preferred here. Furthermore, the absorbance ratio at 260 and 280 nm (A260/280) provides information on whether the AAV capsids are filled or empty. The latter is represented by values between 0.6 and 0.7, while the ratio of filled particles lies between 1.3 and 1.4 [52].

In addition to the absolute molar masses of protein and nucleic acid, MALS allows the determination of the geometric radius of the analyte(s) due to the angular dependency of the scattered light intensity and the particle size. The bigger the particle radius, more precisely the radius of gyration (Rg or rms), the greater the intensity of the scattered

light at lower angles [48]. The variation in the angular dependency allows to draw conclusions on the size and size distribution of components in a sample. The downside of the MALS detector is the lack of sensitivity of small particles. Components with a Rg < 10 nm show no angular variation meaning that all light is scattered equally in each direction (= isotropic scattering). Dynamic light scattering (DLS), however, presents a more sensitive technology compared to MALS that allows the assessment of the hydrodynamic radius (Rh) down to a radius of 1 nm [48]. Compared to static light scattering, DLS takes into account the Brownian motion of the particles which is reflected in the measured fluctuations in the intensity of scattered light over time. These fluctuations are greater for smaller particles due to their movements being faster than larger components. The calculation of the hydrodynamic radius can be assessed using the Stokes-Einstein relation (Equation (3)), with k_b being the Boltzmann constant, T the temperature, η the solution viscosity and D_t the diffusion coefficient of the particle [48]:

$$Rh = \frac{k_b * T}{6 * \pi * \eta * D_t} \quad (3)$$

While SEC is based on the separation of species solely by their hydrodynamic radii, IEC resolves analytes based on their overall charge. This allows the discrimination of same-sized empty and full AAV capsids in terms of the hydrodynamic radius due to the impact of the encapsulated genomic material in filled species contributing to the overall charge of the capsids. Conclusively, IEC-MALS allows a detailed analysis of the biophysical properties of AAVs. A schematic illustration of the IEC-MALS method is given in Figure 1.

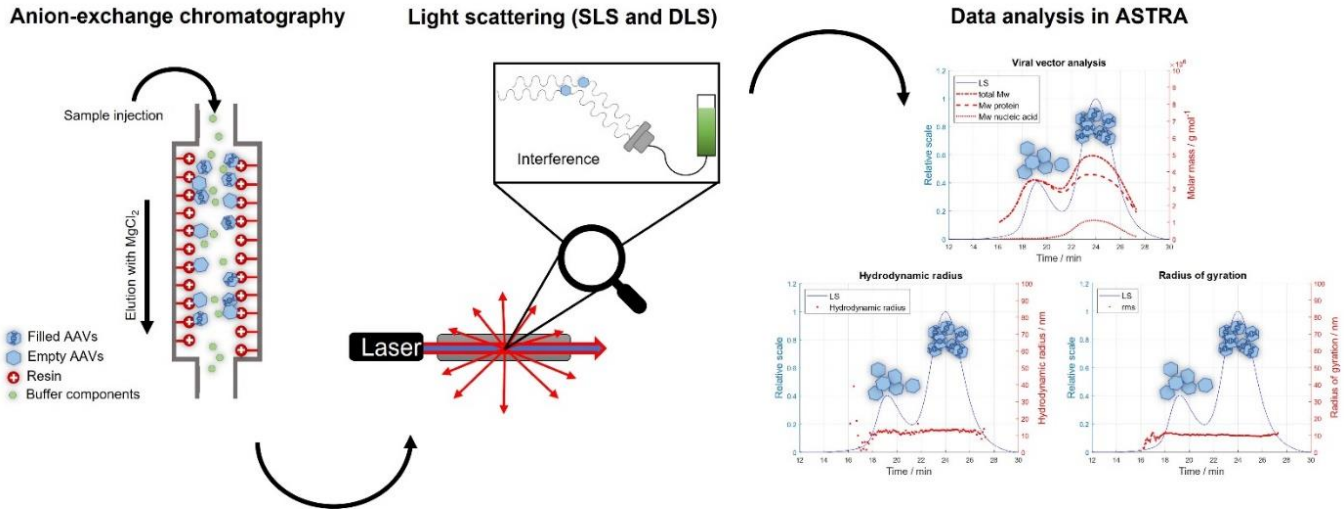

Figure 1. Schematic illustration of the IEC-MALS method. The AAV sample is loaded onto the anion-exchange column, eluted with a salt gradient containing $MgCl_2$ and detected with multi-angle light scattering and UV detectors prior to data analysis using ASTRA software. From Wagner et al. 2022.

Mass Photometry

Despite the many critical quality attributes determinable with IEC-MALS, the resolution of the chromatographic separation is limited to empty and filled AAV particles only. Proportions of AAV capsids containing truncated parts of the payload (partially filled) or genetic cargo beyond the maximum packaging capacity of the virus (overfilled) remain unknown. To date, AUC, TEM or CDMS are the methods of choice for the quantification of empty, partially filled, full and overfull AAV species, however, they lack low turnaround times and high sample throughput [30,31,36]. Furthermore, AUC requires large quantities of purified samples of ~500 µL and genome titers up to 5×10^{12} vg mL^{-1} [37]. CDMS analysis demands 2 h only, as opposed to 6 h for AUC, but is still in development, requires specialised equipment and well-trained personnel [30,37]. Mass photometry represents a faster and more straightforward analysis to gain insight into the homogeneity of an AAV sample with respect to AAV subspecies. It does not require any laborious sample preparation e.g., labelling or immobilisation steps of the analyte and can be operated as an automated instrument, facilitating analysis of large sample numbers [53,54]. The latter makes MP a favoured analytical analysis method over orthogonal techniques, like AUC, TEM and CDMS. Furthermore, sample volumes of 5 - 10 µL and capsid titers around 1×10^{11} cp mL^{-1} are sufficient for MP analysis [55]. The physical principle of MP is based on the interference of light scattered by particles attaching and detaching from a microscopic cover glass and the light which is reflected by the glass slide. The observed contrast of the reversibly binding particles at the solid-liquid interface differs between empty, partially filled, full and overfull AAV capsids. Like MALS, the measured light intensity is directly proportional to the molar mass of the particle, which allows the determination of the molecular weight of the AAV subspecies and consequently the packaged nucleic acid [41,56]. Furthermore, MP provides a rough estimation of the product titer and is based on the registration of the number of binding events which relates to the capsid titer. A schematic illustration is given in Figure 2.

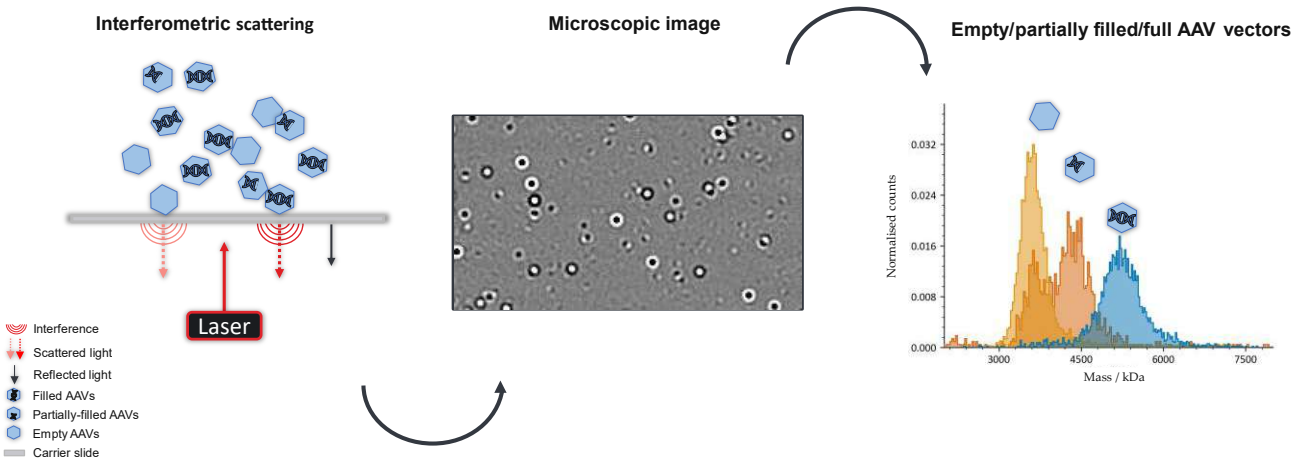

Figure 2. Schematic illustration of a mass photometry measurement. The attachment and detachment of AAVs onto a glass slide result in an interferometric light scattering at the solid-liquid interface. Full and empty particles are visualized in the microscopic image and transformed into a mass histogram according to their ratiometric contrast values. From Wagner et al. 2023.

Results and Discussion

In this thesis, new advanced analytical tools were developed for the in-depth characterization of AAV vectors covering a wide range of critical quality attributes, such as capsid titer, particle size, molecular weights of the protein and payload, polydispersity, and quantities of AAV subspecies including empty, partially filled, full and overfull particles. Furthermore, we established a method for the automated determination of the AAV subpopulations in purified samples using mass photometry and expanded its application to crude cell extracts by developing a fast cleanup procedure for AAVs prior to sample analysis.

A critical part of this thesis was the development of a robust and fast analytical technique for the assessment of multiple CQAs in one single measurement and was the primary focus of **paper I** (Wagner et al. 2022). Due to limited sample material, it is advantageous to develop an analytical approach for the combined determination of multiple CQAs in one measurement. To our knowledge IEC-MALS is the only method, which covers a wide range of CQAs and which does not only save time but also omits laborious sample preparation. Here we developed a novel and robust IEC-MALS method that allows the characterisation and quantification of empty and full AAV vectors of three different serotypes, AAV5, AAV6 and AAV8, without adaptation of the method conditions. This method provides good comparability with orthogonal methods, such as AUC and ELISA with respect to full/empty (F/E) ratio and capsid titer, respectively. Furthermore, we achieved adequate sample recoveries between 70 and 100% which is in agreement with other methods and yielded a high precision with a CV < 5% for product titer, hydrodynamic radius, polydispersity, full-to-total ratio,

absolute molar mass of protein, nucleic acid and total capsid. In addition, good linearity was obtained by diluting the sample to a capsid titer of 2.0×10^{11} cp mL^{-1} (CV < 5%).

Since IEC-MALS lacks chromatographic resolution that would allow the quantification of AAV subspecies, we implemented mass photometry as an orthogonal technology to AUC for the quantification of empty, partially filled, full and overfull AAV vectors and is discussed in detail in **paper II** (Wagner et al. 2023). This simple alternative analytical technique requires no sample preparation, uses minimal sample volumes of 10 µL and capsid titers around 1.0×10^{11} cp mL^{-1}. We observed a linear correlation between sample concentration and measured ratiometric contrast values of product titers between 4.0×10^{10} cp mL^{-1} and 8.0×10^{11} cp mL^{-1}. With a CV < 5%, mass photometry yields a high precision regarding the calculated molecular weight of the incorporated transgene. Additionally, the broad applicability to multiple serotypes without method adaptation makes it a desirable tool in gene therapy analytics.

Due to limitation in the sample number that can be analysed with MP, the installation of a robotic module enabled not only the automated operation of the instrument but allowed a higher sample throughput and was discussed in **paper III** (Wagner et al. 2024). Furthermore, we compared the instrument performance when operated manually and automatically and found that both operation modes performed equally well. In addition, we addressed the differences between the "buffer-free" and the "buffer-dilution" mode used for sample measurement and observed a discrepancy in the number of registered binding events between both focusing options attributed to the lack of mixing the sample with the buffer when using the "buffer-dilution" mode during the automated instrument handling. The feature to estimate the capsid titer and which is calculated from the number of AAV particles binding and unbinding from the glass surface was explored as it has the potential to be used as orthogonal method to titer quantification methods, e.g. ELISA. However, the high variation in the binding count rates biased the calculation of the product titers resulting in an overestimation of the titers when using the "buffer-dilution" focusing as opposed to an underestimation in case of the "buffer free" focusing mode.

Despite mass photometry being a fast and simple analytical tool for the quantification of AAV subspecies, it is limited to purified samples only. Prompted by this, we set up a procedure for the cleanup of AAVs from crude cell extracts prior to MP analysis using single-domain monospecific antibody fragments immobilised on either poly(styrene-divinylbenzene) resin or on magnetic beads and was highlighted in **paper III** (Wagner et al 2024). We were able to gain insight into the heterogeneity of AAV subpopulations

at early stages of the development platform and detected differences in the proportion of empty, partially filled, full and overfull particles between cell extracts which had been generated using two types of transfection reagents.

Concluding Remarks

In this work, we developed an IEC-MALS method for the assessment of multiple CQAs in one measurement covering the determination of the capsid titer, F/E ratio, hydrodynamic radius, radius of gyration, absolute molar masses of the protein and the encapsidated transgene. This assay can be used as orthogonal method to AUC and ELISA with respect to F/E ratio and product titer, respectively. Furthermore, the omission of baseline separation of empty and filled AAV subspecies required for the calculation of above-mentioned parameters and the applicability of the assay to two other serotypes without adaptation of method conditions makes it attractive analytical tool for the in-depth characterisation of gene therapy products.

The lack of chromatographic resolution of IEC-MALS, however, does not disclose information on the AAV subpopulations with incorporated truncated versions of the intended payload (partially filled capsids) or containing more than one copy of the genomic material (overfull capsids). Hence, we implemented mass photometry as fast and simple analytical technique for the quantification of empty, partially filled, full and overfull AAV vectors. Compared to AUC, CDMS and TEM, which are frequently applied in gene therapy, mass photometry can be used as an orthogonal method with the advantage of shorter analysis times (1-2 min.), of being higher in sample throughput, less cumbersome and lower on sample consumption and capsid titers. We managed to calculate the molar mass and quantify AAV subspecies of samples with capsid titers as low as 8.0×10^{11} cp mL^{-1} with a CV < 5% using just 10 µL total sample volume. In addition, we developed a method for the determination of AAV subpopulations in crude harvest material by first, extracting the AAV particles with the aid of single-domain monospecific antibody fragments immobilised on either a poly(styrene-divinylbenzene) resin or on magnetic beads followed by MP analysis. This extraction allows an estimation of AAV subspecies during the upstream process omitting laborious cleanup steps such as diafiltration, ultracentrifugation, affinity chromatography, etc. aiming at a more efficient and less time-consuming screening of different transfection conditions, cell lines, transgenes, etc. that yield high titers of filled AAV capsids.

References

1. Li, C.; Samulski, R.J. Engineering adeno-associated virus vectors for gene therapy. *Nat. Rev. Genet.* **2020**, *21*, 255–272. https://doi.org/10.1038/s41576-019-0205-4.
2. Chandler, R.J.; Sands, M.; Venditti, C.P. rAAV integration and genotoxicity: Insights from animal models. *Hum. Gene Ther.* **2017**, *28*, 4. https://doi.org/10.1089/hum.2017.009.
3. Maestro, S.; Weber, N.D.; Zabaleta, N.; Aldabe, R.; Gonzalez-Aseguinolaza, G. Novel vectors and approaches for gene therapy in liver diseases. *JHEP Rep.* **2021**, *3*, 100300. https://doi.org/10.1016/j.jhepr.2021.100300.
4. Ghosh, S.; Brown, A.M.; Jenkins, C.; Campbell, K. Viral Vector Systems for Gene Therapy: A Comprehensive Literature Review of Progress and Biosafety Challenges. *Appl. Biosaf.* **2020**, *25*, 7–18. https://doi.org/10.1177/1535676019899502.
5. Srivastava, A. In vivo tissue-tropism of adeno-associated viral vectors. *Curr. Opin. Virol.* **2016**, *21*, 75–80. https://doi.org/10.1016/j.coviro.2016.08.003
6. Buning, H.; Huber, A.; Zhang, L.; Meumann, N.; Hacker, U. Engineering the AAV capsid to optimize vector-host-interactions. *Curr. Opin. Pharmacol.* **2015**, *24*, 94–104. https://doi.org/10.1016/j.coph.2015.08.002.
7. Bulcha, J.T.; Wang, Y.; Ma, H.; Tai, P.W.L.; Gao, G. Viral vector platforms within the gene therapy landscape. *Signal Transduct. Target. Ther.* **2021**, *6*, 53. https://doi.org/10.1038/s41392-021-00487-6.
8. Wileys, J. Gene Therapy Clinical Trials Worldwide. Availabe online: https://a873679.fmphost.com/fmi/webd/GTCT (accessed on 14 March 2022).
9. Elevidys. Available online: https://www.fda.gov/vaccines-blood-biologics/tissue-tissue-products/elevidys (accessed on 6 July 2023).
10. Khatwani, S.L.; Pavlova, A.; Pirot, Z. Anion-exchange HPLC assay for separation and quantification of empty and full capsids in multiple adeno-associated virus serotypes. *Mol. Ther.-Methods Clin. Dev.* **2021**, *21*, 548–558. https://doi.org/10.1016/j.omtm.2021.04.003.
11. Oyama, H.; Ishii, K.; Maruno, T.; Torisu, T.; Uchiyama, S. Characterization of Adeno-Associated Virus Capsid Proteins with Two Types of VP3-Related Components by Capillary Gel Electrophoresis and Mass Spectrometry. *Hum. Gene Ther.* **2021**, *32*, 21–22. https://doi.org/10.1089/hum.2021.009.
12. Wang, D.; Tai, P.; Gao, G. Adeno-associated virus vector as a platform for gene therapy delivery. *Nat. Rev. Drug Discov.* **2019**, *18*, 358–378. https://doi.org/10.1038/s41573-019-0012-9.
13. Wright, F.J. Quality Control Testing, Characterization and Critical Quality Attributes of AAV Vectors Used for Human Gene Therapy. *Biotechnol. J.* **2020**, *16*, e2000022. https://doi.org/10.1002/biot.202000022.
14. Hemgenix. Available online: https://www.fda.gov/vaccines-blood-biologics/vaccines/hemgenix (accessed on 17 October 2023).
15. Upstaza. Available online: https://www.ema.europa.eu/en/medicines/human/EPAR/upstaza (accessed on 2 January 2024).

16. Roctavian. Available online: https://www.fda.gov/vaccines-blood-biologics/roctavian (accessed on 2 January 2024).
17. EU/3/12/1091: Orphan Designation for the Treatment of Beta Thalassaemia Intermedia and Major. Available online: https://www.ema.europa.eu/en/medicines/human/orphan-designations/eu3121091 (accessed on 12 April 2023).
18. FDA Approves First Cell-Based Gene Therapy to Treat Adult and Pediatric Patients with Beta-thalassemia Who Require Regular Blood Transfusions. Available online: https://www.fda.gov/news-events/press-announcements/fda-approves-first-cell-based-gene-therapy-treat-adult-and-pediatric-patients-beta-thalassemia-who (accessed on 12 April 2023).
19. Aponte-Ubillus, J.; Barajas, D.; Peltier, J.; Bardliving, C.; Shamlou, P.; Gold, D. Molecular design for recombinant adeno-associated virus (rAAV) vector production. *Appl. Microbiol. Biotechnol.* **2018**, *102*, 1045–1054. https://doi.org/10.1007/s00253-017-8670-1.
20. Rayaprolu, V.; Kruse, S.; Kant, R.; Venkatakrishnan, B.; Movahed, N.; Brooke, D.; Lins, B.; Bennett, A.; Potter, T.; McKenna, R.; Agbandje-McKenna, M.; Bothner, B. Comparative analysis of adeno-associated virus capsid stability and dynamics. *J Virol.* **2013**, *87*, 13150-13160. doi: 10.1128/JVI.01415-13.
21. Geoffroy, M.-C.; Salvetti, A. Helper Functions Required for Wild Type and Recombinant Adeno- Associated Virus Growth. *Curr. Gene Ther.* **2005**, *5*, 265–271. https://doi.org/10.2174/1566523054064977.
22. Buller, R.M.L.; Janik, J.E.; Sebring, E.D.; Rose, J.A. Herpes Simplex Virus Types 1 and 2 Completely Help Adenovirus-Associated Virus Replication. *J. Virol.* **1981**, *40*, 241–247. https://doi.org/10.1128/JVI.40.1.241-247.1981.
23. Nam, H.-J.; Lane, M.D.; Padron, E.; Gurda, B.; McKenna, R.; Kohlbrenner, E.; Aslanidi, G.; Byrne, B.; Muzyczka, N.; Zolotukhin, S.; et al. Structure of Adeno-Associated Virus Serotype 8, a Gene Therapy Vector. *J. Virol.* **2007**, *81*, 12260–12271. https://doi.org/10.1128/jvi.01304-07.
24. Wright, F.J. Product-Related Impurities in Clinical-Grade Recombinant AAV Vectors: Characterization and Risk Assessment. *Biomedicines* **2014**, *2*, 80–97. https://doi.org/10.3390/biomedicines2010080.
25. Venkatakrishnan, B.; Yarbrough, J.; Domsic, J.; Bennett, A.; Bothner, B.; Kozyreva, O.G.; Samulski, R.J.; Muzyczka, N.; McKenna, R.; Agbandje-McKenna, M. Structure and Dynamics of Adeno-Associated Virus Serotype 1 VP1-Unique N-Terminal Domain and Its Role in Capsid Trafficking. *J. Virol.* **2013**, *87*, 4974–4984. https://doi.org/10.1128/jvi.02524-12.
26. Rose, J.A.; Maizel, J.V., Jr.; Inman, J.K.; Shatkin, A.J. Structural Proteins of Adenovirus-Associated Viruses. *J. Virol.* **1971**, *8*, 766–770. https://doi.org/10.1128/jvi.8.5.766-770.1971.
27. Barnes, L.F.; Draper, B.E.; Kurian, J.; Chen, Y.-T.; Shapkina, T.; Powers, T.W.; Jarrold, M.F. Analysis of AAV-Extracted DNA by Charge Detection Mass Spectrometry Reveals Genome Truncations. *Anal. Chem.* **2023**, *95*, 4310–4316. https://doi.org/10.1021/acs.analchem.2c04234.

28. Wörner, T.P.; Bennett, A.; Habka, S.; Snijder, J.; Friese, O.; Powers, T.; Agbandje-McKenna, M.; Heck, A.J.R. Adeno-associated virus capsid assembly is divergent and stochastic. *Nat. Commun.* **2021**, *12*, 1642. https://doi.org/10.1038/s41467-021-21935-5.
29. Wang, C.; Mulagapati, S.H.R.; Chen, Z.; Du, J.; Zhao, X.; Xi, G.; Chen, L.; Linke, T.; Gao, C.; Schmelzer, A.E.; et al. Developing an Anion Exchange Chromatography Assay for Determining Empty and Full Capsid Contents in AAV6.2. *Mol. Ther.—Methods Clin. Dev.* **2019**, *15*, 257–263. https://doi.org/10.1016/j.omtm.2019.09.006.
30. Gimpel, A.L.; Katsikis, G.; Sha, S.; Maloney, A.J.; Hong, M.S.; Nguyen, T.N.T.; Wolfrum, J.; Springs, S.L.; Sinskey, A.J.; Manalis, S.R.; et al. Analytical methods for process and product characterization of recombinant adeno-associated virus-based gene therapies. *Mol. Ther.—Methods Clin. Dev.* **2021**, *20*, 740–754. https://doi.org/10.1016/j.omtm.2021.02.010.
31. Fu, X.; Chen, W.-C.; Argento, C.; Clarner, P.; Bhatt, V.; Dickerson, R.; Bou-Assaf, G.; Bakhshayeshi, M.; Lu, X.; Bergelson, S.; et al. Analytical Strategies for Quantification of Adeno-Associated Virus Empty Capsids to Support Process Development. *Hum. Gene Ther. Methods* **2019**, *30*, 144–152. https://doi.org/10.1089/hgtb.2019.088.
32. Li, T.; Gao, T.; Chen, H.; Dmianova, Z.; Wang, F.; Malik, M.; Luo, J.; Yowanto, H.; Mollah, S. *Determination of Full, Partial and Empty Capsid Ratios for Adeno-Associated Virus (AAV) Analysis*; SCIEX: Framingham, MA, USA, 2020.
33. Refeyn Ltd. Quantifying Heterogeneous AAV Capsid Loading Using Mass Photometry. [White Paper]. 2022. Available online: https://info.refeyn.com/app-note-aav-loading (accessed on 14 June 2023).
34. McIntosh, N.L.; Berguig, G.Y.; Karim, O.A.; Cortesio, C.L.; De Angelis, R.; Khan, A.A.; Gold, D.; Maga, J.A.; Bhat, V.S. Comprehensive characterization and quantification of adeno associated vectors by size exclusion chromatography and multi angle light scattering. *Sci. Rep.* **2021**, *11*, 3012. https://doi.org/10.1038/s41598-021-82599-1.
35. Ye, H. Simultaneous determination of protein aggregation, degradation, and absolute molecular weight by size exclusion chromatography-multiangle laser light scattering. *Anal. Biochem.* **2006**, *356*, 76–85. https://doi.org/10.1016/j.ab.2006.05.025.
36. Pierson, E.E.; Keifer, D.Z.; Asokan, A.; Jarrold, M.F. Resolving Adeno-Associated Viral Particle Diversity With Charge Detection Mass Spectrometry. *Anal. Chem.* **2016**, *88*, 6718–6725. https://doi.org/10.1021/acs.analchem.6b00883.
37. Werle, A.K.; Powers, T.W.; Zobel, J.F.; Wappelhorst, C.N.; Jarrold, M.F.; Lyktey, N.A.; Sloan, C.D.; Wolf, A.J.; Adams-Hall, S.; Baldus, P.; et al. Comparison of analytical techniques to quantitate the capsid content of adeno-associated viral vectors. *Mol. Ther. Methods Clin. Dev.* **2021**, *23*, 254–262. https://doi.org/10.1016/j.omtm.2021.08.009.
38. Stagg, S.M.; Yoshioka, C.; Davulcu, O.; Chapman, M.S. Cryo-electron Microscopy of Adeno-associated Virus. *Chem. Rev.* **2022**, *122*, 14018–14054. https://doi.org/10.1021/acs.chemrev.1c00936.

39. Subramanian, S.; Maurer, A.C.; Bator, C.M.; Makhov, A.M.; Conway, J.F.; Turner, K.B.; Marden, J.H.; Vandenberghe, L.H.; Hafenstein, S.L.; Troxell, B.; et al. Filling Adeno-Associated Virus Capsids: Estimating Success by Cryo-Electron Microscopy. *Hum. Gene Ther.* **2019**, *30*, 1449–1460. https://doi.org/10.1089/hum.2019.041.
40. Amartely, H.; Avraham, O.; Friedler, A.; Livnah, O.; Lebendiker, M. Coupling Multi Angle Light Scattering to Ion Exchange chromatography (IEX-MALS) for protein characterization. *Sci. Rep.* **2018**, *8*, 6907. https://doi.org/10.1038/s41598-018-25246-6.
41. Wyatt, P. Light scattering and the absolute characterization of macromolecules. *Anal. Chim. Acta* **1993**, *272*, 1–40.
42. Sahin, E.; Roberts, C.J. Size-exclusion chromatography with multi-angle light scattering for elucidating protein aggregation mechanisms. *Methods Mol. Biol.* **2012**, *899*, 403–423. https://doi.org/10.1007/978-1-61779-921-1_25.
43. Weihong, Q.; Mingxi, W.; Yaqing, W.; Ruian, X. Scalable Downstream Strategies for Purification of Recombinant Adeno- Associated Virus Vectors in Light of the Properties. *Curr. Pharm. Biotechnol.* **2015**, *16*, 684–695. https://doi.org/10.2174/1389201016666150505122228.
44. Fekete, S.; Beck, A.; Veuthey, J.-L.; Guillarme, D. Ion-exchange chromatography for the characterization of biopharmaceuticals. *J. Pharm. Biomed. Anal.* **2015**, *113*, 43–55. https://doi.org/10.1016/j.jpba.2015.02.037.
45. Tsonev, L.a.I.; Hirsh, A.G. Theory and applications of a novel ion exchange chromatographic technology using controlled pH gradients for separating proteins on anionic and cationic stationary phases. *J. Chromatogr. A* **2008**, *1200*, 166–182. https://doi.org/10.1016/j.chroma.2008.05.076.
46. Zhao, H.; Brown, P.H.; Schuck, P. On the Distribution of Protein Refractive Index Increments. *Biophys. J.* **2011**, *100*, 2309–2317. https://doi.org/10.1016/j.bpj.2011.03.004.
47. Some, D.; Amartely, H.; Tsadok, A.; Lebendiker, M. Characterization of Proteins by Size-Exclusion Chromatography Coupled to Multi-Angle Light Scattering (SEC-MALS). *J. Vis. Exp.: JoVE* **2019, 8, 6907**. https://doi.org/10.3791/59615.
48. Larkin, M.; Wyatt, P. Light scattering techniques and their application to formulation and aggregation concerns. *Formul. Process Dev. Strateg. Manuf. Biopharm.* **2010**, , 269–305.
49. Patel, B.A.; Gospodarek, A.; Larkin, M.; Kenrick, S.A.; Haverick, M.A.; Tugcu, N.; Brower, M.A.; Richardson, D.D. Multi-angle light scattering as a process analytical technology measuring real-time molecular weight for downstream process control. *mAbs* **2018**, *10*, 945–950. https://doi.org/10.1080/19420862.2018.1505178.
50. Wyatt, P. Differential light scattering and the measurement of molecules and nanoparticles: A review. *Anal. Chim. Acta*, **2021**, *7–8*, 2590-1346. https://doi.org/10.1016/j.acax.2021.100070.
51. TOSOH Corporation. Light Scattering for Determination of Molecular Weight and Radius of Gyration *[White Paper]*. 2022. Available online:

https://www.separations.eu.tosohbioscience.com/OpenPDF.aspx?path=~/File%20Library/TBG/Products%20Download/Whitepaper/w20i16a.pdf (accessed on 7 June 2022).
52. Gagnon, P.; Goricar, B.; Mencin, N.; Zvanut, T.; Peljhan, S.; Leskovec, M.; Strancar, A. Multiple-Monitor HPLC Assays for Rapid Process Development, In-Process Monitoring, and Validation of AAV Production and Purification. *Pharmaceutics* **2021**, *13*, 113. https://doi.org/10.3390/pharmaceutics13010113.
53. Takeda, K.; Noda, M.; Maruno, T.; Uchiyama, S. Critical Calibration of Mass Photometry for Higher-Mass Samples Such as Adeno-Associated Virus Vectors. *J. Pharm. Sci.* **2022**, *112*, 1145–1150. https://doi.org/10.1016/j.xphs.2022.10.025.
54. Wu, D.; Piszczek, G. Standard protocol for mass photometry experiments. *Eur. Biophys J.* **2021**, *50*, 403–409. https://doi.org/10.1007/s00249-021-01513-9.
55. Wagner, C.; Fuchsberger, F.F.; Innthaler, B.; Lemmerer, M.; Birner-Gruenberger, R. Quantification of Empty, Partially Filled and Full Adeno-Associated Virus Vectors Using Mass Photometry. *Int. J. Mol. Sci.* **2023**, *24*, 1033. https://doi.org/10.3390/ijms241311033.
56. Sonn-Segev, A.; Belacic, K.; Bodrug, T.; Young, G.; VanderLinden, R.T.; Schulman, B.A.; Schimpf, J.; Friedrich, T.; Dip, P.V.; Schwartz, T.U.; et al. Quantifying the heterogeneity of macromolecular machines by mass photometry. *Nat. Commun.* **2020**, *11*, 1772. https://doi.org/10.1038/s41467-020-15642-w.

Scientific Articles

International Journal of
Molecular Sciences

MDPI

Article

Biophysical Characterization of Adeno-Associated Virus Vectors Using Ion-Exchange Chromatography Coupled to Light Scattering Detectors

Christina Wagner [1,*], Bernd Innthaler [2], Martin Lemmerer [1], Robert Pletzenauer [2] and Ruth Birner-Gruenberger [3]

[1] Analytical Development Europe, Takeda Vienna, 1220 Vienna, Austria
[2] Gene Therapy Process Development, Takeda Orth an der Donau, 2304 Orth an der Donau, Austria
[3] Institute of Chemical Technologies and Analytics, Technische Universität Wien, 1060 Vienna, Austria
* Correspondence: christina.wagner@takeda.com

Abstract: Ion-exchange chromatography coupled to light scattering detectors represents a fast and simple analytical method for the assessment of multiple critical quality attributes (CQA) in one single measurement. The determination of CQAs play a crucial role in Adeno-Associated Virus (AAV)-based gene therapies and their applications in humans. Today, several different analytical techniques, including size-exclusion chromatography (SEC), analytical ultracentrifugation (AUC), qPCR or ELISA, are commonly used to characterize the gene therapy product regarding capsid titer, packaging efficiency, vector genome integrity, aggregation content and other process-related impurities. However, no universal method for the simultaneous determination of multiple CQAs is currently available. Here, we present a novel robust ion-exchange chromatography method coupled to multi-angle light scattering detectors (IEC-MALS) for the comprehensive characterization of empty and filled AAVs concerning capsid titer, full-to-total ratio, absolute molar mass of the protein and nucleic acid, and the size and polydispersity without baseline-separation of both species prior to data analysis. We demonstrate that the developed IEC-MALS assay is applicable to different serotypes and can be used as an orthogonal method to other established analytical techniques.

Keywords: adeno-associated virus vectors; ion-exchange chromatography; multi-angle light scattering; dynamic light scattering; protein characterization; critical quality attributes

Citation: Wagner, C.; Innthaler, B.; Lemmerer, M.; Pletzenauer, R.; Birner-Gruenberger, R. Biophysical Characterization of Adeno-Associated Virus Vectors Using Ion-Exchange Chromatography Coupled to Light Scattering Detectors. *Int. J. Mol. Sci.* **2022**, *23*, 12715. https://doi.org/10.3390/ijms232112715

Academic Editor: Yuri Lyubchenko

Received: 13 September 2022
Accepted: 19 October 2022
Published: 22 October 2022

1. Introduction

Recombinant adeno-associated virus (rAAV) vectors are currently the leading platform for delivering gene therapies in vivo for the treatment of severe and rare diseases in patients. rAAV vectors stand out by their low immunogenicity, long-term gene expression, non-pathogenic behavior and different tissue tropisms due to a vast variety of serotypes [1–3]. The genetic engineering of rAAV vectors that feature an improved transduction efficiency and cope with immunological barriers has been studied extensively in recent years [4]. To date, four gene therapeutics approved by the US Food and Drug Administration (FDA) or the European Medicines Agency (EMA) are on the market [5]. The first gene therapy product (Glybera), based on AAV1, was approved by the EMA in 2012 for the treatment of lipoprotein lipase deficiency, followed by Luxturna, an AAV2-based gene therapeutic, for the treatment of retinal dystrophy, which was approved by the FDA in 2017 and the EMA in 2018. The third, AAV9-based gene therapy product, Zolgensma, was approved by the FDA in 2019 for patients suffering from spinal muscular atrophy [1,6–9]. The fourth lentiviral-based gene therapeutic (Zynteglo) was approved by the EMA in 2019 and only recently by the FDA (September 2022) for the treatment of beta thalassaemia intermedia and major [10,11]. In addition, more than 200 gene therapeutics based on AAV vectors are currently investigated in clinical trials worldwide for the treatment of ocular diseases, cardiovascular diseases and cancer [12].

AAVs belong to the genus *Dependoparvovirus* within the family *Parvoviridae* [4]. They comprise non-enveloped, icosahedral capsids with the ability to insert single-stranded DNA up to 4.7 kb [5]. The capsid itself is made up from three viral proteins: VP1, VP2 and VP3. Those three viral proteins occur in a ratio of 1:1:10, with an overall sum of 60 interlocking proteins forming the icosahedral capsid structure [13,14]. The cellular tropism of the 12 AAV serotypes that have been identified so far is defined by differences in the receptor binding domains on the capsid surface arising from virion assembly [1,15]. The production of the VPs and capsid assembly are encoded by the *cap* gene—one of the open reading frames (ORF) located between two inverted terminal repeats, while the *rep* ORF is crucial for the replication and encapsidation of the viral genome [6,16].

To guarantee a safe and efficacious application of gene therapy products for patients, it is crucial to monitor the product quality to evaluate the critical quality attributes (CQAs), such as capsid titer, packaging efficiency (empty-to-full capsid ratio), viral genome integrity, aggregation content and other process-related impurities [17]. This demands robust and reliable analytical methods with a high throughput and little effort. To date, these attributes are assessed by different methods, varying in their precision and accuracy. While ELISA, PCR and light scattering are used to determine capsid titer, vector genome titer and aggregation content, respectively [18], analytical ultracentrifugation (AUC) and transmission electron microscopy (TEM) are still the leading platforms in the biopharmaceutical industry that provide insight into the quantity of empty, partially-filled and full capsids. Nevertheless, the long turnaround times and lack in high sample throughput limit their application in routine analysis and process development [17,19,20]. To circumvent these issues, orthogonal methods based on a chromatographic separation prior to sample analysis, such as size-exclusion chromatography (SEC) for the quantification of aggregates, can be used due to a faster response and a higher sample throughput. In combination with multi-angle light scattering (MALS), SEC provides a more detailed analysis of AAV samples, as the capsid titer, the polydispersity, the capsid size, the full-to-total capsid ratio, the absolute molar mass of the nucleic acid, the protein and the total capsid can all be assessed simultaneously without the need for column calibration [21,22]. However, the resolution of same-sized particles in the SEC columns is inherently impracticable due to the separation mechanism being based on the hydrodynamic radius of the particles. Furthermore, oligomeric forms are often not fully baseline separated from the monomers due to the properties of the SEC column. This can result in a deviation of the measured absolute molar mass of the monomer from the expected value, as the light scattering (LS) signals of the oligomeric forms are unproportionally higher than the ones of the monomer peak [21,23].

Ion-exchange chromatography (IEC) provides an alternative separation method, which is frequently used for the determination of empty and full AAV capsids. IEC allows more parameters to be optimized in order to enhance the chromatographic resolution of AAV populations compared to SEC, such as buffer medium, pH, temperature, flow rate, salt concentration and composition, gradient slope and column properties. The separation principle is based on the interaction of a positively charged (anion-exchanger) or negatively charged (cation-exchanger) stationary phase with complementarily charged AAV capsids [21]. The choice of ligands depends on the pH of the buffering systems and the stability of AAV vectors at that specific pH. When using an anion-exchange column, the pH of the buffer must exceed the isoelectric point (pI) of the AAV capsids to ensure an overall negative charge of the AAV particles and vice versa when applying a cation-exchanger [24–26].

Like SEC, IEC can be coupled to MALS and thereby enables a more comprehensive characterization of empty and filled AAV capsids due to a separation of both subpopulations prior to sample analysis. This novel application allows the determination of the capsid titer, the full-to-total capsid ratio, the polydispersity, the shape factor, the absolute molar mass of nucleic acid and protein, as well as the hydrodynamic radius and radius of gyration in one single measurement. Based on the physical principle of polarizability of matter, the intensity of scattered light (I_s) at a certain angle (theta, θ) is directly proportional

to the molecular weight (M), the concentration (c) of the analyte and the excess Rayleigh ratio (R) at angle theta assuming that the differential refractive index increment (dn/dc) is a constant value of 0.185 mL/g at ~660 nm (for unmodified proteins in aqueous medium) (Equation (1)) [22,27–30]:

$$I_s(\theta) \propto c * M * \left(\frac{dn}{dc}\right)^2 * R(\theta) \quad (1)$$

The weight-averaged molar mass can be determined as the intercept on the *y*-axis in the Zimm plot by extrapolating to angle zero ($R(0°) = 1$) and concentration zero ($c = 0$). The slope of the extrapolation of the concentration gives the z-averaged radius of gyration [31]. When analyzing AAVs with MALS, the molar masses of the protein and the nucleic acid can be measured simultaneously. This demands two detectors, e.g., UV/RI or a UV detector, measuring at two different wavelengths. In case of IEC, the AAV particles elute from the column by applying a linear salt gradient; thus, a RI detector becomes invalid due to the change in the refractive index caused by the increasing salt concentration introducing a bias in the data analysis. To circumvent this issue, dual wavelength UV-absorption detection can be used, where one wavelength monitors the nucleic acid content (absorption maximum at 260 nm), and the second wavelength detects the protein proportion (absorption maximum at 280 nm) [32].

In addition, the ratio of the absorbance at 260 and 280 nm (A260/280) allows the distinction of empty AAV capsids from filled ones. While values between 0.6–0.7 are indicative for empty AAVs, ratios between 1.3–1.4 represent filled capsids [32]. The ratios can be calculated by integrating the area of both peaks at 260 and 280 nm. A different approach was described by Porterfield et al., who developed a method to quickly assess the protein and nucleic acid content by using light scattering corrected UV absorbance spectroscopy and validated their results by comparison to the orthogonal SEC-MALS technology [33].

Because MALS measures the intensity of the scattered light, it not only allows the calculation of the absolute molar mass of the protein and nucleic acid but also the assessment of the geometric radius of the analyte(s). There is an angular dependency of the scattered light intensity and the particle size, more precisely, the radius of gyration (Rg) of a particle. The bigger the Rg, the greater the scattered light intensity at lower angles [29]. Consequently, it is possible to determine the size and size distribution of the individual components of the sample via the angular variation. However, there is a sensitivity limitation of the MALS detector. Particles with a Rg smaller than 10 nm show no angular dependency of the scattered light intensity. Light is scattered equally in each direction (= isotropic scattering). Compared to static light scattering (MALS), dynamic light scattering (DLS) provides a more sensitive approach and allows the determination of the hydrodynamic radius (Rh) of a particle down to a radius of 1 nm [29]. DLS is based on the time-dependent measurement of fluctuations in the intensity of the scattered light due to the Brownian motion of the particles, which is faster for smaller particles. Rh can then be calculated via the Stokes–Einstein relation (Equation (2)), with k_b being the Boltzmann constant, T the temperature, η the viscosity of the solution and D_t the diffusion coefficient of the particle [29]:

$$Rh = \frac{k_b * T}{6 * \pi * \eta * D_t} \quad (2)$$

Furthermore, the shape of a particle can be determined using the ratio of Rg and Rh. This is particularly important when analyzing heterogeneous samples comprising analytes of different shapes. Rg/Rh ratios of 0.77, 1 and >1 correspond to uniform spheres, hollow spheres and elongated particles, respectively [34].

Conclusively, IEC-MALS provides a detailed assessment of the biophysical properties of AAVs in heterogenous samples. Compared to SEC, where analytes are separated by their hydrodynamic radius, IEC is capable of chromatographically resolving analytes of the same size (Rh) but different overall charge e.g., empty and full AAV capsids.

Here, we present a novel and robust IEC-MALS method for the characterization and quantification of empty and filled AAV capsids without the need for chromatographic baseline separation of both species prior to sample analysis. Our method provides excellent comparability with AUC and ELISA data. Sample recovery (R%) was between 70 and 100%, which is in line with other methods. Good linearity was obtained by diluting the sample to a capsid titer of 2.0×10^{11} cp mL^{-1} (CV < 5%). Furthermore, multiple sample injections yielded a high precision of the assay with a CV < 5% for capsid titer, hydrodynamic radius, polydispersity, full-to-total ratio, absolute molar mass of protein, nucleic acid and total capsid. In addition, the developed IEC method was applied to three different in-house produced serotypes (AAV5, AAV6 and AAV8) without the need for adapting the method conditions and validated by comparison to orthogonal methods, namely AUC and ELISA.

2. Results and Discussion

For the development of an IEC-MALS method, AAV8 was the serotype of choice as it has been reported by Lock et al., to be separatable into filled and empty capsid populations using ion-exchange chromatography [35]. However, to determine whether an anion-exchange (AEX) or cation-exchange (CEX) column was needed, the isoelectric point of the selected serotype was measured using a capillary isoelectric focusing (cIEF) technique. Because the measured pI was 7.4 (net capsid), a CIMac AAV full/empty analytical column (anion-exchanger) was used for the development of the IEC assay. For sample binding and elution, buffers containing 20 mM Tris (pH 8.5, buffer B) and 20 mM Tris + 120 mM $MgCl_2$ (pH 8.5, buffer E), respectively, were selected. The chromatographic separation was carried out using the gradient described in Supplementary Table S1. Due to the difference in their overall negative charge attributed to the encapsidated nucleic acid, empty AAV capsids elute earlier from the column than filled AAV capsids when increasing the salt concentration of the buffer. For sample detection, the AEX column was coupled to a UV detector, a static and a dynamic light scattering detector, which allowed the determination of the absolute molar masses of the protein and nucleic acid, the hydrodynamic radius, the radius of gyration and the polydispersity of the afore-separated empty and filled AAV capsid fractions. The capsid titer and the full-to-total ratio of the sample are additionally assessed. A schematic overview of an IEC-MALS method is given in Figure 1. Unlike SEC-MALS, which uses the UV absorption and the differential refractive index (dRI) detection for the calculation of the above-mentioned parameters, IEC-MALS demands dual wavelength UV-absorption detection, as an RI detector cannot be used when applying salt gradients due to a change in the refractive index with increasing salt concentration (dn/dc).

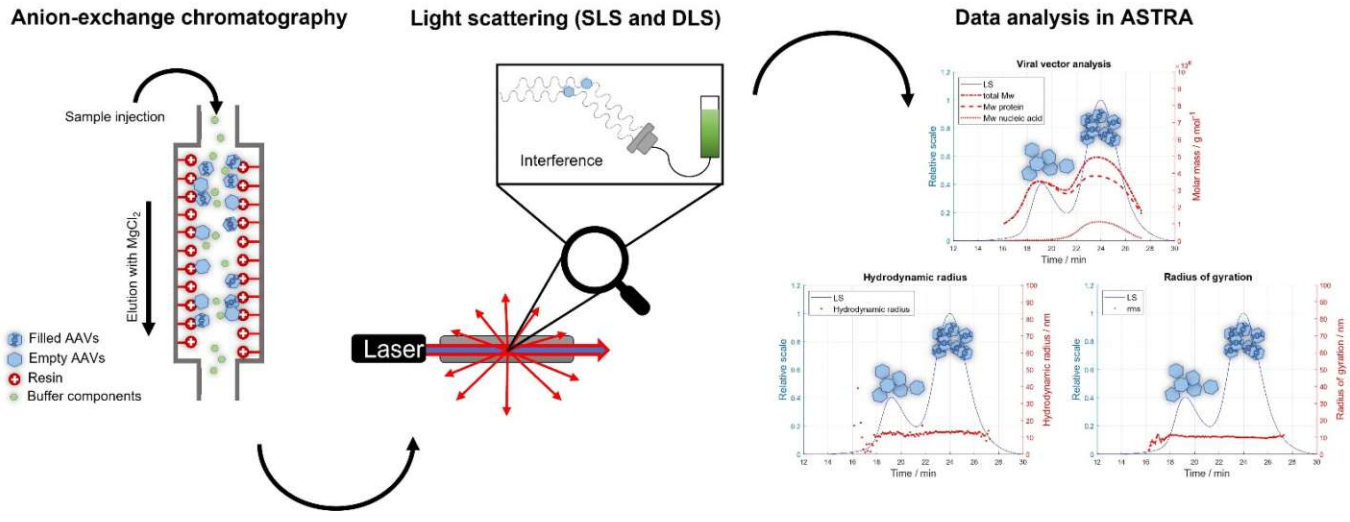

Figure 1. Schematic illustration of the IEC-MALS method. The AAV sample is loaded onto the anion-exchange column, eluted with a salt gradient containing $MgCl_2$ and detected with multi-angle light scattering and UV detectors prior to data analysis using ASTRA software.

2.1. IEC-MALS Development

Like SEC-MALS, IEC-MALS requires the calibration and normalization of the MALS detector prior to sample analysis. Toluene was used as the standard for the calibration of the detector at 90°, while the remaining photodiode detectors were normalized to the 90° detector using bovine serum albumin (BSA), a monodisperse, isotropic scatterer [28]. Because the UV-Vis and light scattering detectors were operated in series, the resulting chromatograms showed shifts in the retention times as the sample is not detected simultaneously. As the sample progresses through the detectors, it becomes more diluted, and broader peaks are observed. To correct for these variations, an alignment and band broadening correction of the UV and LS signals were performed.

2.2. Determination of the UV Extinction Coefficients

The in the software integrated a "viral vector analysis" algorithm allows the calculation of the molecular weights of the total AAV capsid, the proportions of the protein and the transgene, provided that the UV extinction coefficients at 260 and 280 nm of the protein and nucleic acid are known. Because these parameters are specific for each serotype, we experimentally determined the UV extinction coefficients for AAV8 at both wavelengths using ASTRA 8.1 software. Therefore, two samples comprising mostly empty and mostly full AAV8 capsids were measured using an already established SEC-MALS method for the purification of AAV monomers from aggregates. Filled AAV capsids yielded UV extinction coefficients of 14.55 mL (mg cm)$^{-1}$ and 24.65 mL (mg cm)$^{-1}$ at 280 and 260 nm, respectively. Empty AAV capsids yielded UV extinction coefficients of 2.05 mL (mg cm)$^{-1}$ and 1.39 mL (mg cm)$^{-1}$ at 280 and 260 nm, respectively.

2.3. Comparison of %Filled AAV Capsids to Orthogonal Methods

Because AUC is used as the standard analytical technique for the quantification of empty and filled capsids as well as other AAV subspecies, results obtained by IEC-MALS were compared to AUC data regarding the full/empty (F/E) ratio [17,19]. Unlike IEC-MALS, AUC can resolve AAV capsids containing a partial genome from empty and full ones; however, it is a more time-consuming technique with low sample throughput. Another drawback is the need for large sample volumes and high capsid titers [17]. Prompted by this, we developed an IEC-MALS assay which provides a faster and simpler alternative for the determination of the F/E ratio with the advantage of receiving additional information (hydrodynamic radius, radius of gyration, polydispersity and absolute molar mass of protein and nucleic acid) about both AAV populations in one single measurement. Therefore, two AAV8 samples comprising mostly empty (meC) and mostly filled AAV capsids (mfC), respectively, were mixed at different ratios to obtain fractions of various F/E content ranging from 28% to 96% F/E (capsid titers: 1.0×10^{13} cp mL^{-1}). In Figure 2, an excellent linear correlation between data obtained by IEC-MALS (measured %filled) and data generated by AUC (expected %filled) is observed, with a coefficient of determination (R^2) of 0.9968, suggesting that IEC-MALS can be used alternatively for the determination of the F/E ratio. Because ion-exchange chromatography does not provide any information on subpopulations due to a lack of chromatographic resolution, data from AUC for partially-filled and filled particles were added up for the comparison with IEC-MALS data.

2.4. Linearity of the IEC-MALS Method

To test the sensitivity of the IEC-MALS assay, a sample containing an F/E ratio of ~62% was serially diluted covering a concentration range between 1.0×10^{13} cp mL^{-1} and 2.0×10^{11} cp mL^{-1}. Good linearity was obtained when plotting the measured capsid titer against the expected capsid titer determined by ELISA with an R^2 of 0.998 and a CV < 5% (Figure 3a). Sample recovery was between 70–100%. In addition, a linear correlation between the area of the UV signals and the expected capsid titer was observed with a R^2 of 0.999 (Figure 3b). However, at lower sample concentrations, the coefficient of variation exceeded the 5% limit, probably due to the low sensitivity of the LS detector.

Since it is not possible to use neither UV detection at 230 nm (due to other absorbing components in the matrix at that specific wavelength) nor a fluorescence detector (because ASTRA software does not support this instrument in its configuration) as a second concentration detector for the calculations of the molar mass of the nucleic acid or the protein, the sensitivity of the method cannot be improved. Furthermore, ASTRA does not provide information on the signal-to-noise ratio; hence, the LOD and LOQ had to be assessed empirically. In addition, 8.3×10^{10} cp mL^{-1} was the lowest detectable analyte concentration, 2.0×10^{11} cp mL^{-1} was the lowest sample titer, which had been successfully quantified with a CV < 5% and a recovery of 73%. These results are in good agreement with the calculated LOD (8.3×10^{10} cp mL^{-1}) and LOQ (2.5×10^{11} cp mL^{-1}) using the data from Figure 2.

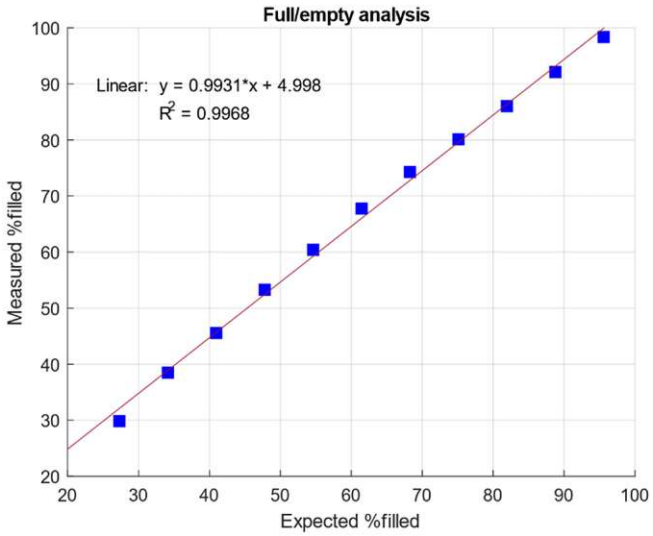

Figure 2. Linear correlation of measured % filled AAV capsids using IEC-MALS and expected % filled AAV capsids by AUC.

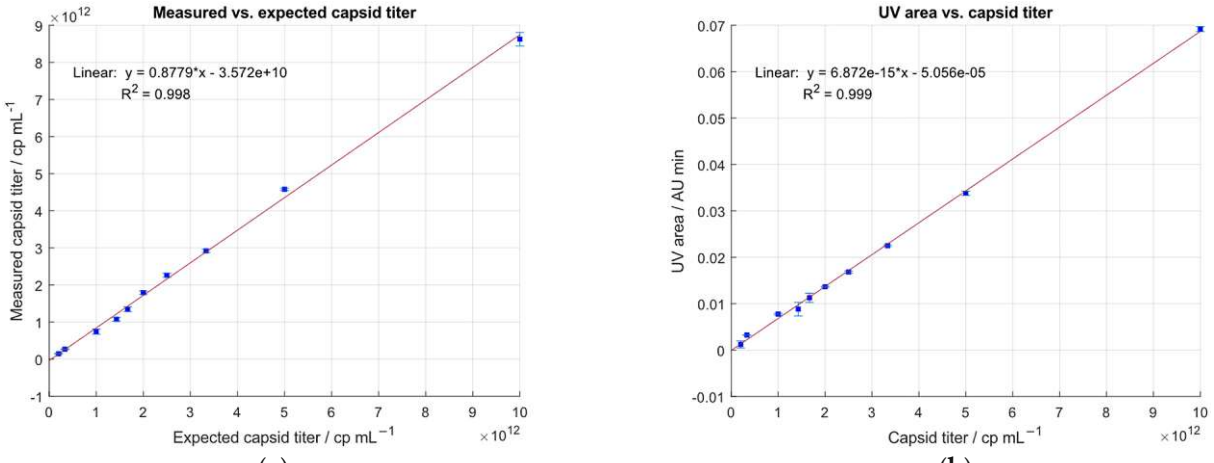

(**a**) (**b**)

Figure 3. Linearity of the developed IEC-MALS method. Plots of expected capsid titers obtained by ELISA vs. (**a**) capsid titer measured with multi-angle light scattering and (**b**) UV area by integration of the UV profiles at 280 nm.

2.5. Robustness of the IEC-MALS Method

To check for the robustness of the optimized IEC-MALS method, different gradients and flow rates were tested with regard to F/E ratio, UV 260/280 ratio, absolute molar masses of the protein, and transgene. Figure 4 shows the obtained chromatograms for the

varied linear gradients and flow rates, respectively. All chromatograms showed two distinct peaks corresponding to empty and filled AAV capsids. When changing the steepness of the salt gradient over the same time period from 0–35% buffer E to 0–45%, 0–55% and 0–65% buffer E using a flow rate of 0.5 mL min^{-1} (Supplementary Table S2), a shift in the retention times is observed. Regardless of whether a flatter ramp (0–35% buffer E) or a steeper gradient (0–65% buffer E) was applied, the calculated results do not differ significantly from one another but match expected values (Table 1). This proves that no baseline separation of empty and full AAV capsids is required prior to data analysis; hence, no further optimization of the developed IEC-MALS method was necessary. In SEC-MALS, however, the influence of the neighboring (aggregate) peak on calculated results of the monomer peak is greater due to the higher molar masses of multimer species impacting the data analysis of the monomers. When analyzing empty and filled AAV capsids, the light scattering intensity of both subspecies is the same; hence, IEC-MALS does not necessarily require baseline-separated empty/full peaks.

Table 1. Overview of IEC-MALS method performance results of empty and full AAV8 capsids obtained by varying the gradient steepness and flow rate of the developed IEC-MALS method.

	Gradient A	Gradient B	Gradient C	Gradient D	Flow Rate 0.5 mL min^{-1}	Flow Rate 0.7 mL min^{-1}	Flow Rate 1.0 mL min^{-1}
Capsid Titer ELISA/cp mL^{-1}	1.00×10^{13}	1.00×10^{13}	1.00×10^{13}	1.00×10^{13}	1.00×10^{13}	1.00×10^{13}	1.00×10^{13}
Measured Capsid Titer/cp mL^{-1}	8.23×10^{12}	8.50×10^{12}	8.35×10^{12}	8.40×10^{12}	8.21×10^{12}	8.75×10^{12}	9.25×10^{12}
RSD/%	1.5	0.3	0.6	0.8	4.3	0.8	0.3
Recovery/%	82	85	84	84	82	88	92
Expected %full	62	62	62	62	62	62	62
Measured %full	66	66	66	67	65	59	59
Difference %full/%	6	6	7	7	5	4	5
Expected Mw Nucleic Acid/kDa	1070	1070	1070	1070	1070	1070	1070
Measured Mw Nucleic Acid/kDa	959	949	956	951	936	904	902
RSD/%	0.1	0.7	0.8	0.7	1.9	0.9	0.1
Difference MW Nucleic Acid/%	10	11	11	11	13	16	16
Measured Mw Protein (Empty)/kDa	3842	3798	3809	3819	3750	3652	3573
RSD/%	1.7	0.5	0.5	0.5	1.0	0.8	0.4
Measured Mw Protein (Full)/kDa	3713	3690	3694	3695	3657	3659	3655
RSD/%	0.3	0.3	0.4	0.3	0.1	0.3	0.0
UV 260/280 Ratio (Empty)	0.69	0.68	0.68	0.65	0.66	0.46	0.74
UV 260/280 Ratio (Full)	1.34	1.32	1.32	1.33	1.34	1.31	1.33

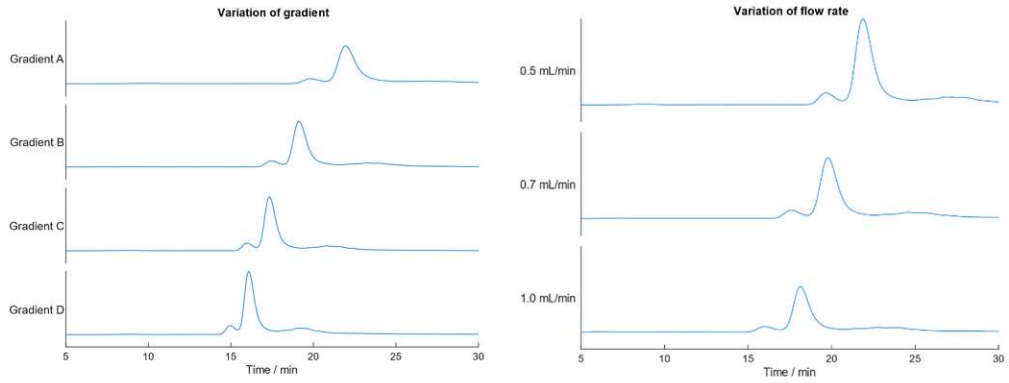

Figure 4. Evaluation of the robustness of the developed IEC-MALS method. (**a**) variation of the linear salt gradient. Gradient A: 0–35% buffer E, gradient B: 0–45% buffer E, gradient C: 0–55% buffer E and gradient D: 0–65% buffer E; (**b**) variation of the flow rate. Flow rates of 0.5 mL min^{-1}, 0.7 mL min^{-1} and 1.0 mL min^{-1} were tested using a linear salt gradient from 0–35% buffer E.

2.6. Application of the IEC-MALS Method to Other Serotpyes

Next, we applied the developed IEC-MALS assay to two different in-house produced serotypes, AAV5 and AAV6. Both serotypes were generated from different downstream process steps, to further prove that the IEC-MALS assay can be applied at different stages of the AAV manufacturing platform. In Figure 5, an overlay of the LS chromatograms and the "viral vector analysis" of AAV5, AAV6 and AAV8 is shown. Results were compared to orthogonal methods, such as AUC and ELISA with respect to full-to-empty ratio and capsid titer, respectively. For the comparison of the measured absolute molar mass of the protein to the expected one, the theoretical ratio (5:5:50, VP1:VP2:VP3) and molar masses (87 kDa (VP1), 73 kDa (VP2) and 62 kDa (VP3)) of the three virus protein subunits in an assembled AAV particle were used to calculate the expected molar mass of the protein [36]. The molar masses of the encapsidated transgenes of the different serotypes were calculated from the 5′-ITR to 3′-ITR of the respective plasmids using SnapGene software 5.1.5 (GSL Biotech LLC, Chicago, IL, USA).

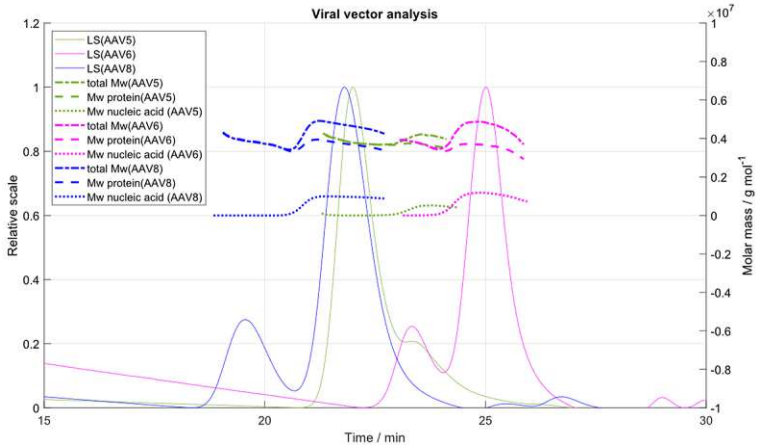

Figure 5. Overlay of the LS chromatograms (solid lines) and molar masses of the total capsid, protein and transgene (dashed lines) of serotypes AAV5 (green), AAV6 (pink) and AAV8 (blue).

For each serotype, two distinct peaks were generated corresponding to the empty and filled AAV populations. Best chromatographic separation of both species was obtained for serotype AAV8, which had been used for the development and optimization of the IEC-MALS assay. Despite the poor peak resolution of serotype AAV5, the measured F/E ratio of ~12% fits well to the expected F/E ratio of 10% (according to AUC). The molar

mass of the protein was lower than the expected theoretical value of ~3.9 MDa; however, more accurate results would have been generated if the exact amino acid composition and the VP ratio of the assembled capsid had been known. This would require a more thorough investigation of the VP stoichiometry of each serotype prior to IEC-MALS analysis and will be investigated in continuing experiments but is beyond the scope of this paper. Because the proportion of the empty AAV capsids of serotype AAV6 was ~24% only (according to AUC), the CV of the measured hydrodynamic radius and radius of gyration was >5% due to a lack of sensitivity of the light scattering detectors. Similar results were obtained for the filled capsid fraction of serotype AAV5 (10% filled capsids) regarding the measured absolute molar mass of the nucleic acid, the hydrodynamic radius and the radius of gyration. For the remaining calculated parameters (capsid titer, full-to-total ratio, polydispersity, absolute molar masses of protein and encapsidated ssDNA), the CV was <5% (see Table 2).

Table 2. Overview of IEC-MALS method performance results of empty and filled AAV8 capsids of different serotypes.

	AAV5	AAV6	AAV8
Capsid Titer ELISA/cp mL^{-1}	6.73×10^{13}	2.12×10^{12}	1.00×10^{13}
Measured Capsid Titer/cp mL^{-1}	6.20×10^{13}	2.28×10^{12}	7.74×10^{12}
RSD/%	3.3	1.4	2.1
Recovery/%	92	107	77
Expected %full	10	68	62
Measured %full	12	66	66
Difference %full/%	15	3	7
Expected Mw Nucleic Acid/kDa	760	1240	1071
Measured Mw Nucleic Acid/kDa	457	1128	970
RSD/%	4.9	1.6	0.9
Difference MW Nucleic Acid/%	40	9	9
Measured Mw Protein (Empty)/kDa	3759	3850	3920
RSD/%	0.8	0.9	1.3
Measured Mw Protein (Full)/kDa	3466	3627	3724
RSD/%	3.1	0.3	0.5
rh (Empty)/nm	12.5	8.4	13
RSD/%	0.3	13.5	2.3
rh (Full)/nm	9	12	14
RSD/%	10.4	0.9	0.5
rms (Empty)/nm	9	8	9
RSD/%	22.4	35.2	11.8
rms (Full)/nm	9	8	8
RSD/%	6.8	13.1	16.4
Polydispersity	1.011	1.040	1.012
RSD/%	1.0	0.3	0.2

2.7. Test of Different Weak and Strong AEX Columns

To evaluate the method performance, the IEC-MALS assay was tested with five different AEX columns of various providers. Comparable results between all AEX columns with respect to hydrodynamic radius, radius of gyration, capsid titer and absolute molar masses of protein and ssDNA were obtained (Figure 6). The CIMac AAv Full/Empty

Analytical Column (BIA Separations, Ljubljana, Slovenia), the ProSwift SAX-1S Column (ThermoFisher Scientific, Waltham, MA, USA) and the UNO Q Polishing Column (BioRad, Hercules, CA, USA) are based on the strong basic nature of quaternary ammonium (QA) groups as counterions for the negatively charged AAVs and are therefore considered as strong anion-exchangers, while the ProSwift WAX-1S Column (ThermoFisher Scientific) and CIMac PrimaS Analytical Column (BIA Separations) are based on multimodal systems that coalesce anion-exchange chromatography and hydrogen bonding interactions. The performance of the UNO Q Polishing Column (BioRad) was diverging most within all five columns regarding the measured F/E ratio, capsid titer and radius of gyration. All other columns yielded comparable results regardless of whether a weak or strong AEX column had been used.

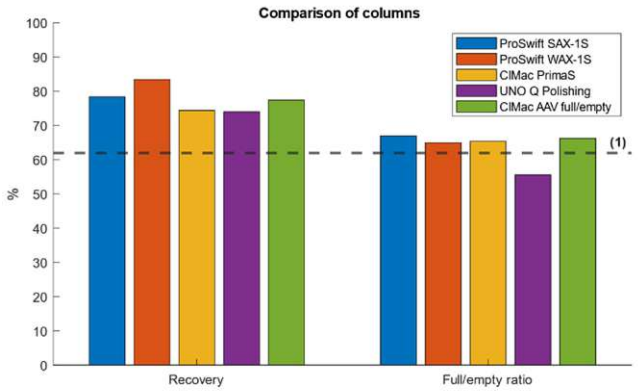

(**a**)

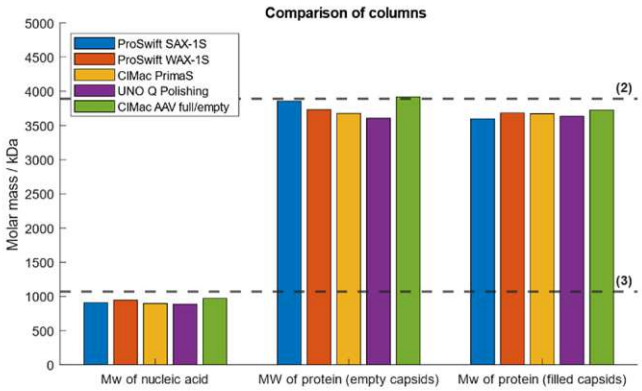

(**b**)

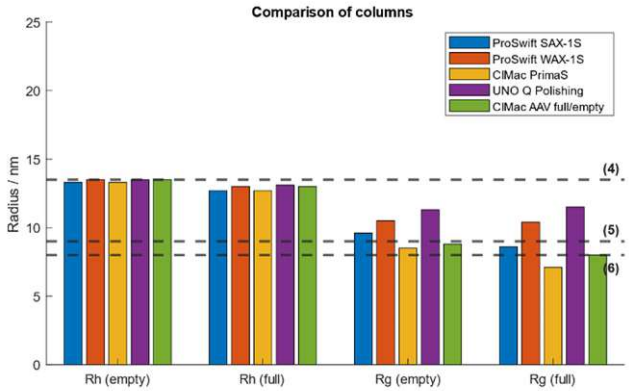

(**c**)

Figure 6. Evaluation of the method performance of the developed IEC-MALS assay using five different anion-exchange columns. The strong AEX columns ProSwift SAX-1S (blue), UNO Q Polishing (purple) and CIMac AAV full/empty (green) and the weak AEX columns ProSwift WAX-1S (orange) and CIMac PrimaS (yellow). Dashed lines (1)–(6) represent (**a**) the expected F/E ratio, (**b**) the absolute molar mass of the protein, the absolute molar mass of the encapsidated ssDNA, (**c**) the hydrodynamic radius, the radius of gyration of empty AAV capsids and the radius of gyration of filled AAV particles, respectively.

2.8. Salt Gradient vs. pH Gradient

Because the application of a pH gradient in combination with a strong AEX column leads to an increase in the interaction of the AAV particles with the QA ligands with rising pH due to the greater overall negative charge of the AAV capsids at high pH, a multimodal system (CIMac PrimaS Analytical Column) was selected for the chromatographic separation

of empty and filled AAV capsids. Therefore, a linear gradient from pH 7 to 10 was used (Supplementary Table S3). As opposed to the pH gradient, the salt gradient yielded higher absolute molar masses of the protein (Table 3). This is probably because of the broad shape of the peaks obtained using the pH gradient (Figure 7), which impacts data analysis. An optimization of the pH gradient conditions, however, would have been out of the scope of this work.

Table 3. Comparison of IEC-MALS method performance results of empty and filled AAV8 capsids obtained by a linear pH gradient and a linear salt gradient.

	pH Gradient	Salt Gradient
Capsid Titer ELISA/cp mL^{-1}	1.00×10^{13}	1.00×10^{13}
Measured Capsid Titer/cp mL^{-1}	9.11×10^{12}	8.87×10^{12}
RSD/%	0.8	1.5
Recovery/%	91	89
Expected %full	62	62
Measured %full	58	68
Difference %full/%	6	9
Expected Mw Nucleic Acid/kDa	1070	1070
Measured Mw Nucleic Acid/kDa	1014	986
RSD/%	0.6	1.1
Difference MW Nucleic Acid/%	5	9
Measured Mw Protein (Empty)/kDa	3359	3802
RSD/%	0.7	1.1
Measured Mw Protein (Full)/kDa	3670	3818
RSD/%	0.3	0.3
UV 260/280 Ratio (Empty)	0.77	0.83
UV 260/280 Ratio (Full)	1.26	1.34

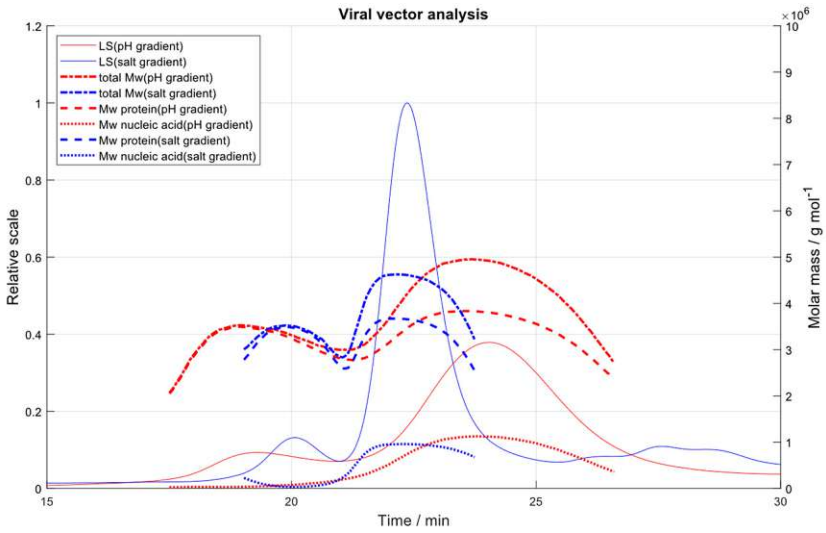

Figure 7. Overlay of the LS chromatograms and "viral vector analysis" of AAV8 obtained by a linear pH gradient (red) or linear salt gradient (blue).

3. Materials and Methods

3.1. Samples and Reagents

Tris (hydroxymethyl) aminomethane (Tris), magnesium chloride hexahydrate ($MgCl_2 \times 6\ H_2O$) and hydrochloric acid (HCl) were purchased from Merck (Darmstadt, Germany). Toluene, BSA and PBS were purchased from Sigma Aldrich (Saint Louis, MO, USA), Thermo Fisher Scientific (Waltham, MA, USA) and Aviva Systems Biology (San Diego, CA, USA), respectively. The binding buffer for the chromatographic separation of empty and filled AAV capsids was prepared by dissolving 20 mM Tris in ultra-purified water (Millipore Purification System, Merck, Darmstadt, Germany) and adjusting to pH 8.5 with 25% HCl. The binding buffer was prepared by dissolving 20 mM Tris and 120 mM $MgCl_2$ in ultra-purified water and adjusting to pH 8.5 with 25% HCl. Both buffers were filtered through a 0.22 µm PES membrane (Steritop Millipore Express PLUS, Merck, Darmstadt, Germany).

The injection volumes of the samples ranged between 10 and 70 µL aiming a total injected mass of ~5–7 µg on the column.

3.2. Instrument Configuration

Analyses were performed on an Agilent HPLC 1260 system (Agilent, Waldbronn, Germany) equipped with a quaternary pump, a degasser, an autosampler and a UV-Vis detector monitoring the absorbance at 260 and 280 nm. In addition, the system was coupled online to a MALS detector (DAWN®, Wyatt Technology, Santa Barbara, CA, USA) with an integrated DynaPro® NanoStar® DLS detector (WyattQELS, Wyatt Technology, Santa Barbara, CA, USA). Prior to sample analysis, the calibration of the MALS detector at a scattering angle of 90° using toluene was carried out, and the remaining scattering angles were normalized to the photodetector at 90° using a monodisperse, isotropic scatterer. Here, we used a solution of 1% BSA (*w*/*v*) in PBS.

For chromatographic separation, CIMac™ AAV full/empty-0.1 Analytical Column was used and compared to four other anion-exchange columns provided by Bio-Rad Laboratories, Herculus, CA, USA (UNO Q Polishing Column), Thermo Fisher Scientific, Waltham, MA, USA (ProSwift™ SAX-1S Column and ProSwift™ WAX-1S Column) and BIA Separations, Ajdovscina, Slovenia (CIMac PrimaS™-0.1 Analytical Column).

Before analyzing the AAV samples, the anion-exchange columns were equilibrated according to the manufacturer's instructions.

3.3. Data Processing

Unlike SEC-MALS, which operates with one eluent only, IEC-MALS requires a gradient for sample elution. Because the ASTRA 8.1 software (Wyatt Technology, Santa Barbara, CA, USA) is restricted to analyses based on one mobile phase only, OpenLAB CDS ChemStation A.02.02 (Agilent, Waldbronn, Germany) had to be additionally used. While the flow rate, the sample injections and the gradient settings were controlled via ChemStation, data analysis was performed with ASTRA 8.1 software solely. This software contains an algorithm ("viral vector analysis"), which is specifically designed for the analysis of virus vectors and provides information on the capsid titer, full-to-empty ratio and molar masses of the protein and encapsidated transgene by using specific input values attributed to the sample e.g., the molecule shape of the analyte (spherical), the extinction coefficients and dn/dc values of the protein and nucleic acid. By combining the sample parameters with light scattering technology and two concentration detectors targeting either the protein or nucleic acid content, the software calculates the above-mentioned sample characteristics using a series of equations, which are described in more detail by Wyatt [22].

4. Conclusions

In this work, we developed a robust and efficient IEC-MALS assay for the characterization and quantification of empty and filled AAV particles with respect to capsid titer, F/E ratio, polydispersity, hydrodynamic radius, absolute molar masses of the protein and the encapsidated transgene. We demonstrated that no baseline separation of the empty

and filled AAV populations is required for calculation of the above-mentioned parameters. Furthermore, the IEC-MALS method is applicable to two other serotypes, AAV5 and AAV6, without the need for adapting method conditions. Results have shown good comparability with orthogonal methods, namely AUC and ELISA, regarding F/E ratio and capsid titer, respectively. Since IEC cannot resolve particles containing truncated versions of the transgene, the measured absolute molar mass of the encapsidated ssDNA can deviate from the expected theoretical value depending on the proportion of the less-filled AAV population in the sample. This should be taken into consideration when interpreting the data. Regardless of this, IEC-MALS provides an alternative analytical technique for the comprehensive characterization of AAV vectors with the advantage of covering a range of various critical quality attributes in one single measurement.

Supplementary Materials: The following supporting information can be downloaded at: https://www.mdpi.com/article/10.3390/ijms232112715/s1.

Author Contributions: Conceptualization, C.W. and M.L.; methodology, C.W. and B.I.; writing—original draft preparation, C.W.; review and editing, B.I., M.L., R.P. and R.B.-G.; supervision, M.L. All authors have read and agreed to the published version of the manuscript.

Funding: Baxalta Innovations GmbH provided all the funding for this research.

Institutional Review Board Statement: Not applicable.

Informed Consent Statement: Not applicable.

Data Availability Statement: Not applicable.

Conflicts of Interest: Authors Christina Wagner, Martin Lemmerer, Bernd Innthaler and Robert Pletzenauer are current full-time employees of Baxalta Innovations GmbH and own company stocks. Ruth Birner-Gruenberger declares no conflict of interest.

References

1. Li, C.; Samulski, R.J. Engineering adeno-associated virus vectors for gene therapy. *Nat. Rev. Genet.* **2020**, *21*, 255–272. [CrossRef] [PubMed]
2. Chandler, R.J.; Sands, M.; Venditti, C.P. rAAV integration and genotoxicity: Insights from animal models. *Hum. Gene Ther.* **2017**, *28*, 4. [CrossRef]
3. Maestro, S.; Weber, N.D.; Zabaleta, N.; Aldabe, R.; Gonzalez-Aseguinolaza, G. Novel vectors and approaches for gene therapy in liver diseases. *JHEP Rep.* **2021**, *3*, 100300. [CrossRef] [PubMed]
4. Aponte-Ubillus, J.; Barajas, D.; Peltier, J.; Bardliving, C.; Shamlou, P.; Gold, D. Molecular design for recombinant adeno-associated virus (rAAV) vector production. *Appl. Microbiol. Biotechnol.* **2018**, *102*, 1045–1054. [CrossRef]
5. Wang, C.; Mulagapati, S.H.R.; Chen, Z.; Du, J.; Zhao, X.; Xi, G.; Chen, L.; Linke, T.; Gao, C.; Schmelzer, A.E.; et al. Developing an Anion Exchange Chromatography Assay for Determining Empty and Full Capsid Contents in AAV6.2. *Mol. Ther.—Methods Clin. Dev.* **2019**, *15*, 257–263. [CrossRef] [PubMed]
6. Oyama, H.; Ishii, K.; Maruno, T.; Torisu, T.; Uchiyama, S. Characterization of Adeno-Associated Virus Capsid Proteins with Two Types of VP3-Related Components by Capillary Gel Electrophoresis and Mass Spectrometry. *Hum. Gene Ther.* **2021**, *32*, 21–22. [CrossRef]
7. Wang, D.; Tai, P.; Gao, G. Adeno-associated virus vector as a platform for gene therapy delivery. *Nat. Rev. Drug Discov.* **2019**, *18*, 358–378. [CrossRef]
8. Wright, F.J. Quality Control Testing, Characterization and Critical Quality Attributes of AAV Vectors Used for Human Gene Therapy. *Biotechnol. J.* **2020**, *16*, 2000022. [CrossRef]
9. Khatwani, S.L.; Pavlova, A.; Pirot, Z. Anion-exchange HPLC assay for separation and quantification of empty and full capsids in multiple adeno-associated virus serotypes. *Mol. Ther.—Methods Clin. Dev.* **2021**, *21*, 548–558. [CrossRef]
10. EU/3/12/1091: Orphan Designation for the Treatment of Beta Thalassaemia Intermedia and Major. Available online: https://www.ema.europa.eu/en/medicines/human/orphan-designations/eu3121091 (accessed on 17 October 2022).
11. FDA Approves First Cell-Based Gene Therapy to Treat Adult and Pediatric Patients with Beta-Thalassemia Who Require Regular Blood Transfusions. Available online: https://www.fda.gov/news-events/press-announcements/fda-approves-first-cell-based-gene-therapy-treat-adult-and-pediatric-patients-beta-thalassemia-who (accessed on 17 October 2022).
12. Wileys, J. Gene Therapy Clinical Trials Worldwide. Available online: https://a873679.fmphost.com/fmi/webd/GTCT (accessed on 14 March 2022).
13. Nam, H.-J.; Lane, M.D.; Padron, E.; Gurda, B.; McKenna, R.; Kohlbrenner, E.; Aslanidi, G.; Byrne, B.; Muzyczka, N.; Zolotukhin, S.; et al. Structure of Adeno-Associated Virus Serotype 8, a Gene Therapy Vector. *J. Virol.* **2007**, *81*, 12260–12271. [CrossRef]

14. Wright, F.J. Product-Related Impurities in Clinical-Grade Recombinant AAV Vectors: Characterization and Risk Assessment. *Biomedicines* **2014**, *2*, 80–97. [CrossRef] [PubMed]
15. Venkatakrishnan, B.; Yarbrough, J.; Domsic, J.; Bennett, A.; Bothner, B.; Kozyreva, O.G.; Samulski, R.J.; Muzyczka, N.; McKenna, R.; Agbandje-McKenna, M. Structure and Dynamics of Adeno-Associated Virus Serotype 1 VP1-Unique N-Terminal Domain and Its Role in Capsid Trafficking. *J. Virol.* **2013**, *87*, 4974–4984. [CrossRef] [PubMed]
16. Rodrigues, G.; Shalaev, E.; Karami, T.; Cunningham, J.; Slater, N.; Rivers, H. Pharmaceutical Development of AAV-Based Gene Therapy Products for the Eye. *Pharm. Res.* **2019**, *36*, 29. [CrossRef]
17. Gimpel, A.L.; Katsikis, G.; Sha, S.; Maloney, A.J.; Hong, M.S.; Nguyen, T.N.T.; Wolfrum, J.; Springs, S.L.; Sinskey, A.J.; Manalis, S.R.; et al. Analytical methods for process and product characterization of recombinant adeno-associated virus-based gene therapies. *Mol. Ther.—Methods Clin. Dev.* **2021**, *20*, 740–754. [CrossRef]
18. McIntosh, N.L.; Berguig, G.Y.; Karim, O.A.; Cortesio, C.L.; De Angelis, R.; Khan, A.A.; Gold, D.; Maga, J.A.; Bhat, V.S. Comprehensive characterization and quantification of adeno associated vectors by size exclusion chromatography and multi angle light scattering. *Sci. Rep.* **2021**, *11*, 3012. [CrossRef] [PubMed]
19. Fu, X.; Chen, W.-C.; Argento, C.; Clarner, P.; Bhatt, V.; Dickerson, R.; Bou-Assaf, G.; Bakhshayeshi, M.; Lu, X.; Bergelson, S.; et al. Analytical Strategies for Quantification of Adeno-Associated Virus Empty Capsids to Support Process Development. *Hum. Gene Ther. Methods* **2019**, *30*, 144–152. [CrossRef]
20. Ye, H. Simultaneous determination of protein aggregation, degradation, and absolute molecular weight by size exclusion chromatography-multiangle laser light scattering. *Anal. Biochem.* **2006**, *356*, 76–85. [CrossRef] [PubMed]
21. Amartely, H.; Avraham, O.; Friedler, A.; Livnah, O.; Lebendiker, M. Coupling Multi Angle Light Scattering to Ion Exchange chromatography (IEX-MALS) for protein characterization. *Sci. Rep.* **2018**, *8*, 6907. [CrossRef]
22. Wyatt, P. Light scattering and the absolute characterization of macromolecules. *Anal. Chim. Acta* **1993**, *272*, 1–40. [CrossRef]
23. Sahin, E.; Roberts, C.J. Size-exclusion chromatography with multi-angle light scattering for elucidating protein aggregation mechanisms. *Methods Mol. Biol.* **2012**, *899*, 403–423. [CrossRef]
24. Weihong, Q.; Mingxi, W.; Yaqing, W.; Ruian, X. Scalable Downstream Strategies for Purification of Recombinant Adeno- Associated Virus Vectors in Light of the Properties. *Curr. Pharm. Biotechnol.* **2015**, *16*, 684–695. [CrossRef]
25. Fekete, S.; Beck, A.; Veuthey, J.-L.; Guillarme, D. Ion-exchange chromatography for the characterization of biopharmaceuticals. *J. Pharm. Biomed. Anal.* **2015**, *113*, 43–55. [CrossRef] [PubMed]
26. Tsonev, L.I.; Hirsh, A.G. Theory and applications of a novel ion exchange chromatographic technology using controlled pH gradients for separating proteins on anionic and cationic stationary phases. *J. Chromatogr. A* **2008**, *1200*, 166–182. [CrossRef]
27. Zhao, H.; Brown, P.H.; Schuck, P. On the Distribution of Protein Refractive Index Increments. *Biophys. J.* **2011**, *100*, 2309–2317. [CrossRef] [PubMed]
28. Some, D.; Amartely, H.; Tsadok, A.; Lebendiker, M. Characterization of Proteins by Size-Exclusion Chromatography Coupled to Multi-Angle Light Scattering (SEC-MALS). *J. Vis. Exp. JoVE* **2019**, *8*, 6907. [CrossRef]
29. Larkin, M.; Wyatt, P. Light scattering techniques and their application to formulation and aggregation concerns. In *Formulation and Process Development Strategies for Manufacturing of a Biopharmaceutica*; Wiley & Sons: New York, NY, USA, 2010; pp. 269–305.
30. Patel, B.A.; Gospodarek, A.; Larkin, M.; Kenrick, S.A.; Haverick, M.A.; Tugcu, N.; Brower, M.A.; Richardson, D.D. Multi-angle light scattering as a process analytical technology measuring real-time molecular weight for downstream process control. *mAbs* **2018**, *10*, 945–950. [CrossRef]
31. TOSOH Corporation. Light Scattering for Determination of Molecular Weight and Radius of Gyration. *[White Paper]*. 2022. Available online: https://www.separations.eu.tosohbioscience.com/OpenPDF.aspx?path=~{}/File%20Library/TBG/Products%20Download/Whitepaper/w20i16a.pdf (accessed on 7 June 2022).
32. Gagnon, P.; Goricar, B.; Mencin, N.; Zvanut, T.; Peljhan, S.; Leskovec, M.; Strancar, A. Multiple-Monitor HPLC Assays for Rapid Process Development, In-Process Monitoring, and Validation of AAV Production and Purification. *Pharmaceutics* **2021**, *13*, 113. [CrossRef]
33. Porterfield, J.Z.; Zlotnick, A. A simple and general method for determining the protein and nucleic acid content of viruses by UV absorbance. *Virology* **2010**, *407*, 281–288. [CrossRef]
34. Some, D.; Johann, C. Characterization of Nanopharmaceuticals with Field-Flow Fractionation and Light Scattering (FFF-MALS-DLS). *[White Paper]*. Available online: https://www.controlledreleasesociety.org/news/characterization-nano-pharmaceuticals-field-flow-fractionation-and-light-scattering-fff-mals (accessed on 7 June 2022).
35. Lock, M.; Alvira, M.R.; Wilson, J.M. Analysis of Particle Content of Recombinant Adeno-Associated Virus Serotype 8 Vectors by Ion-Exchange Chromatography. *Hum. Gene Ther. Methods* **2012**, *23*, 56–64. [CrossRef]
36. Rose, J.A.; Maizel, J.V.; Inman, J.K.; Shatkin, A.J. Structural Proteins of Adenovirus-Associated Viruses. *J. Virol.* **1971**, *8*, 766–770. [CrossRef]

Supplemental Information

Biophysical Characterization of Adeno-Associated Virus Vectors Using Ion-Exchange Chromatography Coupled to Light Scattering Detectors

Christina Wagner, Bernd Innthaler, Martin Lemmerer, Robert Pletzenauer and Ruth Birner-Gruenberger

Supplementary Table S1: Chromatographic separation method using an AEX column and salt gradient with a flow rate of 0.5 mL/min (B = binding buffer, 20 mM Tris, pH 8.5; E = elution buffer, 20 mM Tris + 120 mM $MgCl_2$, pH 8.5).

Time	Salt gradient	
	%B	%E
0	100	0
2	100	0
27	65	35
28	0	100
32	0	100
32.1	100	0
45	100	0

Supplementary Table S2: Chromatographic separation methods for the determination of the robustness using an AEX column and salt gradients A-D and a flow rate of 0.5 mL/min (B = binding buffer, 20 mM Tris, pH 8.5; E = elution buffer, 20 mM Tris + 120 mM $MgCl_2$, pH 8.5).

Time	Gradient A		Gradient B		Gradient C		Gradient D	
	%B	%E	%B	%E	%B	%E	%B	%E
0	100	0	100	0	100	0	100	0
2	100	0	100	0	100	0	100	0
27	65	35	55	45	45	55	35	65
28	0	100	0	100	0	100	0	100
32	0	100	0	100	0	100	0	100
32.1	100	0	100	0	100	0	100	0
45	100	0	100	0	100	0	100	0

Supplementary Table S3: Chromatographic separation methods using an AEX column and salt gradient (B = binding buffer, 20 mM Tris, pH 8.5; E = elution buffer, 20 mM Tris + 120 mM $MgCl_2$, pH 8.5) or pH gradient (B = binding buffer, 20 mM Tris + 10 mM $MgCl_2$ pH 7; E = elution buffer, 20 mM Tris + 10 mM $MgCl_2$, pH 10) with a flow rate of 0.5 mL/min.

Time	Salt gradient		Time	pH gradient	
	%B	%E		%B	%E
0	100	0	0	100	0
2	100	0	2	100	0
27	65	35	32	0	100
28	0	100	36	0	100
32	0	100	36.1	100	0
32.1	100	0	49	100	0
45	100	0			

International Journal of
Molecular Sciences

MDPI

Article

Quantification of Empty, Partially Filled and Full Adeno-Associated Virus Vectors Using Mass Photometry

Christina Wagner [1], Felix F. Fuchsberger [2,*], Bernd Innthaler [2], Martin Lemmerer [1] and Ruth Birner-Gruenberger [3]

[1] Analytical Development Europe, Takeda Vienna, 1220 Vienna, Austria
[2] Gene Therapy Process Development Europe, Takeda Orth an der Donau, 2304 Orth an der Donau, Austria
[3] Institute of Chemical Technologies and Analytics, Technische Universität Wien, 1040 Vienna, Austria
* Correspondence: felix.fuchsberger@takeda.com

Abstract: Adeno-associated viruses (AAV) are one of the most commonly used vehicles in gene therapies for the treatment of rare diseases. During the AAV manufacturing process, particles with little or no genetic material are co-produced alongside the desired AAV capsid containing the transgene of interest. Because of the potential adverse health effects of these byproducts, they are considered impurities and need to be monitored carefully. To date, analytical ultracentrifugation (AUC), transmission electron microscopy (TEM) and charge-detection mass spectrometry (CDMS) are used to quantify these subspecies. However, they are associated with long turnaround times, low sample throughput and complex data analysis. Mass photometry (MP) is a fast and label-free orthogonal technique which is applicable to multiple serotypes without the adaption of method parameters. Furthermore, it can be operated with capsid titers as low as 8×10^{10} cp mL^{-1} with a CV < 5% using just 10 µL total sample volume. Here we demonstrate that mass photometry can be used as an orthogonal method to AUC to accurately quantify the proportions of empty, partially filled, full and overfull particles in AAV samples, especially in cases where ion-exchange chromatography yields no separation of the populations. In addition, it can be used to confirm the molar mass of the packaged genomic material in filled AAV particles.

Keywords: adeno-associated virus vectors; partially filled particles; single-molecule mass photometry; genomic cargo; analytical ultracentrifugation

Citation: Wagner, C.; Fuchsberger, F.F.; Innthaler, B.; Lemmerer, M.; Birner-Gruenberger, R. Quantification of Empty, Partially Filled and Full Adeno-Associated Virus Vectors Using Mass Photometry. *Int. J. Mol. Sci.* **2023**, *24*, 11033. https://doi.org/10.3390/ijms241311033

Academic Editor: Angela Di Capua

Received: 23 May 2023
Revised: 19 June 2023
Accepted: 24 June 2023
Published: 3 July 2023

1. Introduction

Recombinant adeno-associated virus (rAAV) vectors are one of the leading transport vehicles for the introduction of foreign genetic material in vivo to treat severe and rare diseases in patients. The reason for this lies in the characteristics of rAAV vectors, which stand out by their non-pathogenicity, low immunogenicity and long-term gene expression [1–3]. The vast variety of serotypes allows the targeting of specific types of tissues and cells. Furthermore, genetically engineered variants of rAAV vectors to overcome immunological barriers become more attractive and expand the gene therapy portfolio [4]. The high potential of rAAVs in human gene therapy is mirrored in the great number of clinical trials which are currently being investigated worldwide [5]. In addition, three AAV-based and one lentivirus-based gene therapeutics have been approved by the US Food and Drug Administration (FDA) or the European Medicines Agency (EMA) and are commercially available [6–8].

AAVs are members of the *Parvoviridae* family and belong to the genus *Dependoparvovirus* [4]. For efficient replication, they require a helper virus, such as Adenovirus (AV) or Herpes Simplex Virus (HSV) [9,10]. The non-enveloped, icosahedral AAV capsid is made up of 60 protein monomers, which can be grouped into three viral protein isoforms: VP1, VP2 and VP3, occurring in a proportion of 5:5:50 [11]. VP1, VP2 and VP3 share a common region, which is defined as VP3. The latter represents the shortest protein

sequence variant with the lowest molecular weight of 62 kDa. VP1, the longest protein sequence variant, comprises VP2 and differs from VP2 by an N-terminal extension. VP1 and VP2 have molar masses of 87 kDa and 73 kDa, respectively [12–14]. The cargo capacity of the virus is limited to a single-stranded DNA of ~4.7 kb, which is less than for other gene delivery vehicles, such as AV or HSV, which encapsulate double-stranded DNA up to ~8 kb and ~40 kb, respectively [15,16]. To date, there are 13 different AAV serotypes varying in their cellular tropisms due to differences in the capsid surface as a consequence of capsid assembling [17].

During the manufacturing process of AAVs, numerous capsids either lacking genetic cargo (empty), containing truncated versions of the transgene (partially filled) or encapsulating genetic material beyond 4.7 kb (overfill) are co-produced next to the desired AAV vectors loaded with the intact genome of interest (full). Empty, partially filled and overfilled capsids in the final drug product pose a potential risk to the patient and are considered impurities [18,19]. Therefore, it is of high priority to carefully monitor and remove these unwanted byproducts. While the ratio of empty-to-full capsids can be determined easily using, e.g., ion-exchange chromatography in combination with UV detection at 260 and 280 nm, the proportions of partially filled or overfilled particles remain unknown due to the limited resolution of the chromatography system. To date, these subspecies are assessed using analytical ultracentrifugation (AUC), charge-detection mass spectrometry (CDMS) or transmission electron microscopy (TEM). Despite being frequently used in the biopharmaceutical industry, these analytical platforms lack low turnaround times and high sample throughput [20–22]. In addition, AUC demands large quantities of purified samples of ~500 µL and genome titers up to 5×10^{12} vg mL^{-1} [23]. Compared to AUC, CDMS is less time-intensive (2 h instead of 6 h), but the technique is still in development [21]. Furthermore, CDMS requires specialized equipment and well-trained personnel [23].

Mass photometry provides a faster and more straightforward analysis of AAV subspecies by single-molecule counting. It allows the determination of the full-empty ratio (F/E), the molecular weight of empty and filled AAV capsids as well as the mass of the encapsulated genetic material. Moreover, it can resolve and quantify partially filled and overfilled particles. It does not require any laborious sample preparation, including labelling or immobilization of the analyte [24,25]. Equipped with a robotic arm, the MP can be operated as an automated instrument, facilitating analysis of large sample numbers, which provides MP with a tremendous advantage over orthogonal analytical methods, such as AUC, CDMS or TEM. The principle is based on the interference of light scattered by particles reversibly attaching to a microscope glass slide and light reflected by the cover glass. At the interface between the solid cover slide and the sample liquid, a difference in the contrast between empty and filled particles is observed when binding to the glass surface [26]. The intensity of scattered light is directly proportional to the molar mass of the particle [27].

Here we present a simple alternative analytical technique to AUC with no sample preparation for the quantification of empty, partially filled, filled and overfull AAV capsids using minimal sample volumes of 10 µL and capsid titers around 1.0×10^{11} cp mL^{-1}. Furthermore, the single molecule events-based approach allows the determination of the molecular weight of the genomic cargo of an AAV product at different stages of AAV manufacturing. It provides excellent comparability with AUC data and good linearity of capsid titers between 4×10^{10} cp mL^{-1} and 8×10^{11} cp mL^{-1}. Multiple measurements yielded high precision of the method with a CV < 5% for the calculated molecular weight of the incorporated transgene. Furthermore, we show that this technique is applicable to different serotypes (AAV5, AAV8 and AAV9) without any method adaptation.

2. Results and Discussion

To assess the F/E ratio of an AAV sample, ion exchange chromatography (IEC) combined with UV detection is usually the method of choice. However, the separation of AAV9 capsids using a previously published IEC method coupled to light scattering detectors [28]

was not satisfactory, as full and empty species overlapped, probably due to structural changes of the capsid compared to other serotypes. The charge difference between empty and filled AAV vectors is not significant enough to allow a separation of both species, regardless of whether a cation- or anion-exchange approach had been used. Hence, mass photometry provides a simple and fast alternative to quantify both populations in a sample. Additional information on subspecies, like particles containing truncated versions of the genome, is obtained. Compared to IEC, MP requires 5–10 µL of sample, which is one-tenth of the volume used for IEC, omits the need for eluents and is a non-destructive method. In addition, analysis times are reduced to 1–2 min on the mass photometer as opposed to an average 30-min gradient for IEC. A schematic overview of an MP measurement is given in Figure 1. In mass photometry, each event is registered by the instrument, where the intensity of the scattered light is directly proportional to the mass of a capsid [27].

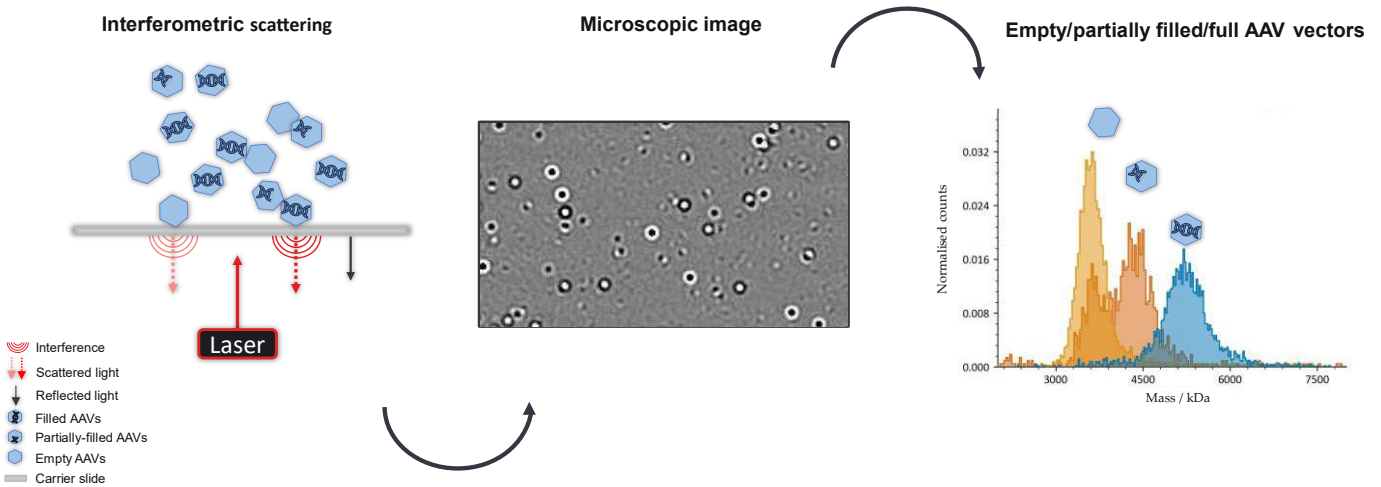

Figure 1. Schematic illustration of a mass photometry measurement. The attachment and detachment of AAVs onto a glass slide result in an interferometric light scattering at the solid–liquid interface. Full and empty particles are visualized in the microscopic image, where white and black circles represent filled and empty AAVs, respectively.

In order to ensure accurate results, clean and dust-free glass slides are required. When reusing microscope coverslips, they were cleaned thoroughly with isopropanol and distilled water before drying them properly with a clean nitrogen stream. Figure 2 depicts the native images of the solid–liquid interface before and after cleaning the glass surface. Furthermore, each sample was diluted prior to measurement to avoid overcrowded microscope images (Figure 2), resulting in lower binding count rates and potential incorrect quantification of AAV vector subpopulations.

2.1. Comparison of % Filled AAV Capsids by Orthogonal Methods

AUC is an orthogonal analytical method to MP for the quantification of empty, partially filled, full and overfull particles. It is based on the different sedimentation velocities of the previously mentioned AAV subpopulations under strong gravitational force due to differences in their size, density, weight and shape [29]. While empty capsids sediment with a sedimentation coefficient (S) between 60 and 64 S, full capsids do so around 100 S. Partially filled AAVs are found in between empty and full populations, while overfilled particles sediment the fastest, hence, have the largest sedimentation coefficient [30]. Consequently, AUC can be applied to confirm the F/E ratio of an AAV sample determined with mass photometry. On the downside, AUC demands large sample volumes and high capsid titers and has low turnaround times and sample throughput [23]. Prompted by this, we implemented mass photometry in our analytics portfolio as a fast and straightforward orthogonal method that provides insight into the homogeneity of an AAV sample.

Therefore, two AAV9 samples comprising mostly empty (meC) and mostly filled AAV capsids (mfC), respectively, were mixed at different ratios to obtain fractions of different F/E ratios ranging from 21% to 86% F/E (capsid titers: ~2 × 10^{11} cp mL^{-1}). Obtained results are depicted in Figure 3. An excellent linear correlation between MP data (measured % filled) and AUC data (expected % filled) with a coefficient of determination (R^2) of 0.9949 is observed. This indicates that mass photometry provides a reliable alternative analysis method for the assessment of the F/E ratio.

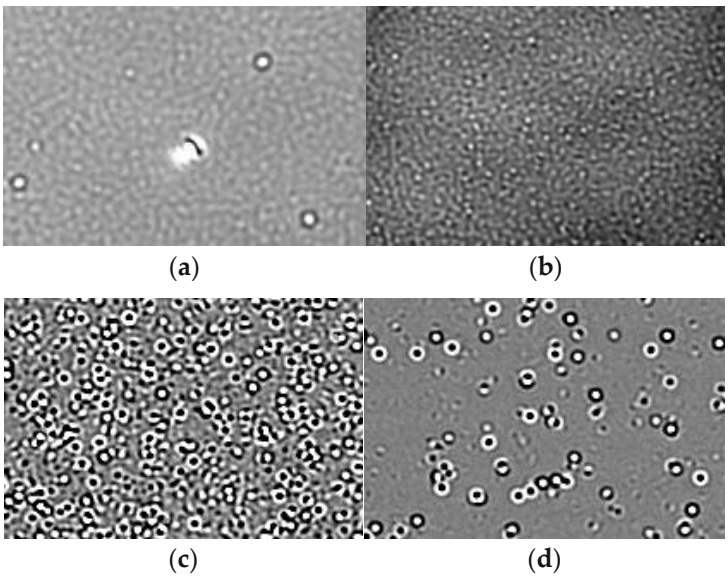

Figure 2. Native microscope images of the solid–liquid interface (**a**) before and (**b**) after cleaning with isopropanol, (**c**) overcrowded with and (**d**) containing an adequate number of AAV particles.

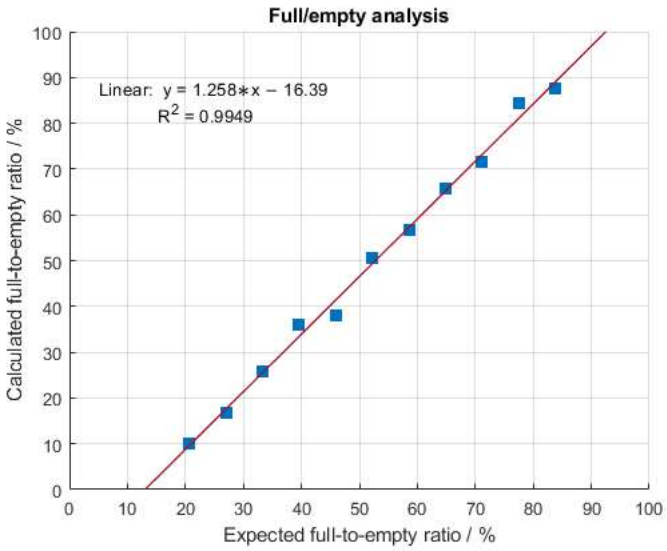

Figure 3. Linear correlation of the measured percentage-filled AAV capsids using mass photometry and expected percentage-filled AAV capsids by AUC.

2.2. Linearity of the Mass Photometer

To assess the sensitivity of the MP, a serial dilution of a sample comprising 1.4% empty, 1.1% partially filled, 86.1% full and 11.4% overfull AAV particles (according to AUC) was conducted, covering a concentration range between 5 × 10^{12} cp mL^{-1} and 4 × 10^{10} cp mL^{-1} (according to ELISA). According to MP manufacturer Refeyn Ltd. (Oxford, UK), 20 µL of a sample with 1 × 10^{11} cp mL^{-1} is the optimal concentration [31]. If

the capsid titer is too high, the microscopic image is overcrowded with AAV particles binding and unbinding from the glass slide (Figure 2). The instrument cannot resolve the single events, and a decrease in the binding counts will be observed, jeopardizing the calculations of the molecular weight and the quantification of the proportions of the AAV subpopulations. We have confirmed this concentration-dependent behavior with capsid titers $\geq 2.5 \times 10^{12}$ cp mL^{-1}. Figure 4 demonstrates the correlation of the binding count rate with increasing sample concentration. Linearity was observed between 4×10^{10} cp mL^{-1} and 8×10^{11} cp mL^{-1}. Despite not being advised by Refeyn Ltd., we have shown that binding count rates < 1000 (60 s recording time) also were suitable for the determination of the molar mass and F/E ratio with relative standard deviations (RSD) < 6% and errors < 9%. Each dilution was measured in triplicates; however, the binding count rates between the measurements fluctuated quite significantly, capturing the limitations of the instrument. If the counting of the single events were highly reproducible throughout multiple measurements of one sample, it would be possible to determine the capsid titer. Hence, the error bars were omitted in Figure 4. Since mass photometry is based on the detection of single events, the LOD stands and falls with the detection of one single particle, e.g., strongly diluted samples that result in a single measured event. However, we need a significant amount of binding events to determine a F/E ratio. The LOQ was found to be 1.8×10^{11} cp mL^{-1} and was calculated using data from Figure 4. Empirically, 8×10^{10} cp mL^{-1} was the lowest analyte concentration, which allowed the calculation of the molar mass and the quantification of the subpopulations with a CV < 5%.

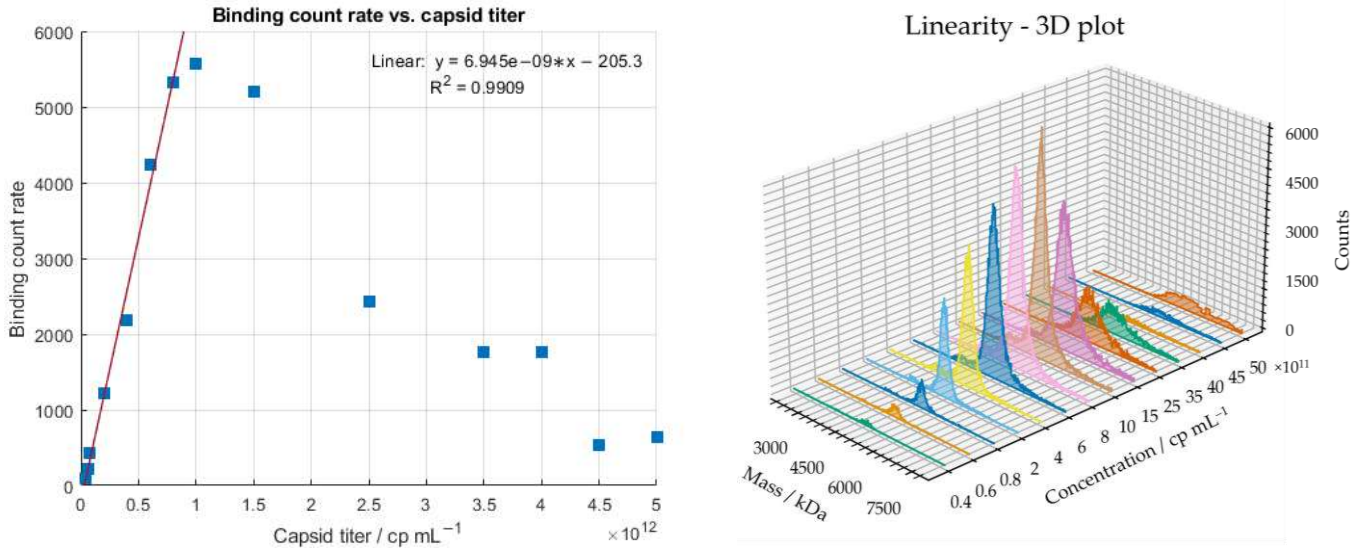

(**a**) (**b**)

Figure 4. (**a**) Linear correlation between binding count rate and capsid titer (determined with ELISA) for sample concentrations between 4×10^{10} cp mL^{-1} and 8×10^{11} cp mL^{-1}. Sample concentrations $\geq 2.5 \times 10^{12}$ cp mL^{-1} result in a significant decrease in the binding count rates. (**b**) 3D plot of measured dilutions.

2.3. Precision of the Mass Photometer

The precision of the MP was tested by measuring an AAV9 sample purified with affinity chromatography (~33% empty, ~6% partially filled, ~52% full and ~8% overfull AAV particles) five times on three consecutive days to additionally check for the impact of repetitive three freeze–thaw (FT) cycles on the AAV integrity. The results show that no significant impact of the FT cycles on the vector integrity was observed regarding the molecular weight of the empty and full AAV species. The average transgene size of 1.45 MDa matches the expected transgene size of 1.40 MDa with an RSD of 2.5% and an error of 3.3% (Table 1). In addition, the measured proportions of the AAV subpopulations are in good agreement with the AUC data. Compared to AUC data, MP underestimates

the overfilled AAV populations; however, this trend was consistent for all repetitive measurements (Table 2). A third orthogonal method could be used to confirm the percentage of overfull AAV particles, but this is out of the scope of this study.

Table 1. Determination of the molar masses of empty and filled subpopulations and confirmation of the transgene size. Data was obtained by five repetitive measurements of an AAV9 sample (~33% empty, ~6% partially filled, ~52% full, and ~8% overfull AAV particles) on three consecutive days (days 1–3).

	Empty AAVs		Full AAVs						
	Average Mass/kDa	RSD/%	Average Mass/kDa	RSD/%	Calculated Transgene Size/kDa	Average Transgene Size/kDa	RSD/%	Expected Transgene Size/kDa	Error/%
Day 1	3583	2.2	4987	2.2	1405				
Day 2	3746	0.9	5217	0.9	1471	1447	2.5	1400	3.3
Day 3	3789	1.3	5253	1.3	1464				

Table 2. Determination of the AAV subpopulations of an AAV9 sample comprising ~33% empty, ~6% partially filled, ~52% full, and ~8% overfull particles. The sample was measured five times on three consecutive days (days 1–3). The obtained results were compared to AUC data. E, PF, F and OF stand for empty, partially filled, full and overfull, respectively.

	MP								AUC			
	Average E/%	RSD/%	Average PF/%	RSD/%	Average F/%	RSD/%	Average OF/%	RSD/%	E/%	PF/%	F/%	OF/%
Day 1	39.7	5.4	7.1	8.7	49.7	2.2	3.5	9.8				
Day 2	40.0	6.8	8.8	9.8	47.8	8.6	2.8	5.4	33.1	6.3	52.3	8.4
Day 3	40.4	3.8	8.3	1.8	48.1	3.1	2.3	8.7				

2.4. Measurement of Different Serotypes

Since mass photometry is insensitive to the size and shape of detected particles [24,25], it is applicable to various serotypes without adaptation of the instrument configurations. To confirm this, we tested three in-house produced serotypes, AAV5, AAV8 and AAV9. Figure 5 illustrates the variations between the detected masses of the three serotypes. Results were compared with AUC data (Figure 6) with respect to the proportion of the subpopulations (% empty, partially filled, full and overfull). Because of the differences in the genetic cargo of each serotype, the AAV limits had to be set individually. Therefore, samples comprising meC and mfC were selected for each serotype to pre-define the limits of the "empty" and "full" AAV capsid fractions. The mass difference between "empty" and "full" was specified as "partially filled". Masses beyond "full" were classified as "overfull". Figure 6 shows that mass photometry agrees well with data obtained by AUC regardless of which serotype (AAV5, AAV8, AAV9) had been used. The percentage of partially filled capsids of AAV8 and AAV9 was accurately captured by the MP, while the percentages of overfilled capsids for AAV5 and AAV9 were slightly underestimated. Nevertheless, obtained results agree well with AUC data highlighting the potential of mass photometry to accurately determine the AAV subpopulations in an AAV sample, regardless of which serotype had been used.

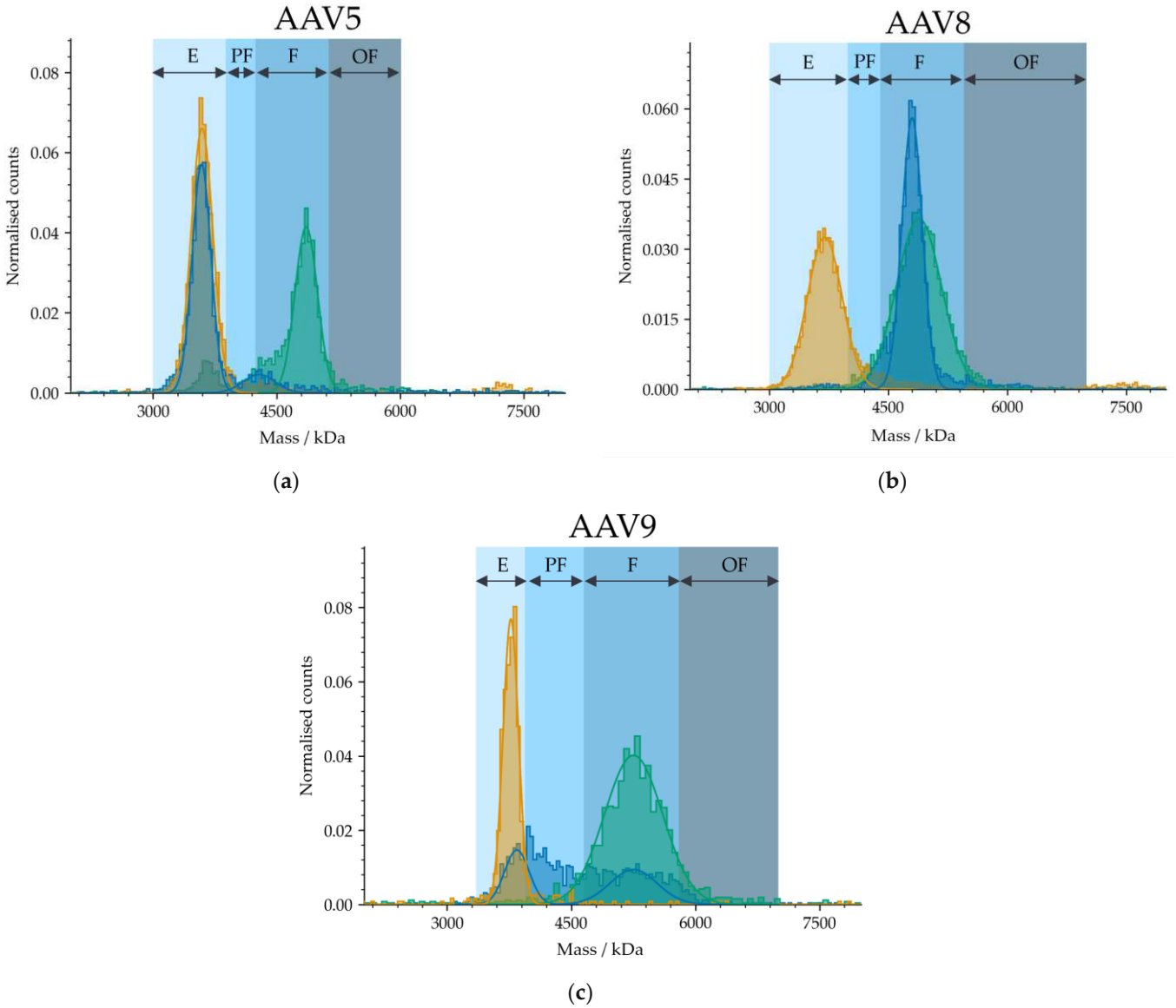

Figure 5. The mass distributions of three AAV serotypes ((**a**) AAV5, (**b**) AAV8, and (**c**) AAV9) comprising different proportions of AAV subpopulations. E, PF, F and OF stand for empty, partially filled, full and overfull, respectively. Samples comprising meC (orange) and mfC (green), respectively, were selected for each serotype to set the AAV limits for the analysis of an AAV sample (blue).

2.5. Confirmation of Transgene Size

To further test the performance of the instrument, three in-house produced AAV9 vectors differing in the size of their encapsulated genomic cargo were measured. The molar mass of the nucleic acid of each AAV9 vector was calculated from the 5′-ITR to the 3′-ITR of the respective plasmid using SnapGene software 5.1.5 (GSL Biotech LLC, Chicago, IL, USA) and compared to the calculated transgene sizes determined with MP. The results in Table 3 confirm that MP allows differentiating between AAV vectors with similar transgene sizes. AAV9_a, AAV9_b, and AAV9_c contained transgenes with decreasing sizes ranging from 1400 kDa to 1370 kDa and 890 kDa, respectively (according to SnapGene software). Serotype AAV9_a showed the highest deviation of the calculated transgene size (MP) from the expected one (SnapGene) with an error of 7.4%. In the case of the shortest encapsulated transgene, MP agrees well with the expected data with an error of 0.0%. The capability to distinguish between transgenes of 890, 1370 and 1400 kDa can be attributed to the high resolution of the instrument. As opposed to SEC-MALS, which can also be used for the

confirmation of the transgene size, MP does not require any knowledge of the analyte prior to measurement, e.g., the molar extinction coefficient of the nucleic acid. Furthermore, MP provides results within one minute only and does not demand any method of development, omitting long turnaround times as in the case of SEC-MALS.

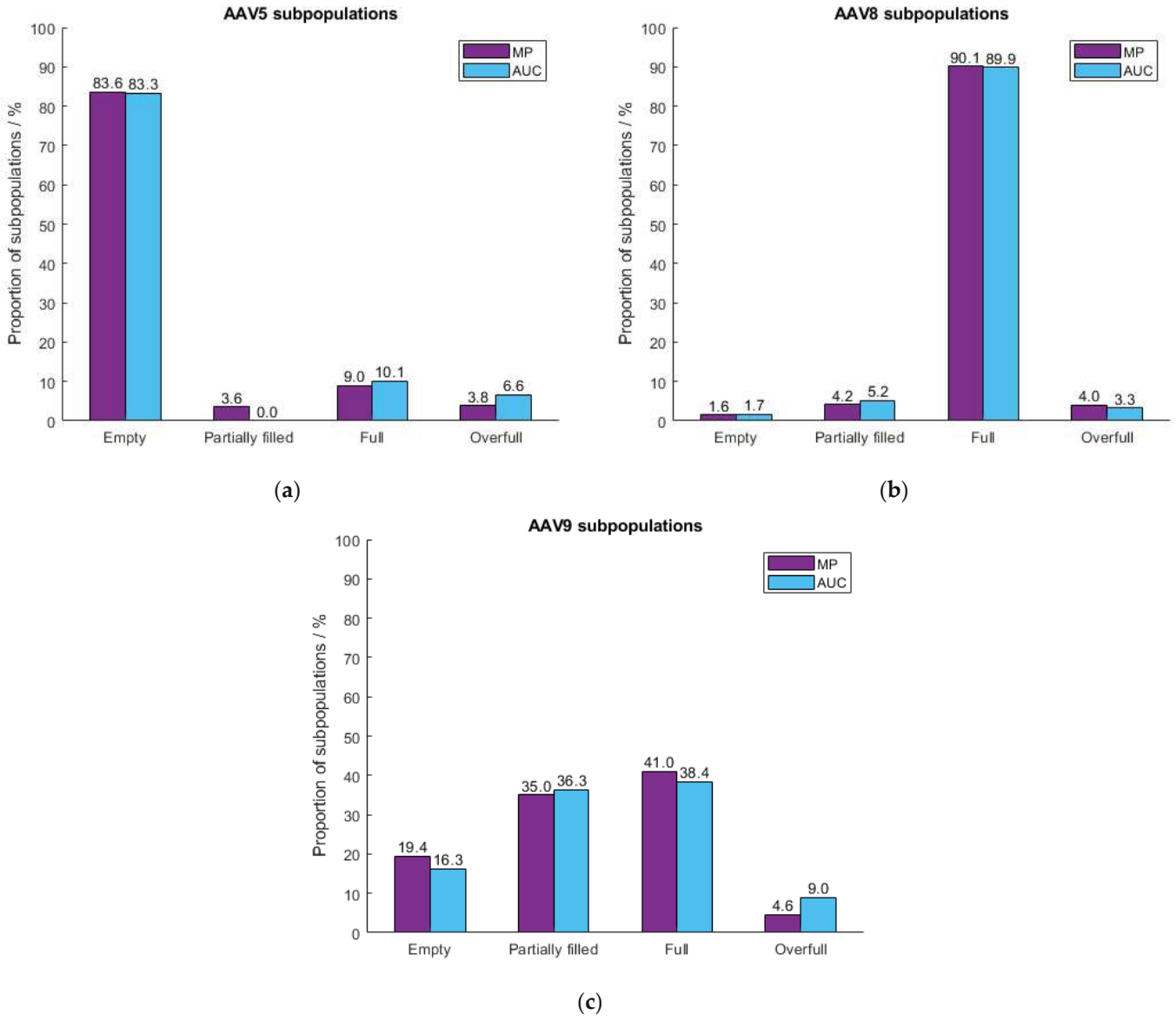

Figure 6. Evaluation of the MP performance using three different in-house produced serotypes (**a**) AAV5, (**b**) AAV8 and (**c**) AAV9. Obtained MP results (purple) were compared to the AUC data (blue).

Table 3. Comparison of three in-house-produced AAV9 vectors differing in their genomic cargo (a, b, and c).

Serotype	Empty AAVs/kDa	Full AAVs/kDa	Calculated Transgene Size/kDa	Expected Transgene Size/kDa	Error/%
AAV9_a	3750	5253	1503	1400	7.4
AAV9_b	3992	5319	1327	1370	3.1
AAV9_c	3754	4644	890	890	0.0

3. Materials and Methods

3.1. Sample Preparation

HPLC-grade phosphate-buffered saline (PBS) was purchased from Sigma Aldrich (Saint Louis, MO, USA). AAV samples were produced in-house. Isopropanol, which is used for cleaning the silicon sample gaskets and the glass slides, was obtained from Merck (Darmstadt, Germany). "Empty" AAV9 and Thyroglobulin (TG), which function as calibrants, were purchased from Progen (Heidelberg, Germany) and Sigma Aldrich (Saint Louis, MO, USA), respectively. "Empty" was used in a final concentration of 3.3×10^{11} cp mL^{-1}, TG at a final concentration of ~100 µg mL^{-1}. Samples were prediluted with PBS and further diluted 1:2 in the well of the silicon gasket (Refeyn Ltd., Oxford, UK) installed in the instrument. The final concentrations of the measured samples ranged between 8×10^{10} and 2×10^{11} cp mL^{-1}. No sample preparation was required; however, the samples should not contain major impurities.

3.2. Measurements and Experimental Setup

The AUC measurements were performed at 15,000 rpm and 18 °C on a Beckman AUC Optima instrument (Beckman Coulter, Brea, CA, USA) equipped with an An-50 Ti analytical rotor (Beckman Coulter, Brea, CA, USA) using a total number of 150 scans per sample. The MP measurements were carried out on the SamuxMP instrument (Refeyn Ltd., Oxford, UK). Compared to previous devices such as OneMP and TwoMP, the SamuxMP features a higher resolution tailored especially for the analysis of AAV vectors. The cover glasses and the silicon gaskets containing six sample wells were purchased from Refeyn Ltd. (Oxford, UK). Prior to each measurement a calibration was conducted using the "empty" AAV9 vector (3.74 MDa) and TG (670 kDa). The molar mass of the "empty" AAV9 had been determined by CDMS and was provided by Progen (Heidelberg, Germany). For the generation of the calibration curve, 10 µL of PBS was pipetted into the well of the sample cassette before automatically adjusting the focus and adding 10 µL of AAV9 calibrant to the loaded PBS by mixing it vigorously. The measurement time was set to 60 s resulting in the acquisition of a movie visualizing the binding and unbinding events. The calibrant was measured twice, and the results of both measurements were merged into one calibrant mass. Thyroglobulin was measured under the same conditions as the AAV9 calibrant.

3.3. Data Collection and Processing

The measurements were recorded for 60 s using AcquireMP 2.4.2 (Refeyn Ltd., Oxford, UK) and analyzed with DiscoverMP (v2023 R1.2) (Refeyn Ltd., Oxford, UK). The binding width was set to 40 for all measurements. The ratiometric contrast distribution was fitted by a Gaussian function to obtain the molecular weight of the respective subpopulation. The F/E ratio and linearity were visualized using MATLAB R2020b (MathWorks, Natick, MA, USA).

4. Conclusions

In this study, we demonstrated that mass photometry could be used as a fast and simple orthogonal method to the cumbersome and more complex AUC, CDMS and TEM. MP provides a useful non-destructive screening tool operating under native conditions. It offers information on the quantities of empty, partially filled, full and overfull AAV populations and can be used to confirm the molecular weight of the genomic cargo. It does so by using minimal sample volumes and low capsid titers. We managed to calculate the molar mass and quantify AAV subpopulations of samples with capsid titers as low as 8×10^{10} cp mL^{-1} with a CV < 5% using just 10 µL total sample volume. In addition, multiple samples can be measured within a short period of time, giving MP an advantage over the more laborious AUC, CDMS and TEM. Good comparability between MP and AUC data was observed regarding the F/E ratio and potential subpopulations. Furthermore, the single event-based light scattering technology allows for the measurement of various serotypes without the adaption of the instrument configurations. The possibility

of estimating the capsid titer with high precision based on the number of binding events would favor the mass photometer over ELISA, as the latter is a serotype-dependent analytical technique that requires different antibodies for different serotypes. Additionally, the recent release of a robotic module for the mass photometer paves the way for automated instrument operation and allows a higher sample throughput. The great potential of mass photometry to quickly assess unwanted byproducts (empty, partially filled, and overfilled AAV particles) in an AAV sample alongside the desired full AAV capsids could provide a more user-friendly and less laborious alternative to AUC in the future and allows to make gene therapy products safer for patients.

Author Contributions: Conceptualization, C.W. and M.L.; methodology, C.W. and F.F.F.; writing—original draft preparation, C.W.; writing—review and editing, M.L., F.F.F., B.I. and R.B.-G.; supervision, M.L. and R.B.-G. All authors have read and agreed to the published version of the manuscript.

Funding: Baxalta Innovations GmbH provided all the funding for this research.

Institutional Review Board Statement: Not applicable.

Informed Consent Statement: Not applicable.

Data Availability Statement: Not applicable.

Conflicts of Interest: Authors C.W., F.F.F., B.I. and M.L. were employed by the company Takeda. The remaining authors declare that the research was conducted in the absence of any commercial or financial relationships that could be construed as a potential conflict of interest. The authors declare that this study received funding from Baxalta Innovations GmbH (part of Takeda). The funder had the following involvement with the study: employer of C.W., F.F.F., B.I. and M.L.

References

1. Li, C.; Samulski, R.J. Engineering adeno-associated virus vectors for gene therapy. *Nat. Rev. Genet.* **2020**, *21*, 255–272. [CrossRef] [PubMed]
2. Chandler, R.; Sands, M.S.; Venditti, C.P. Recombinant Adeno-Associated Viral Integration and Genotoxicity: Insights from Animal Models. *Hum. Gene Ther.* **2017**, *28*, 314–322. [CrossRef] [PubMed]
3. Maestro, S.; Weber, N.D.; Zabaleta, N.; Aldabe, R.; Gonzalez-Aseguinolaza, G. Novel vectors and approaches for gene therapy in liver diseases. *JHEP Rep.* **2021**, *3*, 100300. [CrossRef]
4. Aponte-Ubillus, J.J.; Barajas, D.; Peltier, J.; Bardliving, C.; Shamlou, P.; Gold, D. Molecular design for recombinant adeno-associated virus (rAAV) vector production. *Appl. Microbiol. Biotechnol.* **2018**, *102*, 1045–1054. [CrossRef]
5. Wileys, J. Gene Therapy Clinical Trials Worldwide. Available online: https://a873679.fmphost.com/fmi/webd/GTCT (accessed on 12 April 2023).
6. EU/3/12/1091: Orphan Designation for the Treatment of Beta Thalassaemia Intermedia and Major. Available online: https://www.ema.europa.eu/en/medicines/human/orphan-designations/eu3121091 (accessed on 12 April 2023).
7. FDA Approves First Cell-Based Gene Therapy to Treat Adult and Pediatric Patients with Beta-thalassemia Who Require Regular Blood Transfusions. Available online: https://www.fda.gov/news-events/press-announcements/fda-approves-first-cell-based-gene-therapy-treat-adult-and-pediatric-patients-beta-thalassemia-who (accessed on 12 April 2023).
8. Wang, C.; Mulagapati, S.H.R.; Chen, Z.; Du, J.; Zhao, X.; Xi, G.; Chen, L.; Linke, T.; Gao, C.; Schmelzer, A.E.; et al. Developing an Anion Exchange Chromatography Assay for Determining Empty and Full Capsid Contents in AAV6.2. *Mol. Ther. Methods Clin. Dev.* **2019**, *15*, 257–263. [CrossRef]
9. Geoffroy, M.-C.; Salvetti, A. Helper Functions Required for Wild Type and Recombinant Adeno- Associated Virus Growth. *Curr. Gene Ther.* **2005**, *5*, 265–271. [CrossRef]
10. Buller, R.M.L.; Janik, J.E.; Sebring, E.D.; Rose, J.A. Herpes Simplex Virus Types 1 and 2 Completely Help Adenovirus-Associated Virus Replication. *J. Virol.* **1981**, *40*, 241–247. [CrossRef]
11. Venkatakrishnan, B.; Yarbrough, J.; Domsic, J.; Bennett, A.; Bothner, B.; Kozyreva, O.G.; Samulski, R.J.; Muzyczka, N.; McKenna, R.; Agbandje-McKenna, M. Structure and Dynamics of Adeno-Associated Virus Serotype 1 VP1-Unique N-Terminal Domain and Its Role in Capsid Trafficking. *J. Virol.* **2013**, *87*, 4974–4984. [CrossRef]
12. Rose, J.A.; Maizel, J.V., Jr.; Inman, J.K.; Shatkin, A.J. Structural Proteins of Adenovirus-Associated Viruses. *J. Virol.* **1971**, *8*, 766–770. [CrossRef] [PubMed]
13. Barnes, L.F.; Draper, B.E.; Kurian, J.; Chen, Y.-T.; Shapkina, T.; Powers, T.W.; Jarrold, M.F. Analysis of AAV-Extracted DNA by Charge Detection Mass Spectrometry Reveals Genome Truncations. *Anal. Chem.* **2023**, *95*, 4310–4316. [CrossRef] [PubMed]
14. Wörner, T.P.; Bennett, A.; Habka, S.; Snijder, J.; Friese, O.; Powers, T.; Agbandje-McKenna, M.; Heck, A.J.R. Adeno-associated virus capsid assembly is divergent and stochastic. *Nat. Commun.* **2021**, *12*, 1642. [CrossRef] [PubMed]

15. Oyama, H.; Ishii, K.; Maruno, T.; Torisu, T.; Uchiyama, S.; Troxell, B.; Tsai, I.-W.; Shah, K.; Knuckles, C.I.; Shelton, S.; et al. Characterization of Adeno-Associated Virus Capsid Proteins with Two Types of VP3-Related Components by Capillary Gel Electrophoresis and Mass Spectrometry. *Hum. Gene Ther.* **2021**, *32*, 1403–1416. [CrossRef] [PubMed]
16. Ghosh, S.; Brown, A.M.; Jenkins, C.; Campbell, K. Viral Vector Systems for Gene Therapy: A Comprehensive Literature Review of Progress and Biosafety Challenges. *Appl. Biosaf.* **2020**, *25*, 7–18. [CrossRef] [PubMed]
17. Srivastava, A. In vivo tissue-tropism of adeno-associated viral vectors. *Curr. Opin. Virol.* **2016**, *21*, 75–80. [CrossRef]
18. Wright, J.F. Product-Related Impurities in Clinical-Grade Recombinant AAV Vectors: Characterization and Risk Assessment. *Biomedicines* **2014**, *2*, 80–97. [CrossRef]
19. Li, T.; Gao, T.; Chen, H.; Demianova, Z.; Wang, F.; Malik, M.; Luo, J.; Yowanto, H.; Mollah, S. *Determination of Full, Partial and Empty Capsid Ratios for Adeno-Associated Virus (AAV) Analysis*; SCIEX: Framingham, MA, USA, 2020.
20. Fu, X.; Chen, W.C.; Argento, C.; Clarner, P.; Bhatt, V.; Dickerson, R.; Bou-Assaf, G.; Bakhshayeshi, M.; Lu, X.; Bergelson, S.; et al. Analytical Strategies for Quantification of Adeno-Associated Virus Empty Capsids to Support Process Development. *Hum. Gene Ther. Methods* **2019**, *30*, 144–152. [CrossRef]
21. Gimpel, A.L.; Katsikis, G.; Sha, S.; Maloney, A.J.; Hong, M.S.; Nguyen, T.N.; Wolfrum, J.; Springs, S.L.; Sinskey, A.J.; Manalis, S.R.; et al. Analytical methods for process and product characterization of recombinant adeno-associated virus-based gene therapies. *Mol. Ther. Methods Clin. Dev.* **2021**, *20*, 740–754. [CrossRef]
22. Pierson, E.E.; Keifer, D.Z.; Asokan, A.; Jarrold, M.F. Resolving Adeno-Associated Viral Particle Diversity With Charge Detection Mass Spectrometry. *Anal. Chem.* **2016**, *88*, 6718–6725. [CrossRef]
23. Werle, A.K.; Powers, T.W.; Zobel, J.F.; Wappelhorst, C.N.; Jarrold, M.F.; Lyktey, N.A.; Sloan, C.D.; Wolf, A.J.; Adams-Hall, S.; Baldus, P.; et al. Comparison of analytical techniques to quantitate the capsid content of adeno-associated viral vectors. *Mol. Ther. Methods Clin. Dev.* **2021**, *23*, 254–262. [CrossRef]
24. Takeda, K.; Noda, M.; Maruno, T.; Uchiyama, S. Critical Calibration of Mass Photometry for Higher-Mass Samples Such as Adeno-Associated Virus Vectors. *J. Pharm. Sci.* **2022**, *112*, 1145–1150. [CrossRef]
25. Wu, D.; Piszczek, G. Standard protocol for mass photometry experiments. *Eur. Biophys J.* **2021**, *50*, 403–409. [CrossRef]
26. Sonn-Segev, A.; Belacic, K.; Bodrug, T.; Young, G.; VanderLinden, R.T.; Schulman, B.A.; Schimpf, J.; Friedrich, T.; Dip, P.V.; Schwartz, T.U.; et al. Quantifying the heterogeneity of macromolecular machines by mass photometry. *Nat. Commun.* **2020**, *11*, 1772. [CrossRef] [PubMed]
27. Wyatt, P.J. Light scattering and the absolute characterization of macromolecules. *Anal. Chim. Acta* **1993**, *272*, 1–40. [CrossRef]
28. Wagner, C.; Innthaler, B.; Lemmerer, M.; Pletzenauer, R.; Birner-Gruenberger, R. Biophysical Characterization of Adeno-Associated Virus Vectors Using Ion-Exchange Chromatography Coupled to Light Scattering Detectors. *Int. J. Mol. Sci.* **2022**, *23*, 12715. [CrossRef] [PubMed]
29. Benefits and Applications of Analytical Ultracentrifugation (AUC). Available online: https://www.nanolytics.com/ (accessed on 14 June 2023).
30. Saleun, S.; Mas, C.; Le Roy, A.; Penaud-Budloo, M.; Adjali, O.; Blouin, V.; Ebel, C. Analytical ultracentrifugation sedimentation velocity for the characterization of recombinant adeno-associated virus vectors sub-populations. *Eur. Biophys. J.* **2023**, *52*, 1–11. [CrossRef] [PubMed]
31. Refeyn Ltd. Quantifying Heterogeneous AAV Capsid Loading Using Mass Photometry. [White Paper]. 2022. Available online: https://info.refeyn.com/app-note-aav-loading (accessed on 14 June 2023).

International Journal of
Molecular Sciences

MDPI

Article

Automated Mass Photometry of Adeno-Associated Virus Vectors from Crude Cell Extracts

Christina Wagner [1], Felix F. Fuchsberger [1,*], Bernd Innthaler [1], Robert Pachlinger [1], Irene Schrenk [1], Martin Lemmerer [1] and Ruth Birner-Gruenberger [2]

[1] Pharmaceutical Sciences, Baxalta Innovations (Part of Takeda), 1220 Vienna, Austria
[2] Institute of Chemical Technologies and Analytics, Technical University of Vienna, 1040 Vienna, Austria
* Correspondence: felix.fuchsberger@takeda.com

Abstract: Mass photometry (MP) is a fast and simple analysis method for the determination of the proportions of subpopulations in an AAV sample. It is label-free and requires minimal sample volumes between 5–10 µL, which makes it a promising candidate over orthogonal techniques such as analytical ultracentrifugation (AUC), cryo-transmission electron microscopy (Cryo-TEM) or charge-detection mass spectrometry (CDMS). However, these methods are limited in their application to purified samples only. Here we developed a purification step based on single-domain monospecific antibody fragments immobilised on either a poly(styrene-divinylbenzene) resin or on magnetic beads prior to MP analysis that allows the quantification of empty, partially filled, full and overfull AAV vectors in crude cell extracts. This is aimed at identifying potentially promising harvest conditions that yield large numbers of filled AAV vectors during the early stages of the viral vector development platform, e.g., the type of transfection reagent used. Furthermore, we provide a direct comparison of the automated and manual handling of the mass photometer with respect to the quantities of AAV subspecies, molar mass of the capsid and payload, and highlight the differences between the "buffer-free" sample measurement and the "buffer-dilution" mode. In addition, we provide information on which candidates to use for calibration and demonstrate the limitations of the mass photometer with respect to the estimation of the capsid titer.

Keywords: adeno-associated virus vectors; nanobodies; magnetic beads; automated mass photometry; analytical ultracentrifugation

Citation: Wagner, C.; Fuchsberger, F.F.; Innthaler, B.; Pachlinger, R.; Schrenk, I.; Lemmerer, M.; Birner-Gruenberger, R. Automated Mass Photometry of Adeno-Associated Virus Vectors from Crude Cell Extracts. *Int. J. Mol. Sci.* **2024**, *25*, 838. https://doi.org/10.3390/ijms25020838

Academic Editor: József Tőzsér

Received: 1 December 2023
Revised: 3 January 2024
Accepted: 8 January 2024
Published: 9 January 2024

1. Introduction

In gene therapy, recombinant adeno-associated viruses are one of many vector platforms for the transportation of genomic cargo in patients for the treatment of rare diseases. As opposed to, e.g., retroviruses or lentiviruses, recombinant adeno-associated viruses (rAAVs) are characterised by their low immunogenicity and toxicity, which makes them attractive genomic material delivery systems [1–3]. There are currently seven commercially available AAV-based gene therapy products approved by the European Medicines Agency (EMA) or the US Food and Drug Administration (FDA) aimed at treating lipoprotein lipase deficiency (Glybera), retinal dystrophy (Luxturna), spinal muscular atrophy (Zolgensma), Duchenne muscular dystrophy (Elevidys), hemophilia B (Hemgenix), aromatic L-amino acid decarboxylase (AADC) deficiency (Upstaza) and haemophilia A (Roctavian), respectively [4–11]. In addition, Zynteglo, a lentivirus-based gene therapy product has been approved by the EMA and FDA for patients suffering from beta thalassemia intermedia and major [12,13].

AAV capsids are non-enveloped viruses of about 25 nm in diameter and belong to the genus *Dependoparvovirus* within the family *Parvoviridae* [14,15]. As the genus already suggests, AAVs depend on a helper virus for efficient replication, such as the herpes simplex virus (HSV) or adenovirus (Ad) [16–18]. They are made up of three viral proteins VP1, VP2

and VP3 differing in the length of their N-terminus. VP1, VP2 and VP3 occur in a ratio of about 1:1:10 yielding a total sum of 60 interlocking proteins which form the icosahedral capsid structure [7,19–21]. The packaging capacity of an AAV particle is restricted to single stranded DNA up to 4.7 kb [22]. To date, there are 12 naturally occurring serotypes, which vary in their receptor binding domains defining the tropism of the AAV vectors [1,23]. The genetic engineering of variable regions on the capsid surface allows for the manipulation of the transduction efficiency of the AAV particles and expands the possibilities of designing tailored AAV vector-based gene therapeutics for specific diseases [1,24].

As the production of AAV vectors is a complex process that is influenced by multiple factors such as cell line or plasmid ratios, not only are filled AAV particles generated but also empty and partially loaded capsids [25]. The latter represent AAV species that incorporate only parts of the intended payload and are considered neither full nor empty. In addition to the incorporation of fragmented versions of the vector genome, it is possible that more than one copy of the genomic material is inserted into the AAV capsid but is limited to the maximum loading capacity of the virus particle. This is considered an overfilled particle and, together with empty and partially filled AAV capsids, makes up the unwanted byproducts that are coproduced alongside the desired filled AAV particles. To guarantee a safe and efficacious application of a gene therapeutic, it is crucial to assess certain critical quality attributes (CQAs). One of the CQAs is the determination and quantification of impurities (empty, partially filled and overfull AAV vectors) as they may pose a risk to the recipient due to potential adverse health effects [26–29]. To date, these impurities are assessed by analytical ultracentrifugation (AUC), transmission electron microscopy (TEM) or charge-detection mass spectrometry (CDMS) [30–33]. As opposed to chromatography-based methods in combination with UV detection at 260 nm and 280 nm, AUC, TEM and CDMS are able to distinguish between AAV subspecies other than empty and filled particles, which is attributed to the high resolution of the instruments. Despite providing quantitative information on the proportions of AAV subpopulations, these methods are limited in their sample throughput and lack short turnaround times [31,34]. While CMDS and TEM demand less sample material than AUC, the latter is still the standard method for the assessment of the proportions of AAV subspecies [35].

Mass photometry (MP) offers a fast and simple alternative to the previously mentioned analytical techniques for the quantification of empty, partially filled, full and overfull AAV particles. With analysis times of 1–2 min, MP is significantly superior to orthogonal techniques, such as CDMS (2 h), TEM (2 h–6 h) and AUC (6 h), respectively [26]. In addition, mass photometry stands out by its low sample consumption of 5–10 µL containing 1×10^{11} cp mL^{-1} and minimal sample preparation, as no labelling nor immobilization steps are required [36,37]. Furthermore, the possibility of operating the instrument in an automated manner allows for a higher sample throughput than with CDMS, TEM or AUC. MP is based on the detection of reflected light from the cover slip interfering with scattered light from AAV particles attaching and detaching from the glass slide at the solid–liquid interface. The attaching and detaching of the particles are considered as binding and unbinding events, respectively. All detected binding events are summarised under the term “binding count rate”. Depending on the detected contrast, particles are registered as empty, partially filled, full or overfull AAV fractions and can subsequently be assigned a molecular mass. Hence, it is possible to confirm the molar mass of the packaged transgene in filled AAV particles, which has been described in our previous article [38].

Here we present an extended investigation of the mass photometer following up on our previously published article on the quantification of empty, partially filled and full adeno-associated virus vectors using mass photometry [38]. We provide additional information on the instrument’s performance when operated automatically and manually and compare the “buffer-dilution” mode with the “buffer-free” mode, as both can be used for sample measurement. Furthermore, we show that the variation in the number of binding events between repetitive measurements results in high deviation of the estimated capsid titer to ELISA titer, regardless of manual or automated mass photometry. In addition, we

developed a method to assess AAV subspecies from crude cell material using single-domain monospecific antibody fragments immobilised on either a poly(styrene-divinylbenzene) resin or on magnetic beads followed by MP analysis. This shortcut allows for an estimation of AAV subspecies during the upstream process omitting labour-intensive cleanup steps such as diafiltration, ultracentrifugation, affinity chromatography, etc. aiming at a more efficient and less time-consuming screening of different transfection conditions, cell lines, transgenes, etc. that yield high titers of filled AAV capsids. We observed differences in the proportions of AAV subspecies when applying two different transfection reagents which are used for the introduction of plasmids into the cells. While transfection mix A yielded large quantities of partially filled and small numbers of filled AAV vectors, transfection mix B increased the titer of filled AAV capsids almost threefold according to MP.

2. Results and Discussion

In our previous article we established a method for the quantification of empty, partially filled and full AAV vectors using the Samux Mass Photometer (Refeyn Ltd., Oxford, UK) [38]. Despite being a fast analytical method (1–2 min analysis times) that requires small sample volumes (2–10 µL), the manual operation of the instrument requires constant control and supervision. The number of samples per run is limited to six, which demands frequent replacement of the sample gasket and glass slides. To address this challenge, Refeyn Ltd. launched an additional robotic module (AUTO SamuxMP, Refeyn Ltd., Oxford, UK) that enables the automatic operation of the Samux MP, including sample dilution prior to measurement. The number of analysed samples was increased from six to twenty four, which allows a higher sample throughput before exchanging the sample gasket. The automated pre-dilution of a sample in a 96-well plate additionally saves time and effort and makes mass photometry a more attractive analytical technique for the quantification of the proportions of the AAV subpopulations as opposed to AUC, TEM or CDMS, which require more labour-intensive sample preparation.

2.1. Selection of Calibration Samples

Prior to sample measurement, a calibration curve is set up which assigns a measured ratiometric contrast value to a given molar mass. This allows the determination of the molar mass of each registered binding event. First, we investigated the effect of different calibration analytes of different molecular weights. Thyroglobulin (TG) was selected as the low molecular weight calibrant with a molar mass of 670 kDa. The second, high molecular weight calibrant, was a commercially available empty AAV9 (AAV9e) purchased from Progen, with a molar mass of 3.74 MDa. These analytes had been used in our previous study [38]. In addition, we investigated whether we could replace TG with the zero point. At the zero point, the molar mass and the ratiometric contrast are zero. This would save not only time but also omit the use of another calibration sample. The third option we tested was to include all three data points (zero, TG and AAV9e) for the generation of the calibration curve. As the analyte, we selected an AAV9 sample consisting of ~33% empty, ~6% partially filled, ~52% full, ~8% overfull AAV particles determined with AUC and confirmed with MP [38]. Figure 1 depicts the obtained results regarding the calculated molar masses of the empty and full AAVs, the transgene and the proportions of the AAV subpopulations. As expected, there is no significant difference in the calculated % of AAV subpopulations and molar masses of the capsids and transgene between the three calibrations models (Supplementary Tables S1 and S2). The three data points-based calibration (zero, TG and AAV9e) had a coefficient of determination (R^2) < 1 as opposed to the calibration models using two data points (TG and AAV9e; zero and AAV9e; Supplementary Figure S1). For further experiments we used the zero point and AAV9e for mass calibration, as this calibration model omits the use of a second calibration standard, thus, qualifies for working in a more convenient and time-efficient manner.

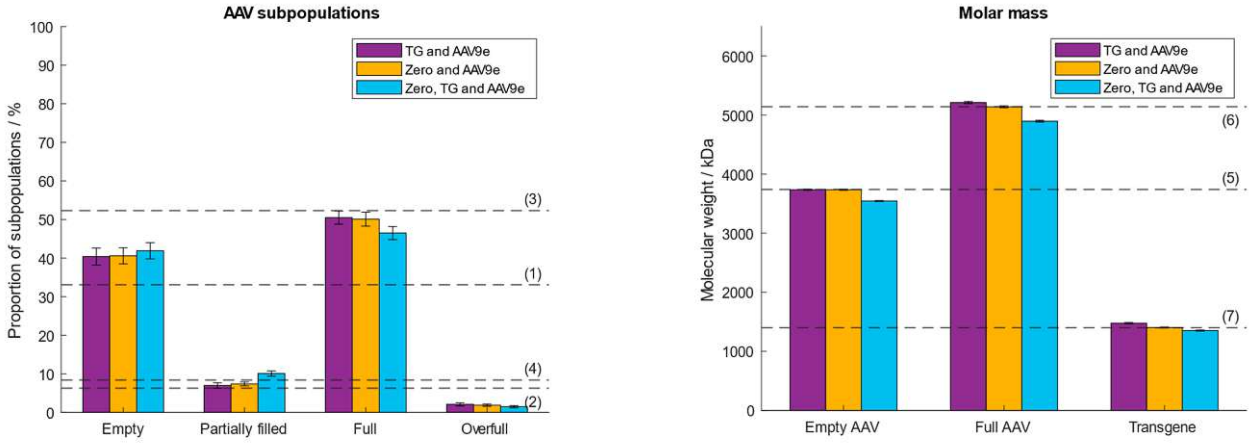

(**a**) (**b**)

Figure 1. Evaluation of the performance of different calibration curves using either TG and AAV9e (purple), zero and AAV9e (orange) or zero, TG and AAV9e (blue). Dashed lines (1–7) represent (**a**) the expected proportion of the empty, partially filled, full and overfull AAV populations, (**b**) the absolute molar masses of the empty and filled AAVs capsids and the transgene, respectively.

2.2. Instrument Focusing with and without Buffer

There are two options to measure a sample on the mass photometer. The "dilution-free" mode is based on automatically adjusting the focus on the interface between the solid phase (glass slide) and the gas phase (air). The "buffer-dilution" approach uses buffer instead of air, where the buffer is pipetted into the well of the gasket, followed by the focusing step and finally adding the sample which leads to an additional dilution of the sample. A schematic illustration is given in Figure 2.

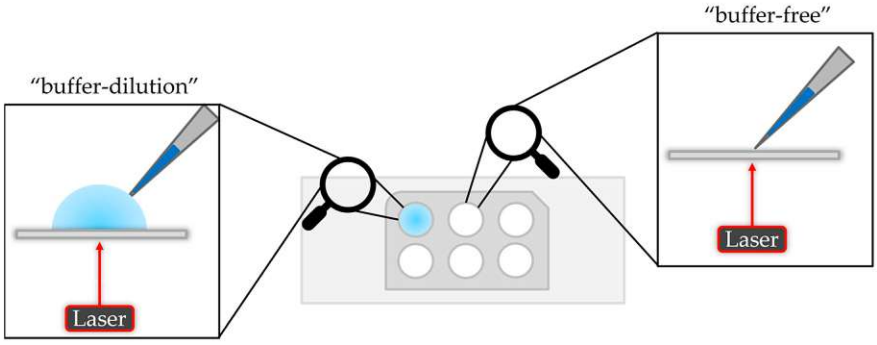

Figure 2. Schematic illustration of the "buffer-dilution" and "buffer-free" sample measurement.

In our previously published article we used the "buffer-dilution" focusing without exception as a dilution step prior to measurement was necessary for all samples due to high capsid titers. However, according to Refeyn Ltd. both options are suitable for the generation of accurate results. Thus, we tested the "buffer-dilution" and "dilution-free" focusing modes and compared the results with respect to the quantities of AAV subpopulations, molar mass of empty/full AAVs and transgene, and binding count rates (Figure 3). Therefore, we selected the same AAV9 sample as described in Section 2.1 comprising ~33% empty, ~6% partially filled, ~52% full, ~8% overfull AAV particles. For the "buffer-free" mode the sample was pre-diluted manually. All subsequent measurements were carried out under automated instrument operation. Results show that the "buffer-free" approach performed better with respect to the calculated molar mass of the empty/full AAVs and transgene (Figure 3). In general, the variation between the samples measured using the "buffer-free" mode is higher than for the "buffer-dilution" mode which is reflected in higher standard deviations (Supplementary Tables S3–S5). The variation in the number

of binding events between both modes is attributed to the lack of mixing the sample with the buffer when using the "buffer-dilution" mode. When operating the instrument manually, the sample had been mixed vigorously in the well by pipetting it up and down before measurement to ensure a homogenous distribution and adequate dilution of the AAV capsids (part of our previous publication [38]). When doing the automated "buffer-dilution", we observed, that the robot does not mix the sample with the buffer but pipettes it onto the bottom of the sample well displacing the buffer from the bottom resulting in a higher number of binding and unbinding events than when mixing it manually. However, for the determination of quantities of AAV subspecies and molecular weight of empty/full capsids and the payload both measurement modes are suitable.

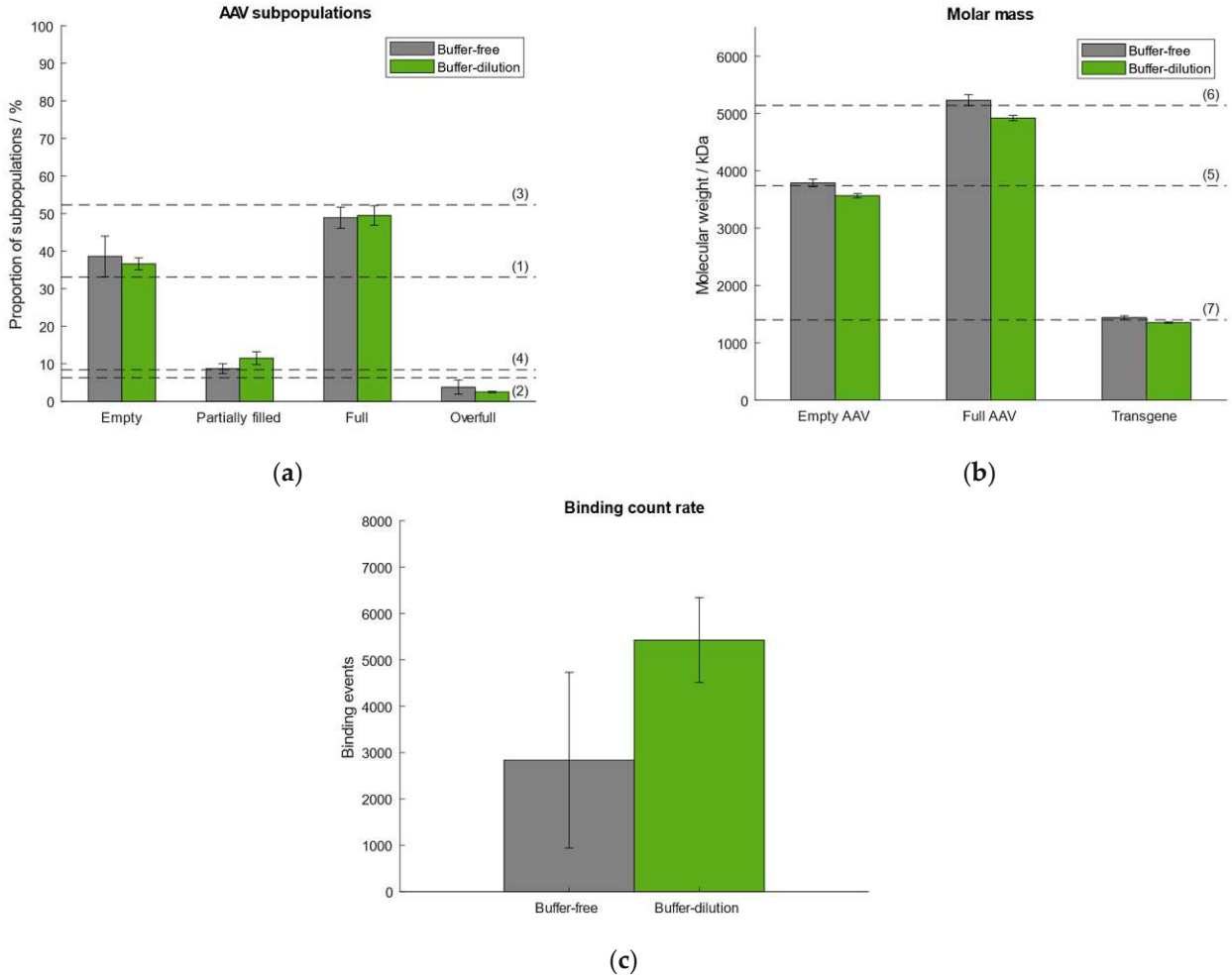

Figure 3. Comparison of performance using either buffer-free (grey) or buffer-dilution (green) focusing mode. Dashed lines (1–7) represent (**a**) the expected proportion of the empty, partially filled, full and overfull AAV populations, (**b**) the absolute molar masses of the empty and filled AAVs capsids and the transgene, respectively. (**c**) Comparison of binding count rates between both focusing modes.

2.3. Manual vs. Automated Instrument Operation

As a consequence of lacking sample homogeneity when using the "buffer-dilution" mode under automatic instrument operation, we investigated and compared the performance when operating the Auto SamuxMP manually and automatically with respect to quantities of AAV subpopulations, molar mass of the capsids and transgene, and binding count rate. Therefore, an AAV9 sample (~33% empty, ~6% partially filled, ~52% full, ~8% overfull capsids) was measured five times by automated pipetting and results were compared to data obtained under manual instrument operation that had been investigated

in our previous publication [38]. The comparison of both operation modes is visualised in Figure 4. Data from the automated handling is given in Supplementary Tables S6 and S7. The results of manual instrument operation had been published in our previous article [38]. Figure 4 shows good comparability between both operation modes. While generally higher standard deviations were observed for measurements that had been carried out under automated operation with respect to the calculated quantities of AAV subspecies, the deviation of the calculated transgene size from the expected value was 2.5% (automated handling), which is lower than for the manual instrument operation (3.3% [38]). The highest RSD was <19% with respect to the measured proportions of the AAV subpopulations and molar mass of capsids and payload (automated handling), as opposed to a max. RSD ~10% for the manual instrument operation [38]. However, there are no significant differences between automated and manual instrument operation regarding the calculated proportions of AAV subspecies and molar masses of the capsids and genomic cargo. The variation in the number of binding events under automated instrument handling is a consequence of the omitted mixing of the sample by the robotic arm when pipetted into the sample gasket containing the buffer and had been observed when investigating the "buffer-free" and "buffer-dilution" focusing modes in Section 2.2.

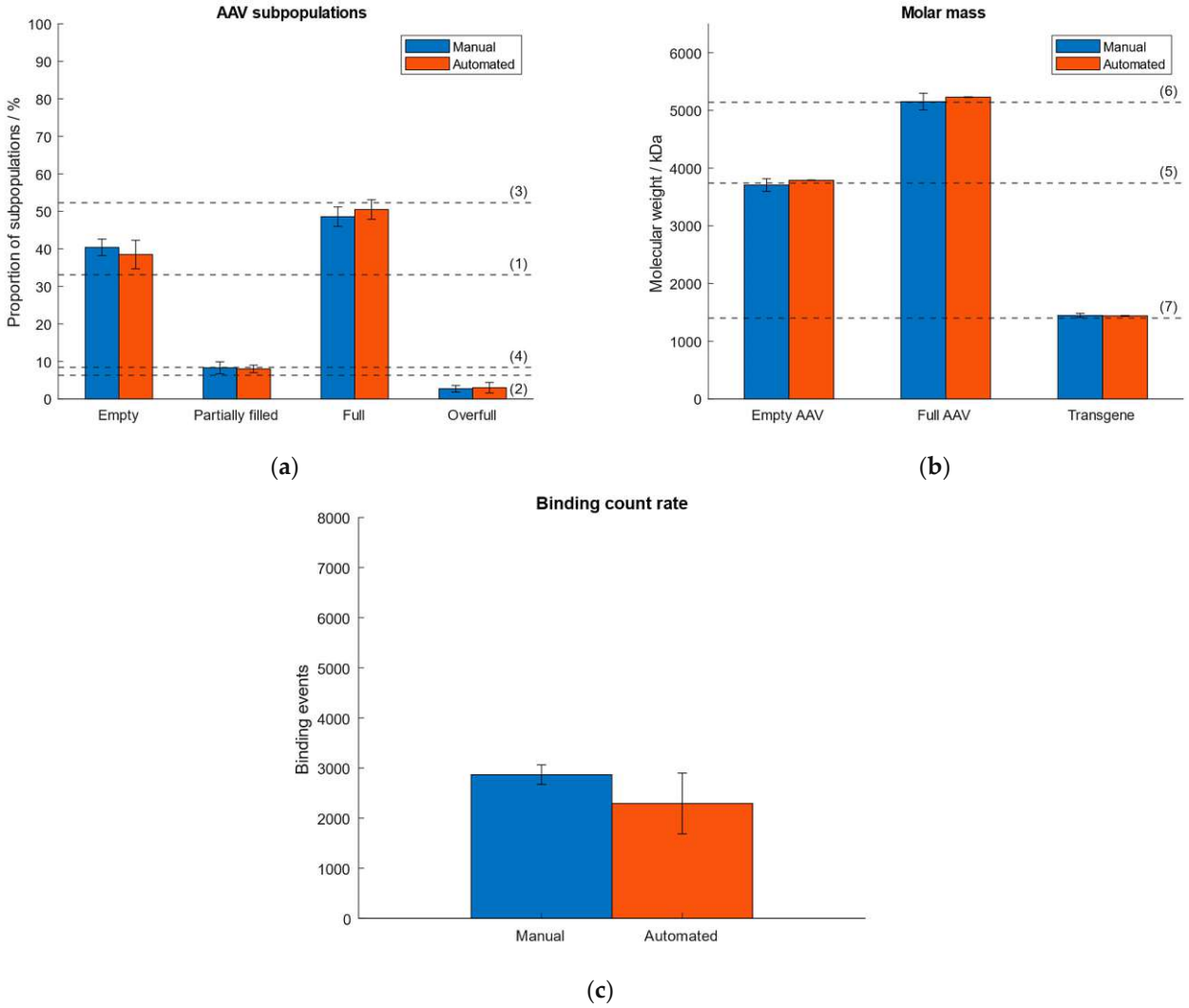

Figure 4. Comparison of manual and automated instrument operation. Dashed lines (1–7) represent (**a**) the expected proportion of the empty, partially filled, full and overfull AAV populations, (**b**) the absolute molar masses of the empty and filled AAVs capsids and the transgene, respectively. (**c**) Comparison of binding count rates between manual and automated operation mode.

2.4. Titer Estimation

Furthermore, we explored a feature of the SamuxMP that provides a rough estimation of the capsid titer and is based on the registration of the number of binding events. However, Refeyn Ltd. does not explicitly define, how precisely the mass photometer estimates the sample titer. Since it is not possible to generate constant binding/unbinding count rates with the MP when measuring a sample multiple times, a precise determination of the sample titer is not possible. To investigate this, we tested four AAV samples differing in their serotype (AAV8 and AAV9) and concentration (4.3×10^{11}, 2×10^{11}, 1.5×10^{11} and 1×10^{11} cp mL^{-1}). All samples were measured in five replicates. Because we have encountered that manual instrument operation yields a smaller RSD of binding events as opposed to running the mass photometer in an automatic mode (Figure 4), we additionally tested, if the calculated titers better matched the expected ones when screening the samples manually. The results in Figure 5 confirm that under the automatic operation of the instrument, the standard deviation is generally higher than for the manual handling of the instrument. The significant fluctuation of the binding count rates between the measurements demonstrates the limitation of the instrument. When measured in manual mode, AAV8 samples yield lower capsid titers as opposed to the automatic handling of the instrument due to fewer particles attaching and detaching from the glass surface. The AAV9 samples show smaller standard deviations and a better comparison between manual and automated operation regarding AAV concentration than the AAV8 samples. In general, the calculated capsid titers (generated with MP) were lower compared to expected sample titers obtained with ELISA.

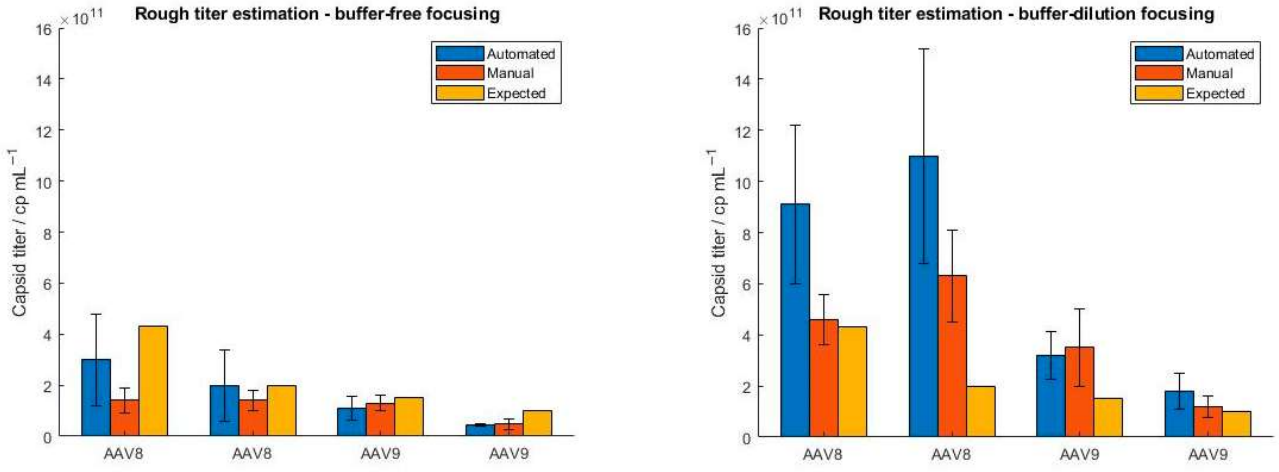

(**a**) (**b**)

Figure 5. Evaluation of the "rough titer estimation" feature of the SamuxMP using two different serotypes (AAV8 and AAV9) at four different concentrations (4.3×10^{11}, 2×10^{11}, 1.5×10^{11} and 1×10^{11} cp mL^{-1}). The samples were measured under automated (blue) and manual (orange) instrument operation and obtained capsid titers were compared to ELISA data (yellow). (**a**) buffer-free focusing, (**b**) buffer-dilution focusing mode.

To further address this, we repeated the experiments but selected the buffer-dilution focusing option instead of the buffer-free focusing option as we found that the latter showed a greater standard deviation in the binding events than when using the buffer-dilution mode (Section 2.2). The results show an overestimation of the capsid titers when using the buffer-dilution focusing compared to the buffer-free focusing regardless of whether the instrument was operated manually or automatically and irrespective of the serotype used. When running the instrument manually, lower standard deviations were obtained than for the automated handling of the instrument. In addition, we observed a significant overestimation of the capsid titers under automated performance which is attributed to the

lack of mixing the sample with the buffer. In general, the standard deviation was smaller for titers obtained with buffer-free focusing compared to buffer-dilution focusing. However, we have found no correlations so far that indicate a concentration- or serotype-dependency of the "rough titer estimation" feature but will be explored further.

2.5. Cleanup of AAVs from Harvest

The determination of full/empty ratios in crude AAV harvests is a very challenging task, hence, we developed a purification process which is based on the manufacturer's protocol [39] and which provides an easy and relatively fast insight into the heterogeneity of AAV subpopulations at early stages of the development platform and could aid in adapting and optimising vector manufacturing conditions. Promising transfection conditions, e.g., the type of transfection reagent, which result in high quantities of the desired filled AAV capsids can be easily identified omitting laborious purification steps for the generation of relatively pure sample material required for MP analysis. To demonstrate this, we developed an easy purification procedure based on nanobodies immobilised on poly(styrene-divinylbenzene) beads (POROS™ CaptureSelect™ AAV9 Affinity Resin) which allows to specifically extract AAV9 capsids from crude cell material for the relative quantification of AAV species (empty, partially filled, full and overfull) using MP. A schematic illustration of the cleanup process is given in Figure 6.

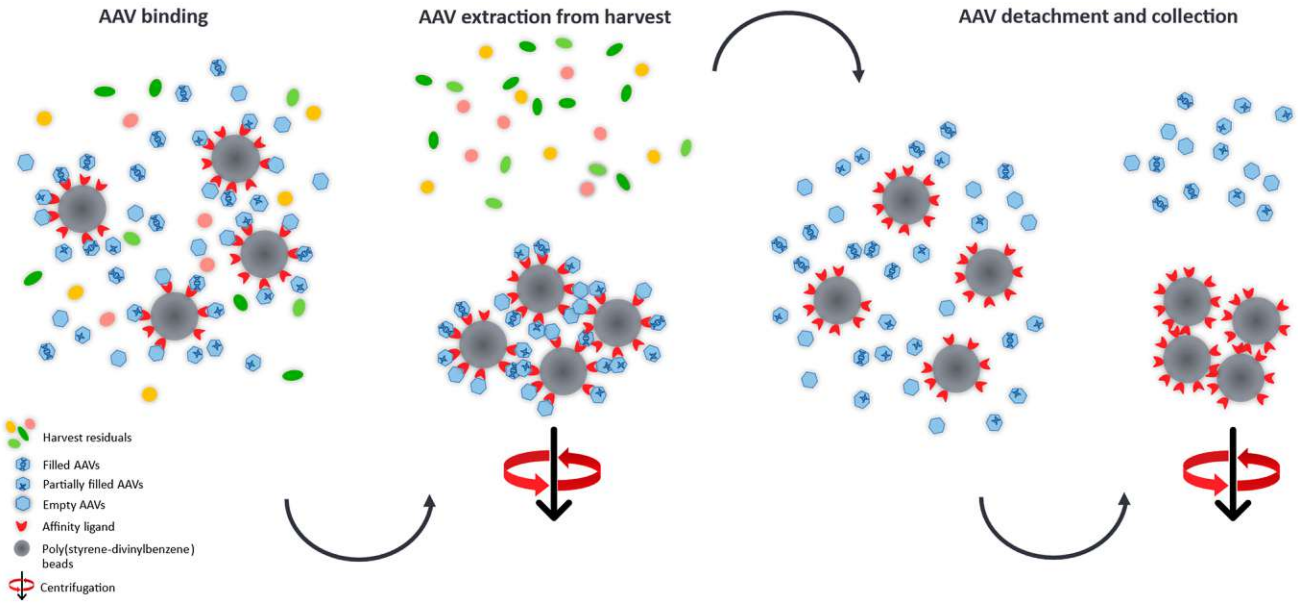

Figure 6. Schematic illustration of the AAV cleanup from harvest material using nanobodies covalently attached to poly(stryrene-divinylbenzene) beads. The immobilised affinity ligands selectively capture the AAVs from the crude cell extract and can then be separated from the harvest residuals by gravitational force. After elution from the binding sites, the AAVs are collected and measured by mass photometry for the quantification of AAV subpopulations.

After determining the best operating conditions of the instrument, we proceeded with the clean-up of AAV9 capsids from harvest material and applied our protocol to two different cell extracts which had been generated using two types of transfection reagents (transfection mix A and B). To confirm the proportion of the different AAV subpopulations after cleanup from harvest material, we performed an AUC analysis. The results in Figure 7 show that MP and AUC data agree well with one another with respect to quantities of AAV subpopulations. However, for AAV capsids generated with transfection mix A, the quantities of filled particles differed between MP (11.2%) and AUC (1.6%). Compared to MP, AUC overestimates the fraction containing empty and underestimates the quantity of filled AAV capsids. However, the findings demonstrate the great potential of mass

photometry to assess AAV subpopulations in crude cell extracts and acts as fast and simple alternative to AUC.

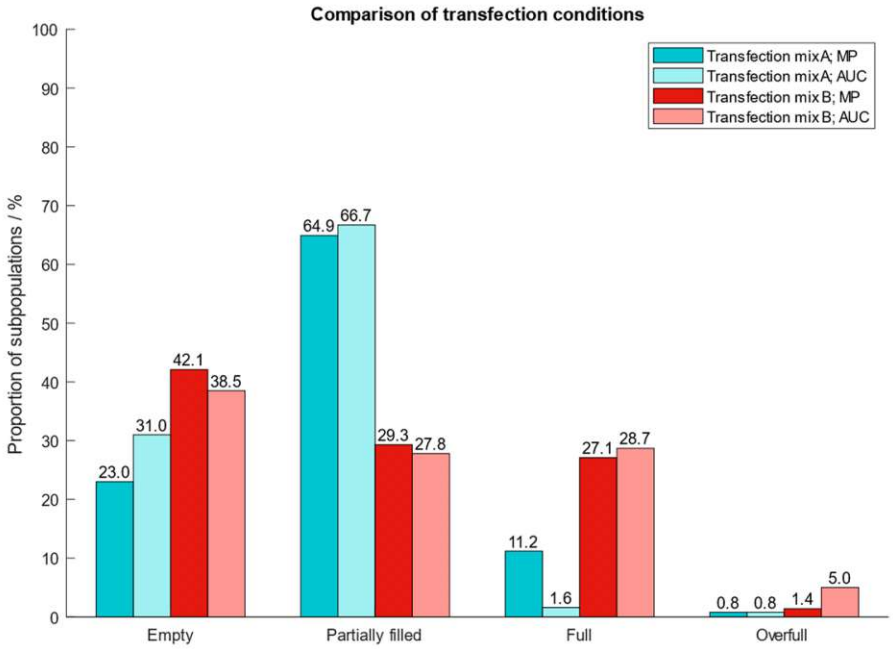

Figure 7. Proportion of AAV9 subspecies purified from crude cell extracts which had been produced by using two different transfection reagents for the introduction of plasmids into the cells. Blue: transfection mix A; red: transfection mix B.

Magnetic Beads

Because our cleanup protocol using POROS™ CaptureSelect™ AAV9 Affinity Resin does not have the potential to be fully automated due to centrifugation steps during the cleanup process, we used magnetic beads for the purification of AAVs from harvest samples. We developed a procedure based on the manufacturer's manual [40] for the extraction of AAVs from crude cell material using Dynabeads™ CaptureSelect™ AAVX Magnetic Beads that has the potential to be run automatically with pipetting robots, such as Andrew+, and will be explored further in future studies but will not be discussed here. The broad range of applicable serotypes include AAV1 to AAV8, AAVrh10 and synthetic serotypes [40] due to the AAVX affinity ligand. Hence, we have observed lack of affinity against AAV9. However, Florea et al. tested the POROS™ CaptureSelect™ AAVX Affinity Resin containing the same nanobody as immobilised on the magnetic beads and were able to bind AAV9 with relatively high efficiency [41]. Because we have found no specific binding of AAVX ligands to AAV9 capsids, we tested the magnetic beads on AAV8-based cell extracts. The mass histogram in Figure 8 shows two defined fractions which can be assigned to the empty and filled AAV populations according to MP and is therefore less homogeneous than the mass histogram of AAV9. AUC measurements were omitted here, due to limitations in the sample volumes and capsid titers required for analysis. However, orthogonality between both analysis techniques was observed in previous investigations (see Section 2.5) and will be explored further in follow-up studies.

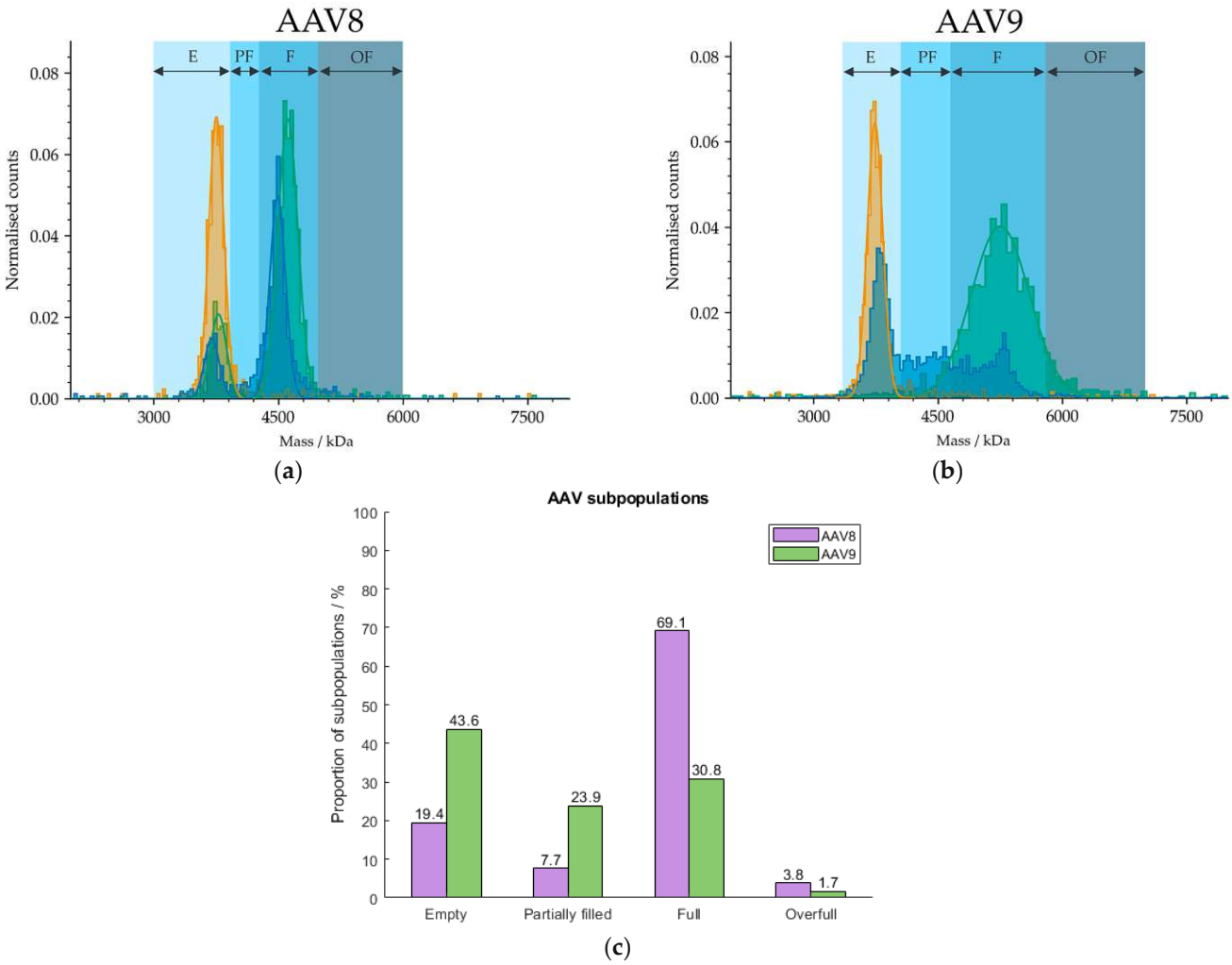

Figure 8. Mass histograms of (**a**) AAV8 and (**b**) AAV9. AAV8 and AAV9 capsids were extracted from curde cell extracts using Dynabeads™ CaptureSelect™ AAVX Magnetic Beads and POROS™ CaptureSelect™ AAV9 Affinity Resin, respectively. E, PF, F and OF stand for empty, partially filled, full and overfull, respectively. Samples comprising meC (orange) and mfC (green), respectively, were selected for each serotype to set the AAV limits for the analysis of an AAV sample (blue). (**c**) Barplot visualising the proportions of AAV subspecies in the AAV8 (purple) and AAV9 (green) extracts from harvest material. Results were obtained with MP.

3. Materials and Methods

3.1. Sample Preparation

For the AAV cleanup from crude cell material, POROS™ CaptureSelect™ AAV9 Affinity Resin and Dynabeads™ CaptureSelect™ AAVX Magnetic Beads were purchased from ThermoFisher Scientific (Waltham, MA, USA). The affinity resin/magnetic beads were washed twice with TBS-based buffer and mixed with our in-house produced cell debris-free supernatant containing the desired AAV9/AAV8 capsids, respectively. The mixtures were incubated at room temperature for 20 min, spun down/magnetically separated, the supernatant discarded and the resin/magnetic beads washed twice with TBS-based buffer and water, respectively. The captured AAV capsids were then eluted from the resin/magnetic beads using an HCl-based buffer at pH 3 and immediately neutralised with Tris-based solution of slightly alkaline pH before analysed on the mass photometer. All in-house produced AAV samples were diluted prior to MP measurement to a final concentration between 1×10^{11} and 2×10^{11} cp mL^{-1} using HPLC-grade phosphate-buffered saline (PBS) obtained from Sigma Aldrich (Saint Louis, MO, USA). Isopropanol,

necessary for cleaning the silicon sample gaskets was purchased from Merck (Darmstadt, Germany). "Empty" AAV9 capsids used for calibration was purchased from Progen (Heidelberg, Germany) and was used at a final concentration of ~3.3 × 10^{11} cp mL^{-1}.

3.2. Measurements and Experimental Setup

AUC analysis was carried out at 15,000 rpm and 18 °C on a Beckman AUC Optima instrument (Beckman Coulter, Brea, CA, USA) equipped with an An-50 Ti analytical rotor (Beckman Coulter, Brea, CA, USA) and a total number of 150 scans per sample. The MP measurements were performed on the SamuxMP Auto (Refeyn Ltd., Oxford, UK) instrument. Compared to the standard SamuxMP, the SamuxMP Auto features automated sample handling due to an integrated robotic arm omitting constant instrument supervision and control. The 24-well sample gaskets and the glass slides were purchased from Refeyn Ltd. (Oxford, UK). A calibration was carried out prior to each measurement using the zero point as the first data point and the "empty" AAV9 vector (3.75 MDa, Progen Biotechnik GmbH, Heidelberg, Germany) as second data point. For the establishment of the calibration, "empty" AAV9 was measured at the beginning and ending of each run sequence. Since in the automated operation mode, the robot does not mix sample with the buffer provided in the well of the gasket when selecting "buffer-dilution" as measurement option, the samples were manually pre-diluted before pipetting 10 µL of the solution directly into the well of the cassette and performing the "buffer-free" focusing of the laser. Each sample was recorded in a movie for 60 s visualising the binding and unbinding events of the AAV particles which are then converted into a histogram representing the distribution of the registered molecular masses.

3.3. Data Collection and Processing

Measurements were recorded using AcquireMP 2.4.2 (Refeyn Ltd., Oxford, UK) and analysed with DiscoverMP (v2023 R1.2) (Refeyn Ltd., Oxford, UK). For data analysis, the bin width was set to 40 for all measurements. A Gaussian function was used to fit the ratiometric contrast distribution yielding the molecular weight of the respective subpopulation. All bar plots were visualised with Matlab R2020b (MathWorks, Natick, MA, USA).

4. Conclusions

Following up on our recent publication, where we demonstrated the high potential of mass photometry as opposed to AUC, TEM and CDMS for the quantification of AAV subspecies, we further investigated the instrument's capabilities by comparing the newly featured instrument automation to manual sample handling with respect to the proportion of AAV subpopulations, molar masses of the capsid and payload, and binding count rates. In general, there are no significant differences between automated and manual instrument operation. However, we observed higher standard deviations for measurements carried out under automated operation than when handling the instrument manually with respect to the calculated quantities of AAV subspecies, the binding count rate and the rough estimation of the capsid titer. The latter demonstrates the limitation of the instrument as significant fluctuations in the registered binding events were observed. The more AAVs attach and detach from the glass surface, the higher the calculated capsid titer. The variation in the binding count rates between samples measured multiple times is reflected in a high standard deviation. If constant binding count rates between the replicates were achieved, it would be possible to gain precise information on the AAV titer. The calculation of the capsid titer using MP would have the potential to replace the more laborious ELISA in the future.

Furthermore, we compared the "buffer-dilution" mode with the "buffer-free" mode, as both can be used for sample measurement. While the first introduces an additional dilution step, the latter measures the sample in its initial state. The results showed, that under automated instrument operation and using the "buffer-dilution" option, the sample

is not mixed with the buffer that had been provided in the sample well. The robot pipettes the sample onto the bottom of the well of the gasket resulting in a displacement of the buffer from the bottom which is mirrored in a higher number of binding and unbinding events than when using the "buffer-free" mode (manual pre-dilution prior to analysis). However, both analysis options are suitable for the assessment of the quantities of AAV subpopulations and the molecular weight of the incorporated genomic cargo.

After the identification of the best operating conditions, we proceeded with the cleanup of AAVs from harvest material using single-domain monospecific antibody fragments covalently attached onto the surface of poly(styrene-divinylbenzene) beads. We were able to distinguish between AAV fractions that had been generated using two types of transfection reagents (A and B) by first, extracting the AAVs from the crude cell material and then, analysing it with mass photometry and AUC. The MP and AUC data of extracted AAVs agreed well with one another demonstrating the good comparability between these orthogonal methods. To expand this further, we used nanobodies immobilised on magnetic beads for the isolation of AAVs from harvest material followed by MP analysis as these procedures have the potential to be fully automated and are paving the way for high throughput full/empty analyses, especially during the early development phase within the upstream process. During this stage, potentially promising harvest conditions that yield a high number of the desired filled AAV vectors can be easily selected and pursued further in follow-up experiments up to large-scale approaches.

Supplementary Materials: The following supporting information can be downloaded at: https://www.mdpi.com/article/10.3390/ijms25020838/s1.

Author Contributions: Conceptualization, C.W. and F.F.F.; methodology, C.W. and F.F.F.; writing—original draft preparation, C.W.; writing—review and editing, M.L., F.F.F., B.I., R.P., I.S. and R.B.-G.; supervision, M.L. and R.B.-G.; All authors have read and agreed to the published version of the manuscript.

Funding: Baxalta Innovations GmbH provided all the funding for this research.

Institutional Review Board Statement: Not applicable.

Informed Consent Statement: Not applicable.

Data Availability Statement: Data are contained within the article and Supplementary Materials.

Conflicts of Interest: Authors Christina Wagner, Felix F. Fuchsberger, Bernd Innthaler, Robert Pachlinger, Irene Schrenk and Martin Lemmerer were employed by the company Takeda. The remaining authors declare that the research was conducted in the absence of any commercial or financial relationships that could be construed as a potential conflict of interest. The authors declare that this study received funding from Baxalta Innovations GmbH (part of Takeda). The funder had the following involvement with the study: Employer of Christina Wagner, Felix F. Fuchsberger, Bernd Innthaler, Robert Pachlinger, Irene Schrenk and Martin Lemmerer.

References

1. Li, C.; Samulski, R.J. Engineering adeno-associated virus vectors for gene therapy. *Nat. Rev. Genet.* **2020**, *21*, 255–272. [CrossRef] [PubMed]
2. Ghosh, S.; Brown, A.M.; Jenkins, C.; Campbell, K. Viral Vector Systems for Gene Therapy: A Comprehensive Literature Review of Progress and Biosafety Challenges. *Appl. Biosaf.* **2020**, *25*, 7–18. [CrossRef] [PubMed]
3. Chandler, R.J.; Sands, M.; Venditti, C.P. rAAV integration and genotoxicity: Insights from animal models. *Hum. Gene Ther.* **2017**, *28*, 314–322. [CrossRef] [PubMed]
4. Elevidys. Available online: https://www.fda.gov/vaccines-blood-biologics/tissue-tissue-products/elevidys (accessed on 6 July 2023).
5. Khatwani, S.L.; Pavlova, A.; Pirot, Z. Anion-exchange HPLC assay for separation and quantification of empty and full capsids in multiple adeno-associated virus serotypes. *Mol. Ther.-Methods Clin. Dev.* **2021**, *21*, 548–558. [CrossRef] [PubMed]
6. Oyama, H.; Ishii, K.; Maruno, T.; Torisu, T.; Uchiyama, S. Characterization of Adeno-Associated Virus Capsid Proteins with Two Types of VP3-Related Components by Capillary Gel Electrophoresis and Mass Spectrometry. *Hum. Gene Therapy* **2021**, *32*, 1403–1416. [CrossRef] [PubMed]

7. Wang, D.; Tai, P.; Gao, G. Adeno-associated virus vector as a platform for gene therapy delivery. *Nat. Rev. Drug Discov.* **2019**, *18*, 358–378. [CrossRef] [PubMed]
8. Wright, F.J. Quality Control Testing, Characterization and Critical Quality Attributes of AAV Vectors Used for Human Gene Therapy. *Biotechnol. J.* **2020**, *16*, e2000022. [CrossRef]
9. Hemgenix. Available online: https://www.fda.gov/vaccines-blood-biologics/vaccines/hemgenix (accessed on 17 October 2023).
10. Upstaza. Available online: https://www.ema.europa.eu/en/medicines/human/EPAR/upstaza (accessed on 2 January 2024).
11. Roctavian. Available online: https://www.fda.gov/vaccines-blood-biologics/roctavian (accessed on 2 January 2024).
12. EU/3/12/1091: Orphan Designation for the Treatment of Beta Thalassaemia Intermedia and Major. Available online: https://www.ema.europa.eu/en/medicines/human/orphan-designations/eu3121091 (accessed on 12 April 2023).
13. FDA Approves First Cell-Based Gene Therapy to Treat Adult and Pediatric Patients with Beta-thalassemia Who Require Regular Blood Transfusions. Available online: https://www.fda.gov/news-events/press-announcements/fda-approves-first-cell-based-gene-therapy-treat-adult-and-pediatric-patients-beta-thalassemia-who (accessed on 12 April 2023).
14. Aponte-Ubillus, J.; Barajas, D.; Peltier, J.; Bardliving, C.; Shamlou, P.; Gold, D. Molecular design for recombinant adeno-associated virus (rAAV) vector production. *Appl. Microbiol. Biotechnol.* **2018**, *102*, 1045–1054. [CrossRef]
15. Kotterman, M.A.; Schaffer, D.V. Engineering adeno-associated viruses for clinical gene therapy. *Nat. Rev. Genet.* **2014**, *15*, 445–451. [CrossRef]
16. Buller, R.M.; Janik, J.E.; Sebring, E.D.; Rose, J.A. Herpes simplex virus types 1 and 2 completely help adenovirus-associated virus replication. *J. Virol.* **1981**, *40*, 241–247. [CrossRef]
17. Geoffroy, M.-C.; Salvetti, A. Helper Functions Required for Wild Type and Recombinant Adeno-Associated Virus Growth. *Curr. Gene Ther.* **2005**, *5*, 265–271. [CrossRef] [PubMed]
18. Wu, Z.; Asokan, A.; Samulski, R.J. Adeno-associated virus serotypes: Vector toolkit for human gene therapy. *Mol. Ther.* **2006**, *14*, 316–327. [CrossRef] [PubMed]
19. Xie, Q.; Bu, W.; Bhatia, S.; Hare, J.; Somasundaram, T.; Azzi, A.; Chapman, M.S. The atomic structure of adeno-associated virus (AAV-2), a vector for human gene therapy. *Proc. Natl. Acad. Sci. USA* **2002**, *99*, 10405–10410. [CrossRef] [PubMed]
20. Mietzsch, M.; Jose, A.; Chipman, P.; Bhattacharya, N.; Daneshparvar, N.; McKenna, R.; Agbandje-McKenna, M. Completion of the AAV Structural Atlas: Serotype Capsid Structures Reveals Clade-Specific Features. *Viruses* **2021**, *13*, 101. [CrossRef]
21. Worner, T.P.; Bennett, A.; Habka, S.; Snijder, J.; Friese, O.; Powers, T.; Agbandje-McKenna, M.; Heck, A.J.R. Adeno-associated virus capsid assembly is divergent and stochastic. *Nat. Commun.* **2021**, *12*, 1642. [CrossRef] [PubMed]
22. Maestro, S.; Weber, N.D.; Zabaleta, N.; Aldabe, R.; Gonzalez-Aseguinolaza, G. Novel vectors and approaches for gene therapy in liver diseases. *JHEP Rep.* **2021**, *3*, 100300. [CrossRef] [PubMed]
23. Bulcha, J.T.; Wang, Y.; Ma, H.; Tai, P.W.L.; Gao, G. Viral vector platforms within the gene therapy landscape. *Signal Transduct. Target. Ther.* **2021**, *6*, 53. [CrossRef] [PubMed]
24. Buning, H.; Huber, A.; Zhang, L.; Meumann, N.; Hacker, U. Engineering the AAV capsid to optimize vector-host-interactions. *Curr. Opin. Pharmacol.* **2015**, *24*, 94–104. [CrossRef] [PubMed]
25. Zhao, H.; Lee, K.-J.; Daris, M.; Lin, Y.; Wolfe, T.; Sheng, J.; Plewa, C.; Wang, S.; Meisen, W.H. Creation of a High-Yield AAV Vector Production Platform in Suspension Cells Using a Design-of-Experiment Approach. *Mol. Ther. Methods Clin. Dev.* **2020**, *18*, 312–320. [CrossRef]
26. Gimpel, A.L.; Katsikis, G.; Sha, S.; Maloney, A.J.; Hong, M.S.; Nguyen, T.N.; Wolfrum, J.; Springs, S.L.; Sinskey, A.J.; Manalis, S.R.; et al. Analytical methods for process and product characterization of recombinant adeno-associated virus-based gene therapies. *Mol. Ther.-Methods Clin. Dev.* **2021**, *20*, 740–754. [CrossRef]
27. Fu, X.; Chen, W.-C.; Argento, C.; Clarner, P.; Bhatt, V.; Dickerson, R.; Bou-Assaf, G.; Bakhshayeshi, M.; Lu, X.; Bergelson, S.; et al. Analytical Strategies for Quantification of Adeno-Associated Virus Empty Capsids to Support Process Development. *Hum. Gene Ther. Methods* **2019**, *30*, 144–152. [CrossRef] [PubMed]
28. Li, T.; Gao, T.; Chen, H.; Dmianova, Z.; Wang, F.; Malik, M.; Luo, J.; Yowanto, H.; Mollah, S. *Determination of Full, Partial and Empty Capsid Ratios for Adeno-Associated Virus (AAV) Analysis*; SCIEX: Framingham, MA, USA, 2020.
29. Refeyn Ltd. Quantifying Heterogeneous AAV Capsid Loading Using Mass Photometry. [White Paper]. 2022. Available online: https://info.refeyn.com/app-note-aav-loading (accessed on 14 June 2023).
30. Ebberink, E.; Ruisinger, A.; Nuebel, M.; Thomann, M.; Heck, A.J.R. Assessing production variability in empty and filled adeno-associated viruses by single molecule mass analyses. *Mol. Ther. Methods Clin. Dev.* **2022**, *27*, 491–501. [CrossRef] [PubMed]
31. Werle, A.K.; Powers, T.W.; Zobel, J.F.; Wappelhorst, C.N.; Jarrold, M.F.; Lyktey, N.A.; Sloan, C.D.; Wolf, A.J.; Adams-Hall, S.; Baldus, P.; et al. Comparison of analytical techniques to quantitate the capsid content of adeno-associated viral vectors. *Mol. Ther. Methods Clin. Dev.* **2021**, *23*, 254–262. [CrossRef] [PubMed]
32. Pierson, E.E.; Keifer, D.Z.; Asokan, A.; Jarrold, M.F. Resolving Adeno-Associated Viral Particle Diversity with Charge Detection Mass Spectrometry. *Anal. Chem.* **2016**, *88*, 6718–6725. [CrossRef] [PubMed]
33. Barnes, L.F.; Draper, B.E.; Kurian, J.; Chen, Y.-T.; Shapkina, T.; Powers, T.W.; Jarrold, M.F. Analysis of AAV-Extracted DNA by Charge Detection Mass Spectrometry Reveals Genome Truncations. *Anal. Chem.* **2023**, *95*, 4310–4316. [CrossRef] [PubMed]
34. Subramanian, S.; Maurer, A.C.; Bator, C.M.; Makhov, A.M.; Conway, J.F.; Turner, K.B.; Marden, J.H.; Vandenberghe, L.H.; Hafenstein, S.L.; Troxell, B.; et al. Filling Adeno-Associated Virus Capsids: Estimating Success by Cryo-Electron Microscopy. *Hum. Gene Ther.* **2019**, *30*, 1449–1460. [CrossRef]

35. Stagg, S.M.; Yoshioka, C.; Davulcu, O.; Chapman, M.S. Cryo-electron Microscopy of Adeno-associated Virus. *Chem. Rev.* **2022**, *122*, 14018–14054. [CrossRef]
36. Takeda, K.; Noda, M.; Maruno, T.; Uchiyama, S. Critical Calibration of Mass Photometry for Higher-Mass Samples Such as Adeno-Associated Virus Vectors. *J. Pharm. Sci.* **2023**, *112*, 1145–1150. [CrossRef]
37. Wu, D.; Piszczek, G. Standard protocol for mass photometry experiments. *Eur. Biophys. J.* **2021**, *50*, 403–409. [CrossRef]
38. Wagner, C.; Fuchsberger, F.F.; Innthaler, B.; Lemmerer, M.; Birner-Gruenberger, R. Quantification of Empty, Partially Filled and Full Adeno-Associated Virus Vectors Using Mass Photometry. *Int. J. Mol. Sci.* **2023**, *24*, 1033. [CrossRef]
39. POROS™ CaptureSelect™ AAV Resins: AAV8, AAV9, AAVX. Available online: https://www.thermofisher.com/order/catalog/product/A27354 (accessed on 2 January 2024).
40. Dynabeads™ CaptureSelect™ AAVX Magnetic Beads. Available online: https://www.thermofisher.com/order/catalog/product/2853522001?SID=srch-srp-2853522001 (accessed on 2 January 2024).
41. Florea, M.; Nicolaou, F.; Pacouret, S.; Zinn, E.M.; Sanmiguel, J.; Andres-Mateos, E.; Unzu, C.; Wagers, A.J.; Vandenberghe, L.H. High-efficiency purification of divergent AAV serotypes using AAVX affinity chromatography. *Mol. Ther. Methods Clin. Dev.* **2023**, *28*, 146–159. [CrossRef] [PubMed]

Supplemental Information

Automated Mass Photometry of Adeno-Associated Virus Vectors from Crude Cell Extracts

Christina Wagner, Felix F. Fuchsberger, Bernd Innthaler, Robert Pachlinger, Irene Schrenk, Martin Lemmerer, Robert Pletzenauer and Ruth Birner-Gruenberger

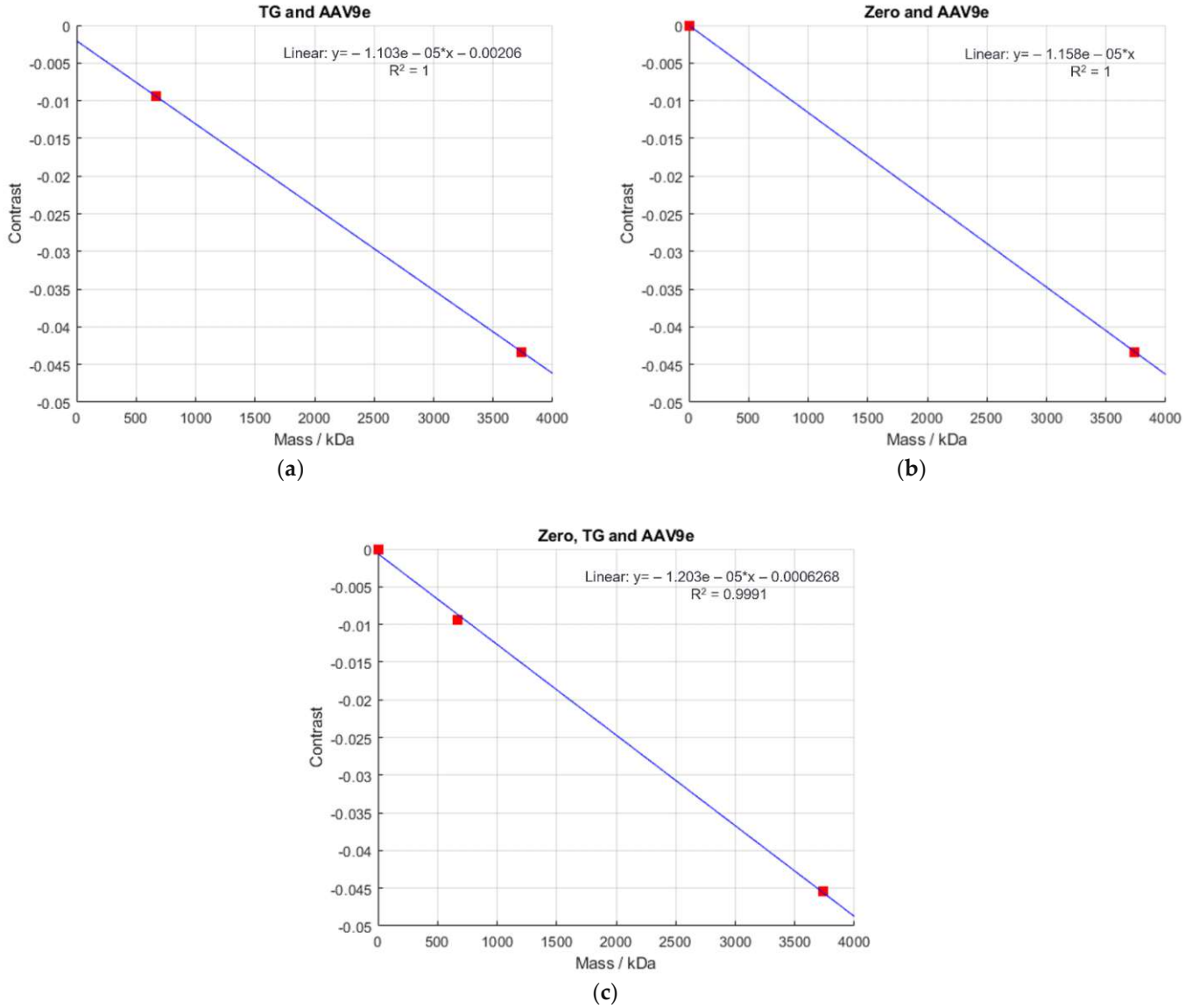

Supplementary Figure S1. Calibration curves obtained with (**a**) TG and AAV9e, (**b**) Zero and AAV9e and (**c**) Zero, TG and AAV9e. The AAV9e and TG datapoints are the average of two independent measurements of the respective sample.

Supplementary Table S1. Determination of the AAV subpopulations of an AAV9 sample consisting of ~33% empty, ~6% partially filled, ~52% full, and ~8% overfull particles under manual operation of the mass photometer using three different calibrations. x: two data points-based calibration with TG and AAV9e; y: two data points-based calibration with the zero point and AAV9; z: three data points-based calibration with the zero point, TG and AAV9e. E, PF, F and OF stand for empty, partially filled, full and overfull, respectively.

	AAV subpopulations							
Calibration	**Average E / %**	**RSD / %**	**Average PF / %**	**RSD / %**	**Average F / %**	**RSD / %**	**Average OF / %**	**RSD / %**
x[1)]	40.4	5.5	7.0	9.3	50.5	3.4	2.1	16.8
y[2)]	40.6	5.2	7.4	6.7	50.1	3.7	1.9	16.6
z[3)]	41.9	5.1	10.1	7.3	46.5	3.8	1.5	20.5

[1)] TG and AAV9e, [2)] Zero and AAV9e, [3)] Zero, TG and AAV9e

Supplementary Table S2. Determination of the molar masses of empty and filled subpopulations and of the transgene size of an AAV9 sample consisting of ~33% empty, ~6% partially filled, ~52% full, and ~8% overfull particles under manual operation of the mass photometer using three different calibrations. x: two data points-based calibration with TG and AAV9e; y: two data points-based calibration with the zero point and AAV9; z: three data points-based calibration with the zero point, TG and AAV9e.

	Empty AAVs		**Full AAVs**					
Calibration	**Average mass / kDa**	**RSD / %**	**Average mass / kDa**	**RSD / %**	**Calculated transgene size / kDa**	**RSD / %**	**Expected transgene size / kDa**	**Error / %**
x[1)]	3736	0.2	5211	0.4	1476	0.8	1400	5.4
y[2)]	3735	0.2	5139	0.3	1403	0.6	1400	0.2
z[3)]	3544	0.2	4896	0.3	1351	0.7	1400	3.5

[1)] TG and AAV9e, [2)] Zero and AAV9e, [3)] Zero, TG and AAV9e

Supplementary Table S3. Determination of the AAV subpopulations of an AAV9 sample consisting of ~33% empty, ~6% partially filled, ~52% full, and ~8% overfull particles under automated operation of the mass photometer using either the "buffer-free" or "buffer-dilution" focusing option. E, PF, F and OF stand for empty, partially filled, full and overfull, respectively.

	AAV subpopulations							
	Average E / %	**RSD / %**	**Average PF / %**	**RSD / %**	**Average F / %**	**RSD / %**	**Average OF / %**	**RSD / %**
Buffer-free	38.6	13.8	8.7	14.9	48.9	5.8	3.8	50.1
Buffer-dilution	36.6	4.4	11.5	14.4	49.5	5.2	2.5	8.0

Supplementary Table S4. Determination of the molar masses of empty and filled subpopulations and of the transgene size of an AAV9 sample consisting of ~33% empty, ~6% partially filled, ~52% full, and ~8% overfull particles under automated operation of the mass photometer using either the "buffer-free" or "buffer-dilution" focusing option.

	Empty AAVs		**Full AAVs**					
	Average mass / kDa	**RSD / %**	**Average mass / kDa**	**RSD / %**	**Calculated transgene size / kDa**	**RSD / %**	**Expected transgene size / kDa**	**Error / %**
Buffer-free	3789	1.8	5230	1.9	1441	2.2	1400	2.9
Buffer-dilution	3566	1.0	4922	0.9	1355	0.9	1400	3.2

Supplementary Table S5. Determination of the binding count rates for "buffer-free" and "buffer-dilution" sample measurements using an AAV9 sample consisting of ~33% empty, ~6% partially filled, ~52% full, and ~8% overfull particles under automated operation of the mass photometer.

	Binding count rate	
	Binding events	**RSD / %**
Buffer-free	2836	66.8
Buffer-dilution	5426	16.9

Supplementary Table S6. Determination of the AAV subpopulations of an AAV9 sample consisting of ~33% empty, ~6% partially filled, ~52% full, and ~8% overfull particles under automated operation of the mass photometer. The sample was measured five times on three consecutive days (days 1-3). E, PF, F and OF stand for empty, partially filled, full and overfull, respectively. E, PF, F and OF stand for empty, partially filled, full and overfull, respectively.

	MP							
	Average E / %	**RSD / %**	**Average PF / %**	**RSD / %**	**Average F / %**	**RSD / %**	**Average OF / %**	**RSD / %**
Day 1	38.5	8.1	8.0	5.4	49.7	6.0	1.4	17.6
Day 2	37.9	7.7	7.3	9.9	51.9	4.1	2.7	18.5
Day 3	37.6	12.8	8.9	13.4	49.6	5.5	4.5	16.7

Supplementary Table S7. Determination of the molar masses of empty and filled subpopulations and of the transgene size under automated operation of the mass photometer. Results were generated by five repetitive measurements of an AAV9 sample (~33% empty, ~6% partially filled, ~52% full, and ~8% overfull AAV particles) on three consecutive days (days 1-3).

	Empty AAVs		**Full AAVs**						
	Average mass / kDa	**RSD / %**	**Average mass / kDa**	**RSD / %**	**Calculated transgene size / kDa**	**Average transgene size / kDa**	**RSD / %**	**Expected transgene size / kDa**	**Error / %**
Day 1	3785	0.5	5222	0.5	1437				
Day 2	3788	1.2	5237	1.6	1448	1440	0.6	1400	2.8
Day 3	3794	1.8	5228	1.7	1434				